Identification and characterization of potential human epidermal stem cells

Dissertation

Faculty of Biosciences
Ruprechts-Karl-University Heidelberg

Elisa Specker
Heidelberg, June 2015

Dissertation

submitted to the

Combined Faculties for the Natural Sciences and for Mathematics

of the Ruperto-Carola University of Heidelberg, Germany

for the degree of

Doctor of Natural Sciences

presented by

Diplom-Biologin Elisa Katharina Specker

born in: Leimen

Oral-examination: July 27th 2015

Identification and characterization
of potential human epidermal stem cells

Referees: Prof. Dr. Andreas Trumpp

Prof. Dr. Petra Boukamp

Danksagung

Mein ganz besonderer Dank gilt an dieser Stelle Frau Prof. Dr. Petra Boukamp, Leiterin der Abteilung Genetik der Hautcarcinogenese am Deutschen Krebsforschungszentrum, für die Möglichkeit, diese Arbeit in ihrer Arbeitsgruppe anfertigen zu können. Danke, dass du mir über viele Jahre hinweg dein Vertrauen entgegengebracht hast und durch viele interessante und hilfreiche wissenschaftliche Diskussionen, stets meine wissenschaftliche Neugier bestärkt und unterstützt hast. Nicht zuletzt hat deine herzliche Betreuung die Laborzeit unvergesslich gemacht!

Herrn Prof. Dr. Andreas Trumpp möchte ich ebenfalls herzlich danken für seine Bereitschaft, sich als Gutachter dieser Arbeit zur Verfügung zu stellen.

Ein besonderer Dank gilt auch Dr. Hans-Jürgen Stark, dein Wissen, dein Engagement und nicht zuletzt dein Humor haben mich durch die vielen schönen Jahre am DKFZ begleitet.

Herzlich bedanken möchte ich mich auch bei Hermann Stammer für seine große Hilfsbereitschaft mich in meinem wissenschaftlichen Arbeiten zu unterstützen.

Ein ganz besonderer Dank gilt Iris Martin und Katrin Schmidt. Eure Unterstützung, die nicht an der Zellkulturtür endete, war einfach großartig!

Danke natürlich an die ganze “Boukamp Familie“: Sabrina Bauer, Manuel Berning, Gaby Blaser, Anja Bort, Svenja Ewert, Lutz Langbein, Elke Laport, Christine Leufke, Iris Martin, Leonard Nevaril, Marco Nici, Katharina Nöske, Elizabeth Pavez-Lorie, Silke Prätzel, Lisa Schardt, Katrin Schmidt, Philipp Scholz, Hermann Stammer, Hans-Jürgen Stark und Marius Tham. Nicht nur, dass ohne euch die Laborzeit nur halb so schön gewesen wäre, es ist auch schön zu wissen, ein paar gute Freunde fürs Leben gefunden zu haben!

Nicht zu vergessen, gebührt auch meinen Mädels, dem Hexenkessel, ein riesen Dankeschön! Ihr habt immer wieder ermutigt, meinen Weg zu gehen und wart immer für mich da. Bei meiner besten Freundin, Julia, möchte ich mich besonders bedanken. Schön, dass es dich gibt!

Ganz besonders möchte ich Kati danken. Ohne deine Hilfe wäre ich verloren gewesen! Ich bin sehr froh, eine so wundervolle Freundin wie dich gefunden zu haben!

In besonderer Weise möchte ich gerne meinen Eltern danken, ohne deren Unterstützung ich all das nie geschafft hätte!

TABLE OF CONTENTS

Zusammenfassung

Trotz seit nunmehr als dreißig Jahren Forschung an epidermalen Stammzellen ist noch nicht verstanden wie die Gewebshomöostase der interfollikulären Epidermis (IFE) reguliert wird. Dies ist hauptsächlich dem Fehlen von eindeutigen Markern für die Identifikation von humanen epidermalen Stammzellen geschuldet. In dem Haarfollikel und Follikel-armer Haut, wie der Epidermis des Mäuseohres, wurden langsam-teilende oder auch *label-retaining* Zellen (LRZ) als Stammzellen beschrieben. Es wird angenommen, dass diese LRZs für die Aufrechterhaltung der Gewebshomöostase verantwortlich sind. Um diese Frage zu beantworten, müssen jedoch Stammzellen in der Haut eindeutig identifiziert werden. Das Ziel dieser Studie war die Isolierung und Charakterisierung von LRZs unter der Annahme, dass das langsame Teilen ein Charakteristikum von epidermalen Stammzellen ist. Da Untersuchungen an der Haut restriktiv sind wurde für diese Studie ein *in vitro* 3D organotypisches Hautmodell verwendet. Für den Nachweis von LRZs wurde ein induzierbarer Tet-Off-H2B-GFP lentiviraler Reporter Vektor verwendet. Dadurch wurde eine Methode entwickelt normale adulte humane Keratinozyten (NHEK) mit diesem lentiviralen Vektor erfolgreich zu infizieren und transduzierte NHEK in Langzeit organotypischen Kulturen (OTK) zu kultivieren. Mit *Pulse-Chase* Experimenten (2 Wochen *pulse*, 6 Wochen *chase*) war es möglich vitale LRZs aus der IFE funktionell als langsam-teilende Zellen zu identifizieren und als GFP-positive Zellen aus OTKs zu isolieren. Zur weiteren Charakterisierung dieser Zellen wurden Microarray-Analysen von den isolierten *label-retaining* basalen Zellen und den entsprechenden unmarkierten basalen Zellen durchgeführt. Die Analyse ergab, dass 102 Gene differentiell in LRZs reguliert sind. Wir konnten zeigen, dass eine hohe Anzahl von Genen der extrazellulären Matrix (EZM) oder EZM modulierenden Gene in LRZs hoch reguliert waren. Dies konnte mittels qRT-PCR verifiziert werden. Um die differentielle Proteinexpression zu bestimmen sind weitere Versuche in Vorbereitung. Anhand dieses Profils nehmen wir jedoch an, dass LRZs imstande sind ihre lokale Umgebung, auch als Nische bezeichnet, aktiv durch die Sekretion von EZM Komponenten zu beeinflussen. Diese besondere EZM kann zur besseren Anhaftung der LRZs in der Nische dienen, sowie als Reservoir für Wachstumsfaktoren, die Zellsignale regulieren können. Die Analyse mit dem Programm Ingenuity Pathway Analyse ergab, dass TGFβ in die Regulierung involviert sein könnte. Stimulierungs-Experimente mit TGFβ ergaben dementsprechend, dass TGFβ-1 die Hochregulation von Genen stimuliert, die auch in LRZs im Gewebe-Kontext sehr hoch reguliert waren. Daher nehmen wir an, dass LRZs ein klar unterscheidbares molekulares Profil im Vergleich zu anderen basalen Zellen der IFE haben, welches ihnen erlaubt ihre Nische spezifisch zu regulieren. Für die funktionelle Rolle der LRZs als epidermale Stammzelle bleiben weitere Untersuchungen abzuwarten.

Summary

Despite more than 30 years of epidermal stem cell research, it is not yet understood how tissue homeostasis is balanced in the interfollicular epidermis (IFE). This is mainly because of the lack of distinct markers to identify human epidermal stem cells. In the hair follicle and the follicle-poor mouse ear epidermis stem cells have been described as slow-cycling cells, also called label-retaining cells (LRCs) (Bickenbach, 1981; Braun et al., 2003; Cotsarelis et al., 1990). It is suggested that these LRCs are responsible for maintaining tissue homeostasis. To address this stem cells need to be identifiable which has yet to be accomplished. Suggesting, that slowly cycling is a characteristic also of epidermal stem cells in the IFE, the aim of this study was the isolation and characterization of LRCs. Since investigation on human skin is restricted, we employed a human *in vitro* 3D organotypic skin model (Muffler et al., 2008). For the detection of LRCs we utilized an inducible Tet-Off-H2B-GFP lentiviral reporter vector. Thus, a method was developed to successfully infect normal human adult keratinocytes (NHEK) with the lentiviral vector and these keratinocytes were further propagated in organotypic cultures (OTC) to establish long-term skin equivalents. In pulse-chase approaches (2 weeks pulse, 6 weeks chase), viable LRCs of the IFE could be functionally identified as slow-cycling cells and isolated as GFP positive cells from OTCs. To further characterize these cells, microarray analysis was performed of the isolated basal LRCs and their respective non-labeled basal cell fraction. This analysis revealed 102 genes to be differentially regulated in the LRCs. We could show that a high fraction of upregulated genes in LRCs were ECM or ECM remodeling genes which could be verified by qRT-PCR. Further characterization on protein level is in progress. From this profile it is suggested, that LRCs actively modulate their local microenvironment, referred to as niche, by secreting unique ECM components. This distinct ECM may well serve for enhanced adhesion of LRCs to the niche as well as a reservoir for growth factors regulating cell signaling. Ingenuity pathway analysis further suggested a role for TGFβ signaling in this regulation. Accordingly, stimulation experiments provided first evidence that TGFβ-1 stimulates upregulation of those genes in NHEKs in 2D cultures that were highly upregulated in LRCs in their tissue context. Thus, we propose that LRCs exhibit a distinct molecular profile that compared to all other basal cells allows them to establish their specific regulatory niche. Their functional role as epidermal stem cells has now to await further investigations.

Abbreviations

°C	Degree Celsius
µg	Microgram
µL	Microlitre
µm	Micrometre
AB	Antibody
Asc. a. ph.	Ascorbic acid phosphate
bFGF	Basic fibroblast growth factor
BM	Basement membrane
BrdU	5'-Bromo-2'-deoxyuridine
BSA	Bovine serum albumine
cDNA	Complementary DNA
cm	Centimetre
CO_2	Carbon dioxide
COL1A1	collagen, type I, alpha 1
Cy3	Indocarbocyanin
D	Day(s)
D10	DMEM with 10% FCS
DAPI	4′,6-Diamidino-2-phenylindol
Dest	de-ionized
DMEM	Dulbecco´s modified Eagle´s medium
DNA	Deoxyribonucleic acid
dNTP	Deoxyribonucleotide triphosphates
ECM	Extracellular matrix
EDTA	Ethylendiamintetraacetate
EGF	Epidermal growth factor
et al.	*et alii/aliae, and others*
EtOH	Ethanol
FA	Formaldehyde
FCS	Fetal calf serum
fdm	Fibroblast-derived matrix
Fig	Figure
g	Gram(s)
G	Gravity constant
GAPDH	Glyceraldehyde-3-phosphate-dehydrogenase
GFP	green fluorescent protein
GO	Gene Ontology
h	Hour(s)
H&E	Hämatoxylin & Eosin
HaCaT	Human adult Calcium Temperature
HBSS	Hank´s balanced salt solution
HCl	Chlorhydric acid
HIST1H2BG	Histone Cluster 1, H2bg
HIST1H4H	Histone Cluster 1, H4h
Hoechst	Bisbenzimide
IdU	Iododeoxyuridine
IFE	Interfollicular epidermis
IFF	Indirect Immunofluorescence
IGFB4	insulin-like growth factor binding protein 4
IGF	Insulin-like growth factor
IL6	Interleukin 6
Ki67	Nuclearprotein associated with proliferation
L	Liter
Lam-PCR	Linear amplification-mediated Polymerase Chain Reaction
LRC	Label-retaining cell
Lrp6	Low-density lipoprotein receptor-related protein 6
MeOH	Methanol
mg	Milligramm
min	Minute(s)
ml	Millilitre
mm	Millimetre
MMP	Matrix metalloprotease
mRNA	messenger RNA
ms	Millisecond
NaN_3	Sodium azide
NaCl	Sodium chloride
nm	Nanometre
NaOH	Sodium hydroxide
NHEK	Normal human epidermal keratinocytes
ON	Over night
OTC	Organotypic coculture
PBS-	Phosphate buffered saline
PBS+	Phosphate buffered saline containing Magnesiochloride and Calciumchloride
PCR	Polymerase Chain Reaction
Pen/Strep	Penicillin / Streptomycin
PFA	Paraformaldehyde
pH	*pondus hydrogenii*
qRT-PCR	Quantitative real-time Polymerase Chain Reaction
RNA	Ribonucleic acid
rpm	rounds per minute
RT	Room temperature
Sca OTC	scaffold-based organotypic coculture
Snai2	snail family zinc finger 2
TGFβ	Transforming growth factor β
TGFβR1	TGFβ receptor type 1
TGFβR2	TGFβ receptor type 2
TGFβR3	TGFβ receptor type 3
THBS1	Thrombospondin-1
TIMP2	metallopeptidase inhibitor 2
V	Volt
Wnt	int/Wingless family

1 Introduction

1.1 The human skin

The skin serves as a protective barrier of the human body and is with an expansion about 1.7m^2 and a proportion up to 16% of the total body weight the largest human organ (Jung, 1995; Williams, 2003). The human skin has a lot of unique and important functions. It protects the human body from infection with pathogens and harmful substances from the environment, for example UV-radiation and exogenous substances. Furthermore the skin plays an important role in the regulation of heat and water, including regulating the electrolyte metabolism. Other functions are the regulation of the immune response through Langerhans cells and the sensation of touch, heat, and cold through Merkel- and nerve cells. The skin is made up of two major compartments, the dermis and the epidermis. Underneath is the deeper subcutaneous adipose and connective tissue (hypodermis). Epidermis and dermis are connected through the basement membrane which mainly contains collagen type IV and collagen type VII, proteoglycans like perlecan and different laminins.

1.1.1 Dermis

The dermis constitutes of a fibroblastic connective tissue and serves as the supporting base for the epidermis (Kanitakis, 2002). The main component of the dermis is a dense network of type I and type III collagen fibrils and elastic fibers embedded in different glycosaminoglycans, a family of water-binding macromolecules (Wilkes et al., 1973). This extracellular matrix (ECM), secreted by dermal fibroblasts, gives the skin high elasticity, and tensile strength as well as compressibility (Deutzmann R, 2007). Fibroblasts are the main cell type in the dermis, but there are also immune cells like macrophages, mast cells and dendrocytes (Fritsch, 2009; Sterry, 2005). Embedded in the dermis are skin appendages such as hair follicles, sebaceous glands and sweat glands.

The dermis comprises two zones, the *stratum reticulare* and the *stratum papillare.* The uppermost layer, the *stratum papillare* is rich in vascular vessels and neuronal cells and contains crypts, the dermal papillae, which interlock with the epidermis (Moll, 2010). These dermal papillae increase the contact area with the epidermis, ensuring optimal nourishment of the epidermis by running blood vessels through the papillae (Kanitakis, 2002). The *stratum reticulare* forms the lower part of the dermis and passes continuously into the subcutis. It consists of a more compact and dense network of collagen fibers giving the skin a high stability (Fritsch, 2009).

1.1.2 Epidermis

The epidermis is a multilayered, stratified, squamous epithelium with a thickness of 40 µm to 0,2 mm depending on age, gender and location (Kanitakis, 2002). Histologically, the epidermis is divided into four different layers, the *stratum basale,* the *stratum spinosum,* the *stratum granulosum and* the *stratum corneum* (Burns, 2004) (Figure 1). The major cell population are keratinocytes (> 90%), but also melanocytes, Langerhans cells and Merkel cells can be found. The epidermis is continuously renewing. Keratinocytes undergo terminal differentiation as the cells migrate from the basal layer to the surface of the skin. Since there are no blood vessels in the epidermis present, the epidermis is supplied via diffusion through the underlying dermis. The downward projections of the epidermis, between the dermal papillae, are called epidermal rete ridges. Keratinocytes build up two independent networks, a network of keratin intermediate filaments and a network of actin filaments. The keratin filaments are connected to the desmosomes (Garrod et al., 2002; Kottke et al., 2006), whereas the actin filaments are part of the adherens junctions (Perez-Moreno et al., 2003; Young et al., 2003). Desmoglein is a typical marker for desmosomes and E-cadherin for adherens junctions, correspondingly. Moreover, there are gap junctions, which allow the exchange of water, ions, and small molecules between adjacent cells (Mese et al., 2007). In addition the basal keratinocytes are firmly anchored to the basement membrane by hemidesmosomes (Figure 1). These intracellular connections allow keratinocytes to communicate and function as a sheet and enable the formation of an epithelial cell polarity (Shin et al., 2006).

The *stratum basale* (or basal cell layer), which is tightly connected to the subjacent basement membrane, is the epidermal regenerative layer. The next overlying layers are the *stratum spinosum* where the keratinocytes change their morphology to a more horizontal and polygonal flattened shape (Figure 1). Moreover, they form intercellular desmosomal connections which lead to a tight cell association providing resistance to physical stress (Kanitakis, 2002). In parallel to this differentiation process the keratinocytes also change their expression profile. While basal keratinocytes express mainly keratin 5 and keratin 14, the expression of keratin 1 and 10 specifies the suprabasal layers, starting at the *stratum spinosum*, and therefore represents the onset of epidermal differentiation.

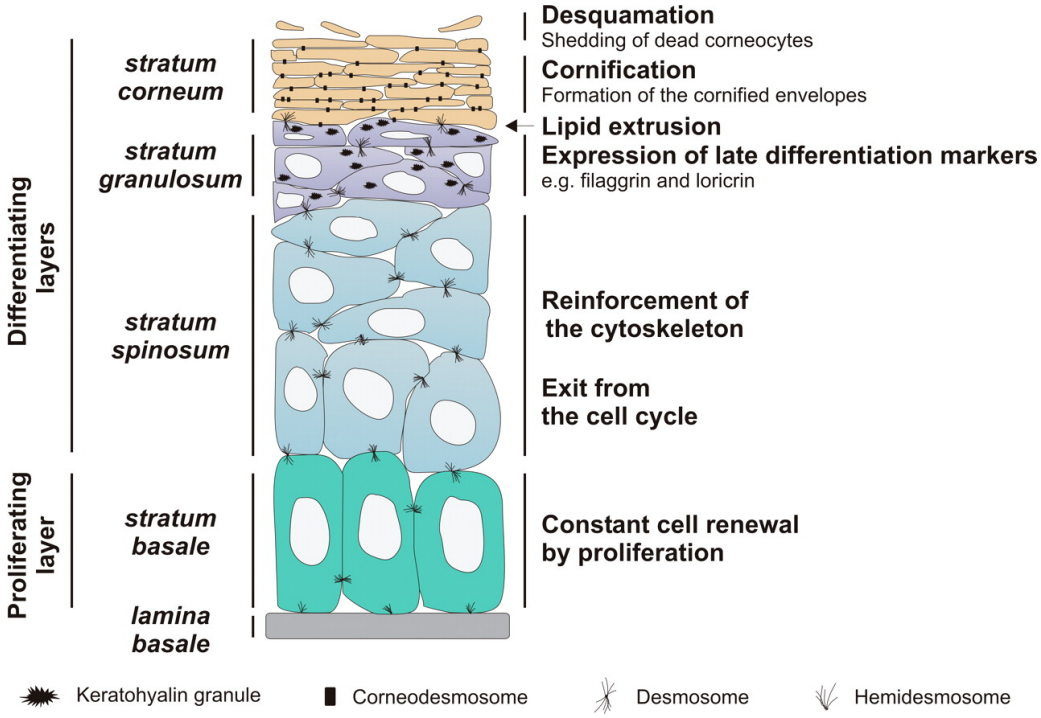

Figure 1: The structure of the epidermis. The stratum basale contains proliferating keratinocytes, from there they detach from the basement membrane and undergo a well defined terminal differentiation program while morphological changes occur. Figure from (Denecker et al., 2008)

The *stratum granulosum* consists of more flattened cells holding abundant keratohyalin granules in their cytoplasm (Chu, 2008). The deeply basophilic keratohyalin granules which contain precursors of the keratin matrix-like profillagrin dissolve and release their content as the cells of the granular layer undergo the terminal differentiation process to a cornified cell (Chu, 2008).

In the most superficial layers, the *stratum corneum,* the cells lose their nuclei and are finally shed off (Figure 1). The cornified layers provide a barrier and protects the epidermis from dehydration (Jackson et al., 1993). The horny cells (corneocytes) form tight junctions and are surrounded by a cornified envelope which is made up of proteins crosslinked by transglutaminases (Moll, 2010). Involucrin, filaggrin, loricrin, small proline rich proteins (SPR), repetin and proteins of the S100-family are components of the cornified envelope and indicate the terminal epidermal differentiation (Steinert and Marekov, 1995; Steinert and Marekov, 1997) (Figure 1).

1.2 Epidermal stem cells

In skin, there is a constant balance between cell proliferation and cell death, called tissue homeostasis. This epithelial balance is maintained by stem cells. Epidermal stem cells play a critical role in human skin homeostasis and wound repair. Adult stem cells in the skin are characterized by their capacity for self-renewal for an extended time period, and the ability to differentiate into multiple lineages derived from their tissue origin (Weissman and Baltimore, 2001).

There have been indentified three different populations of epidermal stem cells in mouse and human skin: in the permanent portion (the bulge region) of the hair follicle, in the sebaceous gland (SG) and in the interfollicular epidermis (Figure 2). Lineage tracing revealed that each compartment is maintained by their own, distinct stem cell population (Clayton et al., 2007; Ghazizadeh and Taichman, 2001; Ito et al., 2005; Levy et al., 2005; Levy et al., 2007). The interfollicular epidermis and the sebaceous glands are constantly self-renewing tissues, while hair follicles cycle between growth (anagen), involution and rest (telogen) (Hardy, 1992).

1.2.1 Hair follicle and sebaceous gland

Most of the knowledge on the regeneration potential of the epidermis comes from intensive research on murine hair follicles (HFs). The best characterized region for stem cells in the HF is the bulge region. Within this bulge region of the HF several suggested markers of stem cells exist including keratin 15 (K15) (Morris et al., 2004) and CD34 (Blanpain et al., 2004; Lyle et al., 1998; Trempus et al., 2003). There are three distinct populations of CD34. In the basal layer of the bulge are α6 integrin high-, K15- and CD34- expressing stem cells located (Figure 2). In the suprabasal layer above is a CD34 positive stem cell population with low levels of α6 integrin (Blanpain et al., 2004) (Figure 2). Lgr5, a known marker for stem cells in the intestinal and gastric epithelium of mice (Barker et al., 2010; Barker et al., 2007), is expressed in the third CD34 positive stem cell population, which is located at the lower part of the bulge region (Figure 2). However, there is a dynamic change of the lgr5 expression during the hair cycle. While lgr5 expression overlaps with CD34 in the resting bulge (telogen), the lgr5 positive cells start proliferating and migrating to the outer root sheath (ORS) to contribute to anagen hair growth while losing their CD34 expression (Jaks et al., 2008). Other markers for stem cell populations in the bulge region are Sox9 (Vidal et al., 2005), Lhx2 (Rhee et al., 2006), and transcription factor 3 (tcf3) (DasGupta and Fuchs, 1999). Furthermore, lineage-tracing demonstrated that there is an lgr6- expressing stem cell population of non dividing cells right above the bulge region located at the isthmus of the HF (Snippert et al., 2010) (Figure 2). This lgr6 stem cell pool can renew the sebaceous gland

and the upper follicle. Moreover, lgr6 lineage-tracing analyses during wound repair shows that this stem cell pool permanently contributes to the newly formed interfollicular epidermis (Snippert et al., 2010). Above the lgr6 positive cell population is a stem cell population located which lacks the expression of CD34 and K15, but is positive for MTS24 and α6 integrin (Nijhof et al., 2006) (Figure 2). MTS24 was suggested as murine progenitor or stem cell marker due to their high clonogenic potential (Nijhof et al., 2006). In the upper part of the HF a quiescent population can be found, which express additionally lrig1. The sebaceous gland, belonging to the HF unit and also named as pilosebaceous tract, has his own stem cell compartment. Here stem cells were identified as CD34 negative, K14 positive and positive for the transcriptional repressor, Blimp1 (Ghazizadeh and Taichman, 2001; Horsley et al., 2006) (Figure 2). This shows that there are multiple stem cell populations in the HF, but it is still elusive if they act independently or if they are organized in a hierarchical manner.

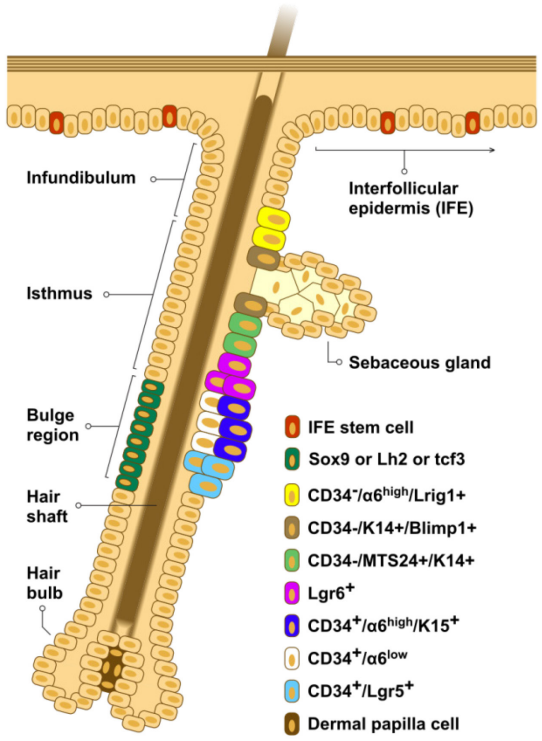

Figure 2: Schematic representation of stem cells in the murine hair follicle. Summary of suggested stem cell marker in the murine hair follicle. There are distinct stem cell populations and yet it has not been resolved if they act independently or in an organized hierarchical manner. Figure modified from (Boehnke et al., 2012).

Importantly, the markers of the mouse HF stem cells could not be detected in the human HF. Instead CD200 was suggested as marker for stem cells in the human bulge, as well as follistatin and the frizzled homolog 1 (Ohyama et al., 2006). This demonstrates that marker characterizing stem cells are different in mouse and human, suggesting that also the regulation may be different. This is substantiated by obvious differences between the

structure of mouse and human skin. Not only the HF density is higher in mouse skin, also the structure and the cycling time of the HF differs. For example are human scalp hair follicles significantly larger than hair follicle in mice. And the growth cycle of the human hair follicles takes years rather than weeks like in mice. Moreover, in mouse hair follicle growth cycling is continuously and hair follicles are highly synchronized for the first two cycles while in human hair follicle cycle independent of each other (Cotsarelis, 2006; Porter, 2003).

1.2.2 The interfollicular epidermis

Despite the fact that earliest studies of skin homeostasis were done in the mouse interfollicular epidermis (IFE), little is known about stem cells in the IFE. Lineage tracing revealed that there is a distinct reservoir of stem cells in the IFE, but after injury also bulge stem cells are able to contribute to the regeneration of the IFE (Ito et al., 2005; Levy et al., 2005). However, also cells of the IFE contribute to the reepithelialized epidermis and bulge-derived cells in the reepithelialized epidermis did not, or at least only very few cells, persist in the regenerated epidermis (Ito et al., 2005; Levy et al., 2005).

Stem cells in the IFE are still difficult to identify. This is mainly because of the lack of definitive markers. Several studies suggested that 1-10% of the basal cells are stem cells (reviewed in (Kaur, 2006)). In mammals many adult stem cells are considered as rarely dividing or slowly cycling cells (Arai et al., 2004; Cotsarelis et al., 1990). Therefore, stem cells can be identified functionally as label-retaining cells (LRCs) (Bickenbach, 1981). This could be first shown *in situ* in the murine IFE; slow cycling cells were able to maintain a DNA label for prolonged periods (Bickenbach, 1981). Young mice were given a pulse with radioactive H^3-thymidine or later with 5-bromo-20-deoxyuridine (BrdU), which is incorporated into their DNA during the high proliferation in this developmental phase of the epidermis. Subsequently, the chase period started and no label was administered for 4-6 weeks. During that time the DNA label is diluted in a proliferation-associated manner and only the infrequently dividing cells were able to keep the label over time (Bickenbach and Chism, 1998; Cotsarelis et al., 1990; Morris and Potten, 1999). These slowly cycling cells were identified as LRCs and were shown to behave like clonogenic cells *in vitro* (Bickenbach, 1981; Mackenzie and Bickenbach, 1982*)*. Moreover, a higher colony forming ability for isolated LRCs of the mouse skin was demonstrated (Morris and Potten, 1994). Several studies could show that LRCs can be detected in the murine IFE and the hair follicle bulge (Bickenbach, 1981; Cotsarelis et al., 1990; Morris et al., 1985). There are hints that also in the human IFE heterogeneity in the proliferative activity can be found. Early studies showed, that there are differences in the colony forming potential of cultured keratinocytes isolated

from the skin. They can be divided in holoclones, which have a high proliferation potential, paraclones with differentiated colonies and meroclones with intermediate characteristics (Barrandon and Green, 1987). Importantly, clonal assays of cultured basal keratinocytes isolated from the human IFE showed that cells which had the highest self-renewal capacity *in vitro* were slow cycling *in vivo* (Jones et al., 1995). Since labeling methods cannot be applied to human skin, this approach was further developed in a human in vitro 3D- organotypic skin model (Muffler et al., 2008). Normal human keratinocytes are able to incorporate nucleotide analogues like iododesoxyuridine (IdU) and to be subsequently cultivated for long-term in OTCs. It was shown that LRCs could be identified in the epidermal basal layer in OTCs (Muffler et al., 2008) (Figure 3 A). However, using nucleotide analogues such as IdU, does not allow isolation of vital LRCs. This is hampered due to the necessary use of fixation methods to visualize the label. This problem could be bypassed by the generation of a tissue-specific Histone 2B-GFP (H2B-GFP)-fusion construct controlled by a tertracycline-responsive regulatory element (Tet-Off) (Tumbar et al., 2004). Tumbar et al. engineered a transgenic mouse with an H2B-GFP tet-off controlled reporter under the control of a keratin 5 (K5) promoter (Tumbar et al., 2004). In order to isolate and characterize LRCs from the mouse epidermis pulse-chase experiments were performed using Doxycycline (Dox) in the drinking water. After a chase period of 4 weeks, with the presence of Dox, <1% of the bulge cells could be detected as label-retaining cells (Tumbar et al., 2004).

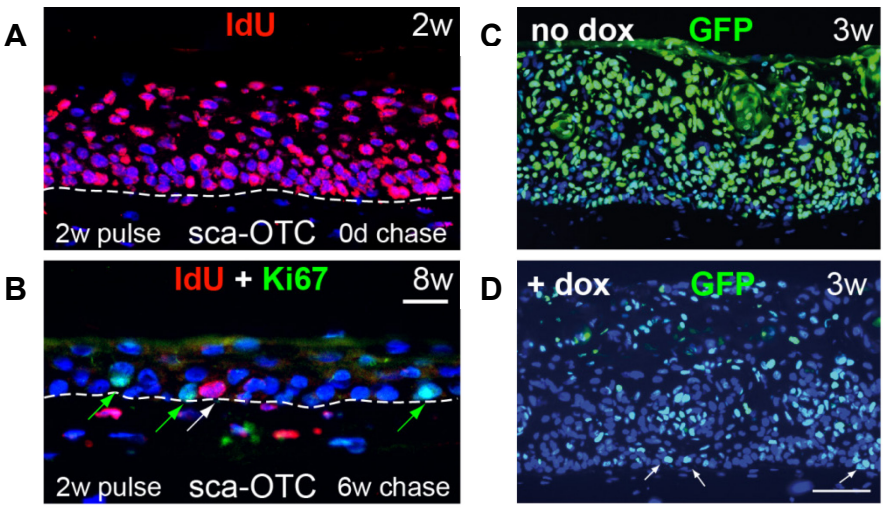

Figure 3: Detection of label-retaining cells (LRCs) in 3D organotypic cultures (OTCs). (A) Normal human keratinocytes after a pulse of 2 weeks with the nucleotide analogue IdU. All cells are labeled (in red). Figure from (Muffler et al., 2008)(B) LRCs could be detected in the basal layer of the epidermis after a chase period of 8 weeks (8w). Figure from (Muffler et al., 2008). (C) 3 week old OTC of HaCaT-ras II4 Tet-Off-H2B-GFP cells under the absence of Dox. All cells remain GFP-positive (in green). Figure from (Falkowska-Hansen et al., 2010) (D) After a chase period of 3 weeks (3w) LRCs can be identified and localized in the basal layer. Figure from (Falkowska-Hansen et al., 2010).

To apply this approach for human cells, a lentiviral-based vector harboring a bicistronic expression cassette was developed allowing transducing the whole regulatory Tet-Off-H2B-

GFP unit in a single step (Falkowska-Hansen et al., 2010). The vector was successfully introduced into human immortal and malignant keratinocytes (HaCaT and HaCaT-rasII4) by viral infection.

Furthermore, it was shown that by using HaCaT-ras II4 Tet-Off-H2B-GFP cells on OTCs the H2B-GFP expression was sustained also under 3D conditions (Figure 3 C). Moreover, it was demonstrated that the cells remained responsive to Dox. The OTCs were cultivated for one week in the absence of Dox in the culture media, this allows the expression of GFP (pulse period). After the addition of Dox to the culture medium for the following weeks, the reporter is turned off and the H2B-GFP expression is declining in all proliferating cells and only slow-cycling cells are able to keep the label (chase period) (Figure 3 D). These slowly cycling, H2B-GFP LRCs, could be successfully detected in the basal layer in OTCs of HaCaT-ras II4 H2B-GFP cells (Falkowska-Hansen et al., 2010) (Figure 3 D).

In the literature several markers for stem cells in the IFE are suggested. The expression of high levels of β1 integrin of human keratinocytes was one of the first marker characterized *in vitro* (Jones and Watt, 1993). These β1 integrin^{high} expressing cells showed higher colony forming ability and better adherence to ECM proteins, like type IV collagen and fibronectin (Jones and Watt, 1993). Also in the human IFE *in vivo* β1 integrin^{high} expressing keratinocytes could be detected at the tips of the dermal papilla from several body sites (Jensen et al., 1999). However, there are high numbers of integrin-bright basal cells, between 25– 50%, depending on body site (Jones et al., 1995). Therefore other markers need to be taken into account for the identification of stem cells. Another suggested marker, which was co-expressed with β1 integrin^{high}, was the Notch ligand delta like 1 (DLL1) (Lowell et al., 2000). There was enhanced Delta1 expression above the dermal papillae. Interestingly, it was shown that if Delta1 was over-expressed in a population of keratinocytes, there was no change on the proportion of stem cells, but neighbouring keratinocytes were driven to entry into the transit amplifying compartment and to differentiate. Therefore Delta1 expression of epidermal stem cells was suggested to block Notch signaling in order to prevent differentiation of themselves and to influence the fate of adjacent keratinocytes (Lowell et al., 2000). Another potential marker which is co-expressed with high levels of β1 integrin was the melanoma chondroitin sulphate proteoglycan (MCSP). However, the combination of β1 integrin^{high} and MCSP did not further increase the colony forming ability as with β1 integrin^{high} alone. But the expression of MCSP was shown to be a marker for mitotically inactive cells and promoting cell-cell adhesion (Legg et al., 2003). On the basis of DLL1 and MCSP expression Watt et al. performed single-cell expression profiling of these cells. These studies suggested Lrig1 as potential stem cell marker, which is important for the

quiescent state of the stem cells. Over-expression of Lrig1 in keratinocytes showed a reduced capacity of proliferation, but did not influence the clonal growth capacity. It was suggested that Lrig1 acts through the downregulation of the EGF receptor responsiveness and a negative regulation of myc (Jensen and Watt, 2006). Lrig1 was also found to be expressed at the top of rete ridges which also express MCSP, DLL1 and β1 integrin^{high} (Jensen and Watt, 2006). Further analysis on the basis of single cell expression discriminated by DLL1 expression suggested the transmembrane glycoprotein, CD46, as new epidermal stem cell marker (Tan et al., 2013). CD46 was also shown to colocalize with β1 integrin and restricted to basal keratinocytes in human skin (Tan et al., 2013). CD46 knockdown experiments further showed a reduction in the growth rate and adhesiveness of these cells as well as an impaired spreading of the cells (Tan et al., 2013). Therefore CD46 could increase the adhesion of the stem cells to basement membrane in the IFE (Tan et al., 2013). Notably, single cell expression profiling of human keratinocytes did not always show an overlap of expression of DLL1, Lrig1, MCSP and β1 integrin^{high} (Jensen and Watt, 2006). However, cells isolated on the basis of these markers had a greater colony forming efficiency in 2D (Tan et al., 2013). In addition, there are also other markers suggested for epidermal stem cells. Kaur et al. demonstrated that keratinocytes isolated from neonatal human and adult murine skin on the basis of high expression of α_6 integrin and low expression of the transferring receptor CD71 represent a quiescent subpopulation (Li et al., 1998). Interestingly, cells with α_6^{bri} and CD71^{dim} expression were detected at the bottom part of the rete ridges in human IFE. Thus these cells were located at the opposite site of the rete ridge as described for β1 integrin^{high} expression (Muffler et al., 2008). Importantly, it was shown that α_6^{bri} and CD71^{dim} expressing cells had the greatest intrinsic tissue-regenerative capacity when transplanted on de-epithelialized rat tracheas (Li et al., 2004; Schluter et al., 2011). Recently, also the Wnt inhibitor, WIF1, was reported as interfollicular stem cell marker and seems to inhibit cell cycle progression in the presence of Wnt ligands (Schluter et al., 2013). Moreover, LRCs in OTCs showed co-expression of WIF1 (Schluter et al., 2013). Taken together, a number of markers are described. It remains unclear which of these markers indeed refers to stem cells and accordingly where the stem cells are located within the IFE. Therefore, the obvious lack of a unifying model to describe the regulation of stem cells in the IFE underlines the need for further investigations in order to clarify the crucial parameters.

1.3 Homeostasis of the skin

Two different models have been proposed for epidermal regeneration. So far the prevailing model for epidermal maintenance was the hierarchical model. This model suggests that the tissue is organized in epidermal proliferative units (EPUs). These EPUs comprise a LRC,

which divides asymmetrically, giving rise to a new stem cell and a short-lived transit-amplifying cell (TAC). The population of TACs leaves the basal layer after 4-6 cell cycles and pass through a differentiation program thereby generating columnar units (Potten, 1974). The number of cell divisions of TACs is thought to be limited due to an internal ‘‘memory’’ prior entering terminal differentiation (Potten, 1981; Strachan and Ghadially, 2008) (Figure 4 A). Nevertheless there are also data which are inconsistent with the hierarchical model. For instance, in various studies LRCs in the IFE could be detected rarely and not that often as expected by the hierarchical model (Allen and Potten, 1974; Braun et al., 2003; Potten, 1974). Furthermore, up to now little is known about the contribution of LRCs to the homeostasis due to the lack of further characterization by transplantation assays. Therefore, *in vivo* lineage-tracing was chosen as a fundamental tool to investigate the fate of individual stem cell and its descendants. To mark a cell and its progeny inducible genetic labeling was applied (Alcolea and Jones, 2013; Clayton et al., 2007; Jones et al., 2007). These studies were interpreted that the basal cell layer of the IFE is composed of a single type of proliferative progenitors with random fate choice, termed as stochastic model (Figure 4 B). All basal cells can have three different outcomes with random choice upon cell division, either two differentiated daughters, two undifferentiated progenitors, which remain in the basal layer and continue to divide, or one of each (Clayton et al., 2007; Doupe et al., 2010; Lim et al., 2013) (Figure 4 B). Long-term homeostasis is ensured through balanced symmetrical cell divisions. Importantly, the stochastic model cannot exclude the existence of a LRC population, assuming that these stem cells make only minimal contribution to epidermal homeostasis and are mainly activated during epidermal wounding (Clayton et al., 2007; Mascre et al., 2012).

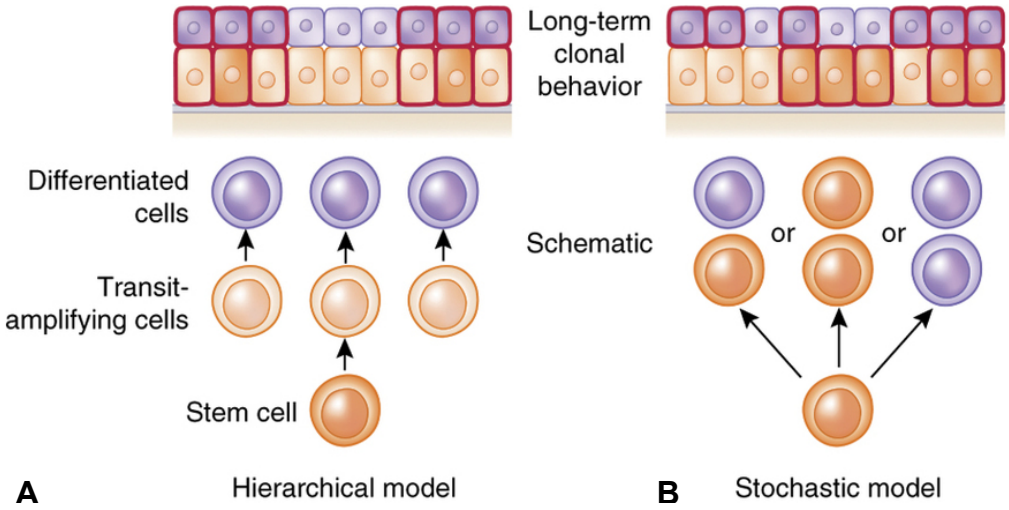

Figure 4: Two models for epidermal homeostasis. (A) In the hierarchical model the epidermis contains a stem cell which rarely divides and gives raise to the rapidly proliferating transit amplifying (TA) cells. They are believed to undergo a limited number of cell divisions before they terminal differentiate. (B) The stochastic model based on lineage tracing suggests that cycling basal keratinocytes can generate three different outcomes: both remain proliferating (in orange); both are differentiating (in purple) or one is differentiating and one remains proliferative. Figure from (Hsu et al., 2014).

So far the stochastic model is only described in mouse skin (Clayton et al., 2007; Gomez et al., 2013; Lim et al., 2013; Mascre et al., 2012). Therefore, the question remains if also the human IFE is maintained by a single type of proliferating cells as suggested by the stochastic model. The situation could be different for the human IFE which has not only many more layers of keratinocytes, but also its basal layer is undulating and tightly connected with the dermis through rete ridges (RR) and dermal papillae (Kanitakis, 2002). Notably, there are also rete ridge-poor parts in human skin, like e.g. human breast skin. Moreover, the density of HF is greatly reduced making the IFE predominant in the human skin (Figure 5).

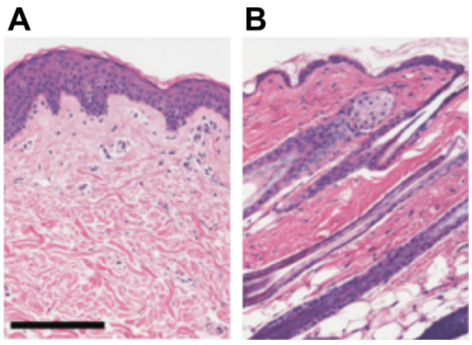

Figure 5: Comparison of normal human and normal mouse skin. (A) Human epidermis is generally thicker and comprises 6–10 cell layers. Furthermore the IFE is predominant in human skin and contains less hair follicles. (No hair follicles are present in this image) (B) The mouse IFE has only three cell layers and has no rete ridges. Mouse epidermis contains only short interfollicular regions with much more hair follicles. Figure from (Gudjonsson and Elder, 2006).Scale bar: 100µm.

1.4 Stem cell niche

Studies on stem cells from diverse systems have shown that stem cells reside in a dynamic and specialized microenvironment often referred to as stem cell niche. The maintenance and survival of stem cells is controlled by extracellular cues from the surrounding microenvironment as well as by intrinsic genetic programs within the stem cell (Fuchs et al., 2004; Jones and Wagers, 2008; Watt and Driskell, 2010). Obviously, epidermal stem cells need an appropriate environment and are dependent on a niche, since they are losing their “stemness” in culture and thus cannot be cultivated for long-term. Studies in OTCs also showed that without the supporting fibroblasts in the dermal part, long-term maintenance of the epithelium is not possible (Boehnke et al., 2007). There is growing evidence that especially the ECM may play an essential role in the stem cell niche, because it can directly or indirectly regulate the maintenance, proliferation, self-renewal and differentiation of cells (Lu et al., 2012). The expression of β1 integrin^{high} expression, which is suggested as epidermal stem cell marker, (Jones et al., 1995; Jones and Watt, 1993; Webb et al., 2004) lead to a higher adhesiveness of stem cells to ECM proteins, e.g. fibronectin and type IV collagen (Jones et al., 1995). Integrins have also the ability to deliver signals into the cell or

from the cell to the ECM (Hynes, 2002) and can enhance the response to growth factors (Brizzi et al., 2012). In accordance with this, also HF bulge stem cells and mouse epidermal LRCs express higher levels of ECM genes, like different collagens, tenascin C and fibulin 1 (Morris et al., 2004; Tumbar et al., 2004). The functional consequences of a distinct ECM protein expression are poorly understood. The ECM could not only serve as anchor for stem cells it could be important for the cell-cell communication and intrinsic regulatory mechanisms. For instance, reduction of Integrin expression drives the cells into differentiation (Grose et al., 2002; Watt, 2002). Furthermore, β1 integrin is essential for spindle orientation along with asymmetric cell division (Lechler and Fuchs, 2005).

1.5 Studying epidermal stem cells

For obvious ethical reasons human epidermal stem cell biology cannot be studied *in vivo* but requires appropriate *in vitro* experimental models. To investigate complex biological processes of the skin *in vitro* 3D organotypic culture systems were developed. Organotypic coculture systems are produced by seeding human keratinocytes onto a dermal equivalent which contains human fibroblasts. 3D organotypic cultures are also known as skin equivalents (Boehnke et al., 2007). The advantage of OTCs is the air exposed cultivation of the keratinocytes hence inducing the tissue specific differentiation process and the development of a terminal differentiated epithelium. First attempts of successful OTCs were described by Bell and colleagues (Bell et al., 1981). The dermal part, called dermal equivalent, can be prepared according to various principles. There are dermal equivalents made up of e.g. collagen seeded with dermal fibroblasts (Bell et al., 1981; Fusenig et al., 1980; Stark et al., 2004) or by de-epidermized dermis (DED) (Ponec et al., 1988; Prunieras et al., 1983). However one major drawback of skin equivalents based on e.g. type I collagen hydrogels is the early degeneration due to high shrinkage and decreased stability of the OTCs. These models are therefore not useful for long-term studies. To investigate epidermal stem cell biology, OTCs with an extended lifespan enabling long-term studies on skin regeneration and homeostasis are necessary. This was fulfilled by the development of DE´s which are reinforced with scaffold and colonized with human skin fibroblasts (Figure 6) (Stark et al., 2006; Stark et al., 2004). Also DEs based on a primary human fibroblast-derived dermal matrix are suitable for long-term studies. In this approach dermal equivalents are generated solely by fibroblasts.

Since fibroblasts are able to synthesize, remodel and maintain all ECM components by themselves human fibroblasts were cultivated without any addition of collagen or a scaffold

and generate a complex extracellular matrix largely similar to the dermis in the human skin (Berning et al., 2015; El Ghalbzouri et al., 2009).

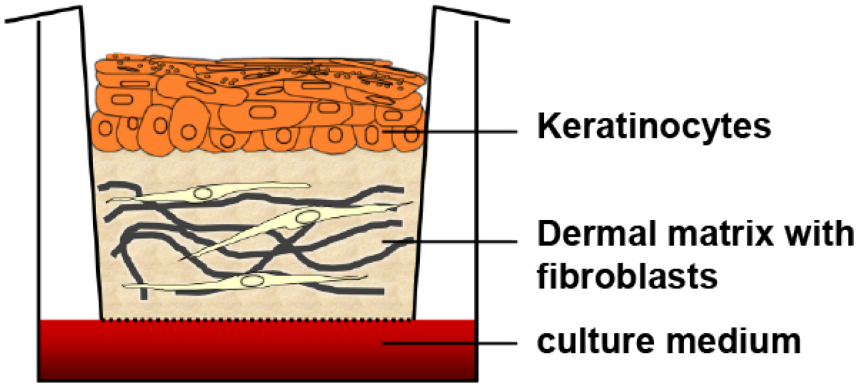

Figure 6: Schematic illustration of a skin equivalent. The dermal equivalent is reinforced with a scaffold and suspended with fibroblasts. Keratinocytes are seeded on top and cultivated air-exposed.

1.6 Aim

Despite more than 30 years of research on epidermal stem cells, stem cells in the human interfollicular epidermis have yet to be identified. This is mainly because of the lack of definitive markers. Stem cells play an essential role for maintaining homeostasis in the epidermis. Because stem cells rarely divide, they can be identified functionally as label-retaining cells (LRCs). However, the role of LRCs for tissue homeostasis is still elusive. Therefore, there is a strong need to isolate and characterize LRCs from the human epidermis.

Since investigations on human skin are very limited and LRC-detection with DNA labels cannot be applied to humans, pulse-chase experiments were further developed in a human in vitro 3D organotypic skin model (Muffler et al., 2008). Normal human keratinocytes are able to incorporate nucleotide analogues like IdU and can be subsequently cultivated in long-term skin OTCs which mimics the human skin under controlled *in vitro* conditions. It was shown that LRCs could be identified in the epidermal basal layer of the epidermis (Muffler et al., 2008). However using nucleotide analogues such IdU, does not allow isolating vital LRCs. This is hampered due to the necessary use of fixation methods to visualize the label.

To circumvent this problem and to detect viable LRCs in the epithelium, alternative methods were established. With the development of an inducible Tet-Off-H2B-GFP lentiviral reporter vector the detection and isolation of living label-retaining cells became possible (Tumbar et al., 2004). Falkowska-Hansen et al. were able to infect immortal and tumorigenic keratinocytes with an similar one-step vector system and to perform pulse-chase experiments to identify LRCs (Falkowska-Hansen et al., 2010). Up to now this approach was not used for human normal keratinocytes (NHEK) in order to detect LRCs. Therefore, the aim of this study was to establish the conditions to infect human adult keratinocytes with this H2B-GFP lentiviral vector, to perform pulse-chase experiments in long-term skin equivalents (OTCs) in order to generate and isolate label-retaining cells (LRCs). Moreover, the regulation of LRCs and new markers for the identification of LRCs, the potential stem cell, should be explored. In this respect the transcriptional analysis from isolated LRCs would promise deeper insight into their regulation and functionality.

2 Material and Methods

2.1 Material

2.1.1 Cells

Normal human keratinocytes and dermal fibroblasts

Primary keratinocytes and primary fibroblasts were routinely isolated in our laboratory from explant cultures of human skin. In this thesis keratinocytes from three different donors and fibroblasts from one donor were used. The internal name of the keratinocytes and fibroblasts is the date of isolation (Table1). The skin samples were kindly provided by Dr. Doebler (ATOS Klinik, Heidelberg) and the women's Hospital in Tübingen with the consent of the Ethics Committee.

internal name	age	gender	area
Fib1 04.04.07	23 years	female	n/s
KH1 04.04.07	23 years	female	n/s
KH17.04.07	43 years	female	breast
KH19.04.12	49 years	female	breast

Table 1: Normal human keratinocytes (KH) and fibroblasts from primary human explants.

HEK293T cells

HEK293T cells were kindly provided by the group of Dr. Jörg Hoheisel.

2.1.2 Cell culture supplements and media

Cell culture supplements

Article	*Supplier*
Adenine	Sigma Aldrich, Steinheim, Germany
Aprotinin (Trasylol®) (1000 I./E./ml)	Bayer Vital, Leverkusen, Germany
Ascorbic acid stock: 50 mg/ml fdmSE medium: 50 µg/ml	Sigma-Aldrich, Taufkirchen, Germany
Choleratoxin	Sigma Aldrich, Steinheim, Germany
DermaLife	LifeLine, CA, USA
DMEM (Dulbecco´s Modified Eagle´s Medium)	Cambrex (Lonza), Verviers, Belgium
EDTA (Ethylenediaminetetraactetate) (0.05% (w/v)) in PBS+ 1 µl/ml phenolred	Serva Electrophoresis GmbH, Heidelberg, Germany
EGF (Epidermal growth factor)	1 ng/ml, Sero-med, Wien, Austria
F12	Cambrex (Lonza), Verviers, Belgium
FCS (Fetal calf serum)	Invitrogen Gibco, Darmstadt, Germany
FGF (Fibroblast growth factor)	Invitrogen Gibco, Darmstadt, Germany
Glycerol	Carl Roth, Karlsruhe, Germany
Hydrocortisone	Sigma Aldrich, Steinheim, Germany

Penicillin / Streptomycin (10U/ml; 10µg/ml)	Biochrom, Berlin, Germany
Penicillin / Streptomycin / Amphotericin	Cambrex (Lonza), Verviers, Belgium
rhInsulin	Sigma Aldrich, Steinheim, Germany
TGF-β1 human recombinant 10 µg/ml dissolved in 4mM HCl with 1mg/ml BSA, OTC medium: 1 ng/ml	R&D Systems, Minneapolis, USA, 240-B/CF
Thrombin S lyophilized 10 I.E./ml in PBS + CaCl2 (5,88 mg/ml)	Baxter, Unterschleißheim, Germany
Tissucol Fibrinogen 1.0 lyophilized, thermo inactivated	Baxter, Unterschleißheim, Germany
Trypsin 0.4% + 0.1% in PBS/1 µl/ml Phenolred	Roche Biochemica, Mannheim, Germany

Cell culture media

Article	*Ingredients*
D10	DMEM + 10% FCS + 1% Penicillin (10U/ml)/Streptavidin (10µg/ml)
FADcomplete	1:1 DMEM / F12, 5 % FCS, 1 % Pen / Strep, 5mg / L Insulin, 10^{-10}M Choleratoxin, 1µg / L rhEGF, 24µg / L Adenin, 0.4µg / mL Hydrocortison
fdm OTCs Medium	1:1 DMEM / F12, 10 % FCS, 1 % Pen / Strep / Amph., 200 µg / mL Asc. Acid, 1 µg / mL TGFβ, 2.5 ng / mL EGF, 5 ng / mL FGF, 5 µg / mL rhInsulin
Sca OTC Medium	1:1 DMEM / F12, 10 % FCS, 1 % Pen / Strep / Amph., 200 µg / mL Asc. Acid, 10^{-10}M Choleratoxin, 1µg/l rhEGF, 250U/ml Aprotinin
Freezing Medium	DMEM containing 20% FCS and 10% (v/v) Glycerol
rFAD	1:1 DMEM / F12, 10 % FCS, 1 % Pen / Strep, 200 µg / mL Asc. Acid, 0.4 µg / mL Hydrocort., 10^{-10} M Choleratoxin
Trypsin / EDTA	0.05%Trypsin/ 0.025% (w/v) EDTA in PBS with Phenolred

2.1.3 Antibodies, kits and primer

Primary antibodies

Epitope	Species	Dilution	Supplier / Order no.
Collagen VII	rabbit	1:5000	L.Bruckner-Tudermann, Freiburg, Deutschland
Decorin	rabbit	1:200	H. Kresse,Münster
Desmoglein 1+2	mouse	1:10	Progen 61002
E-cadherin	mouse	1:20	Progen 10028
Fibronectin	rabbit	1:200	Telios
Filaggrin	Mouse	1:100	Acris FLG01
Involucrin	Mouse	1:100	Sigma I9018
Keratin 10	Mouse monoclonal	1:10	Progen 11414
Keratin 14	mouse	1:100	Abcam 7800
Ki67	Mouse monoclonal	1:20	Dako M724029-2
Ki67	rabbit	1:400	Abcam 15580
Integrin α6	rat	1:500	Progen 10709
Integrin α6	mouse monoclonal	1:20	Millipore CBL458
Integrin α6 PE conjugated	monoclonal	1:100	Millipore CBL458P
phospho-Smad3	rabbit monoclonal	1:100	Abcam 52903

Thrombospondin	mouse	1:20	Immunotech,Marseille,France 0148
Vimentin	guinea pig	1:100	Progen GP53

Secondary antibodies

Host species	Reactive species	Conjugated with	Dilution	Supplier / Order no.
donkey	rabbit	DyLight488	1:500	Invitrogen A21206
goat	rabbit	Cy3	1:500	Jackson 111-165-003
goat	mouse	Alexa488	1:500	Invitrogen A11029
goat	mouse	Cy3	1:500	Jackson 115-165-068
goat	rat	Alexa488	1:500	Jackson 112-545-003
donkey	guinea pig	Cy3	1:500	Dianova 706166148

Kits

Kits	*Supplier*
Färbekit Hämatoxylin & Eosin (H&E)	Morphisto, Frankfurt, Deutschland
Mycoplasma Detection Kit	Sigma-Aldrich, Taufkirchen, Germany
QIAshredder	Qiagen, Hilden, Germany
RNA Isolation Kit ARCTURUS Pico Pure	Lifetechnologies, Darmstadt, Germany
RNase-free DNase Set	Qiagen, Hilden, Germany
RNeasy Mini Kit	Qiagen, Hilden, Germany

Primer

Gene	*Primersequenz (left)*	*Primersequenz (right)*
COL1A1	gaagagaaggccccgttg	cggtagcctttaggtccgata
Decorin	gggctggcagagcataagta	ccttttggtgttgtgtcca
Fibronectin	gaactatgatgccgaccagaa	ggttgtgcagatttcctcgt
Fibulin 1	gctggaggagctgcactg	tccccagcagacagcaat
Fibulin 2	caggtggcctctaacaccat	gcttgcagggtccattgt
GAPDH	agccacatcgctcagacac	gcccaatacgaccaaatcc
HIST14H4	aggctggagtcgttggtg	actttggtcctgcttcttgg
HIST1H2BG	cagtttggctaacgtggttaaa	ccgagtctctgggatgacac
IGFBP4	gagatcgaggccatccag	cgaattttggcgaagtgc
IL6	ccagagctgtgcagatgagt	ctgcagccactggttctgt
Keratin 14	cctctcctcctcccagttct	atcgtgcacatccatgacc
Lumican	gaaagcagtgtcaagacagtaagg	ggccactggtaccaccaa
P21	aggtccccctggaaagaa	catctgatccagggtttcca
Smad3	gtctgcaagatcccaccag	agccctggttgaccgact
Smad7	cgatggattttctcaaaccaa	aggggccagataattcgttc
Snai2	tggttgcttcaaggacacat	gcaaatgctctgttgcagtg
Tenascin C	ggaatacacactgagaatctttgc	aagtctcttggagaatcgaggtc
TGFβ	gcagcacgtggagctgta	cagccggttgctgaggta
TGFβR1	ctgctcctcctcgtgctg	ggtggcagaaacactgtaacg
TGFβR2	tggtgctctgggaaatgac	caccttggaaccaaatggag
TGFβR3	cagatggatgccagcaca	tgatgttgtgtccttgctttg
THBS1	gctccggtacacacagcaa	agggtcagagatcagctaggc
TIMP2	gaagagcctgaaccacaggt	cggggaggagatgtagcac
Vimentin	aaagtgtggctgccaagaac	agcctcagagaggtcagcaa

2.1.4 Technical equipment and consumables

Name	*Supplier*
CASY® cell counter with TTC analysis system	Schärfe System, Reutlingen, Germany
Cell culture incubator HeraCell 240 and 240i	ThermoScientific, Schwerte, Germany
Cell Freezing machine Kryo 10 Series III	Planer, Sunbry-on-thames, UK
Centrifuge 5417 R (for Eppendorf tubes)	Eppendorf, Wesseling-Berzdorf, Germany
Centrifuge Heraeus Laborfuge 400	Thermo Scientific, Fermont, USA
Cryo boxes	Nunc, Wiesbaden, Germany
Cryostat CM3050S Cryotome	Leica, Wetzlar, Germany
Digital Timer, Neolab 2-2002	neoLab, Heidelberg, Germany
Dispensette	Brand, Wertheim, Germany
ELISA Reader Multiskan FC	Thermo Scientific, Schwerte, Germany
Foreceps Dumont	Dumont, Montignez, Switzerland
Gammacell 1000 (137Cs)	Atomic Energy of Canada Limited, Ontario, Canada
Gasprofi 1 micro WLD-Tec	neoLab, Heidelberg, Germany
Laboratory Scale Delta Range PC440	Mettler-Toledo, Gießen, Germany
Lab pipettes, Gilson Pipetman, 10-1000µL	Gilson, Mannheim, Germany
Light Cycler 480 II	Roche Mannheim, Germany
Liquid nitrogen dewar	KGW Isotherm, Karlsruhe, Germany
Micro scales	Sartorius, Göttingen, Germany
Microscope AX-70 (fluorescence) F-View II CCD-camera	Olympus, Hamburg, Germany
Microscope IX-70 (cell culture) AxioCam ERc 5s	Olympus, Hamburg, Germany
Microscope BX-51 (Histology) Color-View I camera	Olympus, Hamburg, Germany
Minifuge RF	Heraeus Intruments, Osterode, Germany
Microcentrifuge II, GMC-060	Daihan Labtech, Corea
NanoDrop 1000	Thermo Scientific, Dreieich, Germany
Nitrogen tank CHRONOS	Messer, Griesheim, Germany
PCR machine DNA Engine Dyad Peltier Thermal Cycler	BioRad, Munich, Germany
pH Meter ph522	WTW, Weinheim, Germany
Pipetboy acu	IBS Integra Biosciences, Zizers, Switzerland
Pipetboy Comfort	IBS Integra Biosciences, Zizers, Switzerland
Pipettes mline	Biohit, Göttingen, Germany
Serological pipettes Stripette, 10-50ml	Corning, Amsterdam, Netherlands
Shaker KS250 basic	IKA Labortechnik, Staufen, Germany
Sliding microtome Leica SM2010 R	Leica Biosystems, Nussloch, Germany
Sterile tissue culture hood, HeraSafe HS18	Heraeus Instruments, Hanau, Germany
Thermomixer 5436	Eppendorf, Hamburg, Germany
Tissue-Tek TEC Tissue Embedding Console	Sakura Finetek, Zoeterwoude, Netherlands
Tissue-Tek VIP 5 Jr. Vacuum Infiltration Processor	Sakura Finetek, Zoeterwoude, Netherlands
Vacuboy and VACUSAFE system	Integra Biosciences, Fernwald, Germany
Vortexer REAX 200	Heidolph Instruments, Schwabach, Germany
Water bath	Köttermann, Hänigsen, Germany

Consumables

Consumables	*Supplier*
6-well deep-well plates BioCoat™ (Scaffold -OTCs)	BD Biosciences, Heidelberg, Germany
6-well Falcon inserts 0.4µm, translucent, High pore density	BD Biosciences, Heidelberg, Germany
12-well deep-well ThinCert-plates (fdm OTCs)	Greiner Bio-One,Frickenhausen, Germany
12-well ThinCert 0.4µm, translucent	Greiner Bio-One,Frickenhausen, Germany
Cell culture dishes and plates, various sizes	BD Biosciences, Heidelberg, Germany
Cell culture tubes CELLSTAR 15ml-50ml	Greiner Bio-One, Frickenhausen, Germany
Cell Strainer 40 and 70µm	BD Bioscience, Heidelberg, Germany
Cover glasses, various sizes	Menzel, Braunschweig, Germany
Cryomold, various sizes	Sakura Tissue-Tek, Zoertewonde, Netherlands
Cryo tube TM Vials	Nunc, Wiesbaden, Germany
Filter tips, various volumina	Nerbe-Plus, Winsen/Luhe, Germany
Filter tips, Tip-One, various volumina	Starlab, Hamburg, Germany
Immersion Oil Immersol 518N	Zeiss, Jena, Germany
Liquid Blocker Pen	Daido, Sangyo, Tokyo, Japan
Microscope slides (Histobond®)	Marienfeld, Lauda-Königshofen, Germany
Microscope slides (uncoated)	Langenbrinck, Teningen, Germany
Object glasses (76x26mm)	Menzel, Braunschweig, Germany
Parafilm M	Bemis Plastic Packaging, Neenah, USA
Paraffin	Vogel, Gießen, Germany
PCR tube, 0.5ml	Eppendorf, Hamburg, Germany
Pipette tips, various sizes	Starlab, Hamburg, Germany
quadriPERM dishes	Greiner Bio-One, Frickenhausen, Germany
Safe-Lock tubes, 1.5ml	Eppendorf, Hamburg, Germany
Superfrost Plus slides	Menzel, Braunschweig, Germany
Syringe Luer Lock tip (5, 10, 30, 50ml)	Terumo, Leuven, Belgium

2.1.5 Buffer, solutions, chemicals and enzymes

Buffer and Turnkey Solutions

Buffer	*Ingredients*
Antibodybuffer	3% BSA/PBS-
Blockingbuffer (IIF and FACS)	3% BSA/PBS-
FACS Buffer	2%FCS/PBS-
Turnkey Solutions	**Company**
Aquaguard-1 and -2	PromoCell, Heidelberg, Germany
CASY® clean	Innovatis AG, Reutlingen, Germany
CASY® ton	Innovatis AG, Reutlingen, Germany
Dako Fluorescent Mounting Medium	DAKO, Glostrup, Denmark
dNTPs	Fermentas, St. Leon-Rot, Germany
Eukitt®	O.Kindler, FREIBURG, Germany

Chemicals

Name	*Supplier*
2-Propanol	Sigma Aldrich, Steinheim, Germany
Acetone	Sigma Aldrich, Steinheim, Germany
ß-mercaptoethanol	Sigma Aldrich, Steinheim, Germany
DAPI	Sigma Aldrich, Steinheim, Germany
Ethanol, absolute	Sigma Aldrich, Steinheim, Germany
Ethanol, denaturated	Berkel AHK Alkoholhandel, Berlin, Germany
Formaldehyde solution wt. 37%	Sigma Aldrich, Steinheim, Germany
Glycerol	Carl Roth, Karlsruhe, Germany
Hematoxylin/Eosin (H/E)	Carl Roth, Karlsruhe, Germany
Methanol	Sigma Aldrich, Steinheim, Germany
Normal goat serum	Dianova, Hamburg, Germany
Nuclease free water	Qiagen, Hilden Germany
PBS (Phosphate Buffered Saline)	Serva Electrophoresis, Heidelberg, Germany
PBS+ (PBS with MgCl2, CaCl2)	Serva Electrophoresis, Heidelberg, Germany
Polybrene	Santa Cruz, Heidelberg, Germany
Polyethylenimine	Polysciences, Eppelheim, Germany
Sodium butyrate	Sigma Aldrich, Steinheim, Germany
SYBR®Green	Invitrogen, Karlsruhe, Germany
Triton®X-100	Sigma Aldrich, Steinheim, Germany

Enzymes

Name	*Company*
DNA Polymerase I	Invitrogen, Karlsruhe, Germany
Reverse transcriptase	Quiagen, Hilden, Germany
Hot Start Taq Polymerase,Fermentas	St.Leon-Rot, Germany
RNase	Roche Applied Sciences, Mannheim, Germany
DNase	Roche Applied Sciences, Mannheim, Germany

2.1.6 Software

Software

Article	*Company*
Adobe CS5	Adobe Systems Incorporated
AxioVision Version 40V 4.8	Carl Zeiss Micro Imaging, Göttingen, Deutschland
Cell^D, Cell^F	Olympus, Hamburg, Deutschland
Chipster Version 3.1.1	Sourceforge.net
GraphPad Prism V 4.0	Statcon, Witzenhausen, Germany
ImageJ Version 1.4	Wayne Rasband, National Institute of Health, USA
Ingenuity IPA	Qiagen, Redwood, USA
LightCycler® 480 1.5.0. SP4	Roche Applied Sciences, Mannheim, Deutschland
Microsoft Excel 2010	Microsoft Corp., USA
Microsoft Power Point 2010	Microsoft Corp., USA
GraphPad Prism Version 4.0	Statcon, Witzenhausen, Deutschland
GenomeStudio	Illumina, Inc., San Diego, USA

2.2 Methods

2.2.1 Cellculture methods

2.2.1.1 *Cultivation and maintenance of human fibroblasts*

The cultivation of human dermal fibroblasts was in Dulbecco's modified Eagle's medium (DMEM) with 10% FCS and 1% Penicillin/Streptavidin (D10). The medium was exchanged three times per weeks. The cells were split at confluency (approx. every 10 days). For passaging the cells the medium was removed, the culture dish was rinsed with 5ml EDTA (0.05%) and incubated for 3 min with 0.1 % Trypsin / EDTA at 37°C. Finally to stop the trypsin-activity 2 volumes D10 was added to the cell suspension. Subsequently the cell suspension was counted with the CASY®-cell counter. The cells were seeded at a density of 6400 - 9500 cells per cm^2.

2.2.1.2 *Feeder cells for the cocultivation with keratinocytes*

To prepare feeder cells human dermal fibroblasts were cultivated and after trypsinization irradiated with 55Gy (Gammacell 1000). In this way they are mitotically inactivated and overgrowth of the fibroblasts is prevented. However the irradiated fibroblasts still have growth-promoting activity through the secretion of factors for keratinocytes. Feeder cells were seeded in FAD medium at a density of 3200 cells per cm^2. For optimal medium precondition keratinocytes were seeded earliest 24 hours after preparation of the feeder cells.

2.2.1.3 *Isolation, cultivation and maintenance of human keratinocytes*

Human adult keratinocytes were obtained from human skin biopsies. The biopsies were placed for 30 min in an antiseptic Betaisodona solution and then washed with PBS+. The epidermis is separated from the dermis by incubating the minced skin biopsie (0,5cm thick and 4cm long) in 0,5mg/ml Thermolysin over night at 4°C. To achieve a single cell suspension the epidermis was subsequently incubated in a 0.8% trypsin-EDTA mixture for 10 min at 37°C and then separated with the help of active pipetting. The reaction was stopped with FAD medium (2x times) before the cell suspension was filtered through a 70µm cell strainer. The cell strainer was washed several times with medium. Cells were counted with the CASY®-cell counter and seeded on feeder culture dishes (35000cells/cm^2). The keratinocytes were trypsinized and frozen in freezing medium at 80% confluency ($2x10^6$ cells/ml per tube, passage 1). After thawing keratinocytes were cultivated in tissue culture-

treated dishes either with feeder cells and FAD medium or without feeder cells in DermaLife medium. Keratinocytes were grown up to 80% confluency and then trypsinized. The cells were washed in EDTA (0.05%) followed by the incubation with EDTA (0.05%) for 3 min at 37°C. Feeder cells were detached by washing the plate with the preincubated EDTA solution, while the keratinocytes remain sticking on the culture dish. Subsequently the dish with EDTA was incubated for another 7 min at 37°C. In contrast to keratinocytes cultivated with feeder cells, the incubation step with EDTA to lose cell-cell contacts by the binding of calcium ions was not necessary when cultivating keratinocytes in DermaLife medium, since the medium contains low amounts of calcium and the cells are not tightly connected. To detach the keratinocytes the culture dish was incubated for 3 min with 0.4 % Trypsin / EDTA at 37°C. The separation of the cells was achieved by active pipetting. For the inhibition of trypsin twice the amount of FCS-containing medium was added. Cells were counted with the CASY®-cell counter. Confluency and appearance of the cells was determined with a phase contrast Olympus IX70 Inverted Microscope. Images were taken using an Axiocam ERc 5s (Zeiss) and computer processed using AxioVision (Zeiss MicroImaging).

2.2.1.4 *Stimulation of cells with TGFβ-1*

NHEKs were seeded in low-calcium medium (DermaLife) in a 6cm petridish. After 24h the medium was changed and the stimulation started with TGFβ. Therefore, the cells were supplied with DermaLife medium with 10pg/ml – 10ng/ml TGFβ-1. Samples were taken after 8 h, 24hrs, 48hrs, 3 d and 4d and the medium was replaced every 48h. As controls served unstimulated cells harvested at the same time points.

2.2.1.5 *Treatment of cells with Y-27632*

NHEKs were seeded either in low-calcium medium (DermaLife) or in calcium-containing FAD medium with 5% FCS and feeder fibroblasts in a 10cm petridish. NHEKs were supplied with medium containing 10µM Y-27632. Keratinocytes were grown up to 80% confluency and then seeded into a new dish.

2.2.1.6 *Proliferation Assay*

To examine the proliferation kinetics of keratinocytes proliferation assays were performed. The different treated cells were seeded on 24 well plate at a density of $2x10^4$ per well, then cultivated for 12 h until the first plate for the standard curve was harvested. Therefore the medium was removed and washed with PBS before stored at -20°C. The plates were

harvested 48 h, 72 h, 96 h. Every group was analysed in octuplicates. To measure the proliferation of the cells at each time point the DNA of the cells was stained. Therefore a lyse buffer (PBS + 0,1% TritonX-100) with SyBr-Green (1:2500) was prepared and 1ml was added into each well and incubated for 1 hour (in the dark at RT). The measurement was done with the Ascent 2.4 Flouroscan with the filter 485-538nm. The total cell number was calculated using the standard plate as reference, where a given fluorescent intensity is correlated with a defined cell number. To determine the proliferation rate in OTCs cryosections of the OTCs were stained with Ki67, a cellular marker for proliferation (staining protocol see 2.2.4.1.). For each sample, five representative images were captured with 20x magnification. The total cell number of basal cells and the number of Ki67-positive cells was determined. The result was expressed as mean ratio in percentage.

2.2.1.7 *Freezing and thawing of cells*

In order to prepare frozen cell stocks the cells are frozen in liquid nitrogen. After trypsinization the cells were counted with the CASY®-cell counter and then centrifuged for 5min at 1000rpm. The cell pellet was resuspended in freezing medium with a final cell concentration of $2x10^6$ cells per ml. The cryotubes were filled with 1ml of the cell suspension and after 30 min incubation at RT, placed in isopropanol filled cryoboxes and incubated for 1h at 4°C. This ensures a slow and gentle cooling process. Subsequently the cryoboxes were transferred to a -80°C freezer over night before they were long term stored in liquid nitrogen. For thawing a new cell stock, the cryotube was taken out of the liquid nitrogen and thawed in the water bath at 37°C. The thawed cell pellet was either resuspended in 5 ml of fresh medium (D10, FAD or DermaLife) and then transferred into a culture dish containing pre-warmed medium or directly transferred into the culture dish. The medium was exchanged one day after thawing.

2.2.1.8 *Mycoplasmtest*

For the rapid and reliable detection of mycoplasma a highly-sensitive PCR technology, the mycoplasma Detection Kit Venor®*GeM,* was used. For the detection of mycoplasma 1ml of the cell culture medium was taken. After a centrifugation step for 6 min with 12000rpm 900µL of the supernatant was removed. 100µl of the sample supernatant was incubated at 95°C for 10 min, followed by a briefly centrifugation for a few seconds to remove cellular debris. Per sample which was testet 2µL of the sample supernatant was added to the PCR reaction tube. The PCR was performed according to manufacturer's instructions. The PCR products were separated by electrophoresis in a 1,5% standard agarose gel. To visualise the DNA

fragments SYBR® Safe DNA Gel Stain was added. If the sample is positive for mycoplasma a distinct 265-278 bp band appeared. All cells used were regularly tested for mycoplasma.

2.2.1.9 *Cell pellets*

For the isolation of RNA the cells were trypsinized and then centrifuged for 5 min at 1000rpm. The cell pellet was resupended in 1ml PBS- and transferred into a 1.5ml Eppendorf tube. After another centrifugation step at 1000rpm for 5 min the supernatant was removed and the pellet was frozen in liquid nitrogen and stored at -80°C.

2.2.1.10 *Scaffold Based Long Term Organotypic cocultures (sca OTCs)*

For scaffold based dermal equivalents 6 well plates with cell culture inserts (0.4µm pore size, high pore density) were used. As scaffold served M3 saffold with a diameter of 21cm which was placed into the cell culture filter. To produce the DE fibroblasts were trypsinized and $1x10^6$ cells were used per DE. The fibroblasts were resuspended in FCS and the same amount of thrombin solution (10I.E./ml) was added. Subsequently 850µL of the thrombin/fibroblast mixture was seeded on top of the scaffold. Then 850µL of fibrinogen/PBS+ (1:1) was added to the thrombin/fibroblast solution and carefully mixed. The final concentration of fibrinogen was 2mg/ml and 2,5 I.E./ml Thrombin. For Polymerisation the DEs were placed to the incubator (5%CO_2, 37°C) for 30 min. Finally D10 medium containing ascorbic acid phosphate (1:1500) and 1ng/ml recombinant human TGF-β1 was added to the bottom well and on top of the DE. The DEs were cultivated for 4-7 days. Before the keratinocytes were seeded sterile glass rings were placed on top of the DEs and cultures were transferred into 6 well deep well plates. Additionally the medium was shifted to rFAD with ascorbic acid phosphate (1:1500) and aprotinin (Trasylol, 1:20). The keratinocytes were trypsinized as described and $1x10^6$ cells per culture in 1ml were seeded inside the ring on top of the DE. The cultures were kept submers for 48 hours until the rings were removed with sterile forceps and the air exposed cultivation started (day 1 of the cultures). The cultures were supplied with rFAD with ascorbic acid phosphate (1:1500) and a reduced aprotinin concentration (1:40). The medium was changed three times per week. For pulse-chase experiments Doxycycline (Dox, 1ng/ml, 1: 1000) was added to the culture medium after 14 days of cultivation for another 6-11weeks. Subsequently, the cultures were harvested or single- cell suspension of the OTCs was performed.

2.2.1.11 *Fibroblast-derived matrix Organotypic cocultures (fdm OTCs)*

Cell dervived matrices DEs were also prepared in 6 well or 12 well deep well plates with cell culture inserts (0.4µm pore size, high pore density). To achieve a cell derived matrices fibroblast are seeded multiple times and cultivated for 4 weeks in fdmDE medium (see 2.1.2). During this precultivation fibroblasts can synthesize, remodel and maintain ECM components and thereby create a cell derived matrix DE. First, fibroblasts are trypsinized as described and seeded with a density of $0{,}5x10^6$ cells (for 12 well cultures) or $1{,}5x10^6$ cells (for 6 well cultures) in one ml per insert. Multiple seeding occurred within one week, in total three times. Each insert has a final amount of $1{,}5x10^6$ (12 well plate) or $6x10^6$ (6 well plate) of fibroblasts. After the precultivation period in fdmDE medium (see 2.1.2) keratinocytes are seeded on top of the DEs. Therefore keratinocytes are trypsinized as describes above and the cell pellet with $0{,}25x10^6$ (12 well plate) or 1 $x10^6$ (6 well plate) is resuspended in 1ml of rFAD with ascorbic acid phosphate (AscP, 1:1500). The cultivation is without aprotinin, since the cell derived matrix prevents the invasion of the keratinocytes. The medium of the cmd DEs is shiftet directly before seeding of the keratinocytes. The skin equivalents are cultivated in rFAD with AscP (1:1500). Pulse-chase experiments were performed as described in 2.2.1.9.

2.2.1.12 *Single cell suspensions of OTCs*

To obtain a single cell suspension of the OTCs first the epidermis needed to be separated from the dermis. Therefore each culture was cut into small pieces and incubated with a freshly prepared Disapse II solution (1mg/ml) for 2 hours at 37°C. Subsequently the epidermis was peeled of the dermis with the help of sterile tweezers. The epidermis was cut into smaller pieces and transferred into a 50ml Falcon tube with prewarmed 0.4 % Trypsin / EDTA solution. The Falcon was incubated for 3 min at 37°C. To separate the cells properly active trypsination by pipetting the solution and chipping the Falcon was necessary. To stop the trypsin activity twice of the amount of D10 Medium was added to the cell/trypsin suspension and filtered through a 70µL cell strainer into a new 50ml Falcon tube. After washing the filter, the cell suspension was counted with the CASY®-cell counter.

2.2.1.13 *FACS Analysis or Sorting*

For FACS analysis the single cell suspensions of the OTCs (see 2.2.1.11) or cell suspensions of cell from culture dishes (for trypsination see 2.2.1.3) were spun down for 5 min at 1000rpm and resuspended in 1ml of PBS (up to $10x10^6$ cells/1ml) and then analysed. For FACS sorting the cells were resuspended in 500µL blocking solution (PBS with 3% BSA) and incubated for 15 min on ice, followed by the incubation of the conjugated antibody for 30

min on ice. Finally the suspension was centrifuged for 5 min at 1000rpm and the pellet was resuspended in 1ml FACS Buffer (PBS with 0,5% FCS). All samples were analyzed by flow cytometry (FACSCalibur) and FlowJo Software. For FACS sorting the samples were sorted by the FACS Core Facility of the Universitätsklinikum Heidelberg. The sorting was performed by the BD FACSAria™ III cell sorter. Cell suspension was mixed with 1 µL 7AAD or Propidium iodide (PI) for live staining of the cells. The cells were collected in 15ml Falcon tubes (up to $5x10^6$ cells) or in a 1.5ml Eppendorf tube (for small samples, below $5x10^4$ cells).

2.2.1.14 *Isolation of LRCs*

To isolate LRCs from OTCs the single cell suspension of the OTCs (see 2.2.11) was counted with the Casy cell counter and centrifuged for 5min at 1000rpm. The cells were resuspended in 500µL blocking solution (PBS with 3% BSA) and incubated for 15 min on ice, followed by the incubation with an anti-CD49f Phycoerythrin (PE) conjugated Antibody, clone 4F10 (Millipore), for 30 min on ice. Finally the suspension was centrifuged for 5 min at 1000rpm and the pellet was resuspended in 1ml FACS Buffer (PBS with 0,5% FCS). LRCs were sorted for PE (α6 integrin) and GFP- positive cells. Basal cells were sorted for PE (α6 integrin) positive and GFP- negative cells. Suprabasal cells were sorted for PE (α6 integrin) negative and GFP- negative cells.

2.2.2 Processing of tissue

2.2.2.1 *Preservation of OTCs*

To further analyse the OTCs one half of the cultures was analysed histologically and the other half was analysed with immunofluorescence stainings. For the histological analysis the OTCs were fixed for at least 24h in a ready to use solution “special fixative for anatomy and histology” (Mephisto). Afterwards the OTCs were dehydrated in increasing concentrations of ethanol (70, 80, 90 and 96%) and then transferred into xylene. Finally the cultures were embedded in paraffin wax and stored at room temperature. The paraffin embedded samples were cut with a sledge microtome with a thickness of 4µm.

For immunofluorescence analysis the cultures were embedded in Tissue Tek and frozen in the gas phase of liquid nitrogen. Frozen tissue sections with a thickness of 6-8µm were made by using a Cryotome. The sections were stored at -20°C.

2.2.2.2 *Cells on cytospins*

From single cell suspension or trypsinized cells cytospins were prepared. A cell number up to 30.000 cells per Cytospin was taken up in 100 µL of medium and transferred into a cytospin funnel. The samples were centrifuged at 1.200 rpm for 5 minutes to attach the cells through a cytofunnel to a glass slide. The glass slides can be then processed for IIF.

2.2.3 Tet-Off-H2B-GFP reporter

2.2.3.1 *Bacterial transformation and plasmid purification*

To produce competent bacteria 3ml of LB media were inoculated with 30µL of the bacteria HB101 and grew overnight at 37°C in a roller drum. The next day 500µL of the overnight culture were inoculated into a sterile Erlenmeyer flask containing 50ml of fresh LB medium. The culture was placed on a shaker and after 2 hours the cell density reached mid-log growth phase. The growth rate of the culture was determined by taking 1ml of the cultures and reading the optical density at 550 nm wavelength using a spectrophotometer. The optimal OD_{550} is 0.5. The cell suspension was centrifuged at 5000rpm for 5 min at 4°C. The cell pellet was resuspended with 20µL ice-cold sterile 50 mM $CaCl_2$ (Solution A). The cell suspension was placed on ice for 15 min. Then the cells were centrifuged at 5000rpm for 5 min. at 4°C. The cell pellet was resuspended in 2,8 ml of sterile ice-cold 100mM$CaCl_2$ (Solution B). For long-term storage 100µL were stored at -80°C until needed. For transformation to 100µL of the bacterial culture 2µL plasmid (0,5ng/µL) was added. The mixture was incubated for 30 min on ice until 900µL of SOC medium was added and incubated at 37°C for 1 hour in a roller drum (250 rpm). 200µL of the cells were plated on selective LB agar containing ampicillin (Amp). The plates were incubated over night at 37°C. 6 single colonies were picked and incubated over night at 37°C in fresh LB medium containing Amp. For the purification of the plasmids the Quiagen EndoFree Plasmid Purification Kit was used. All steps were performed according to manufacturer's instructions.

2.2.3.2 *Virus production*

To produce the viral particles approx. 57.000 HEK293T cells per cm^2 were seeded in a 175 cm^2 cell culture flask and cultivated with DMEM with 10% heat inactivated FCS. The cells had to be even distributed across the substrate surface. The cells were incubated for 24h at 37°C under 5% CO_2. For the transient transfection of the cells with the expression constructs the transfection solutions A and B solution were prepared according to Table 2. A vector map of the tet-off-H2B-GFP vector is shown below.

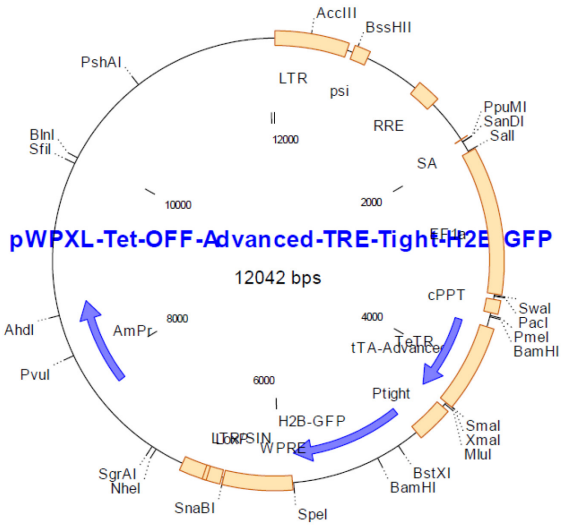

Vector map tet-off H2B-GFP lentiviral vector.

The transfection solution A and B was mixed and the mixture was incubated for 25-30 min at room temperature. Subsequently the mixture was added to the HEK293T culture and incubated for 16-18h. To induce the expression of the transgenes 480 µL sodium butyrate (500mM) was added to 24 ml culture volume of the transiently transfected cells to reach a final concentration of 10mM.

Transfection solution A	psPAX stock sol.	12 µL (= 12 µg)
	pMD2.G stock sol.	4.8 µL (= 4.8 µg)
	pWPXLTTT-H2BGFP stock sol.	16 µL (= 16 µg)
	Hanks´ balanced salt solution	1967 µL
		Σ 2000 µL
Transfection solution B	PEI stock sol.	90 µL (90 =µg)
	Hank´s balanced salt solution	1910 µL
		Σ 2000 µL

Table 2: Instructions to produce viral particles for one 175 cm^2 culture flask.

After 8h the culture medium was exchanged for fresh DMEM with 30% heat inactivated FCS and incubated for 16-18h. Finally the culture supernatant was harvested at 48h and 72h post cells transfection. The culture supernatant was then filtrated through a 0.45µm filter and pooled and stored at -80°C or concentrated by ultracentrifugation. The producer cells were discarded.

2.2.3.3 *Concentration by Ultracentrifugation*

For the preparation of highly concentrated viral stocks the supernatant is concentrated by ultracentrifugation. Therefore 4 ml sucrose (20%) was placed in an ultracentrifuge tube (Beckman Culture) before 30 ml of the supernatant is carefully laid over without disrupting the sucrose cushion. The ultracentrifuge tubes were equalized and placed into the ultracentrifuge buckets into the SW28 rotor. The tubes were centrifuged for 2 hours at 4°C at 25.000rpm. After the centrifugation the supernatant is removed and the pellet is dissolved in DMEM (1:100). The lentiviral stocks were aliquoted in 50µL aliquots and stored at -80°C.

2.2.3.4 *Virus Titration*

The concentration of infectious virus was measured by limiting dilution whereas the viral proteins expressed by infected cells are detected by FACS. Therefore $4x10^5$ keratinocytes where seeded with 2 ml DermaLife medium per well in a 6 well plate. After 5 hours 16µl polybrene/well (1µg/ml) is added into each well. After preparation of a serial dilutions of the virus (1/100-1/100000) the serial dilutions of the virus is added to the pre-plated cells. The plates are then centrifuged for 2500rpm at 37° C for 90 minutes before the virus is removed and replaced with fresh DermaLife Medium. After 48 hours all wells are trypsinized as described in XY and analyzed by FACS. The titer is calculated with the following formula:

Titer (TU/µL) = GFP positive cells/100 x initial cell number x dilution of virus.

2.2.3.5 *Transduction of cells*

For the transduction of keratinocytes 4 x 10^5 keratinocytes were seeded per well in a collagen I coated 6-well plate. After 2 hours the virus supernatant and polybrene (8 µg/ml) is added into each well. Subsequently the plates are centrifuged for 90 min at 2500rpm at 37°C. After this spinoculation the virus was removed and with fresh medium exchanged. The cells were trypsinized after 3 days of cultivation and seeded on OTCs or analyzed by FACS.

2.2.4 Staining methods

2.2.4.1 *Indirect Immunofluorescence*

In indirect immunofluorescence the first antibody (primary) is unlabeled and in order to detect the antigen the second anti-immunoglobulin antibody is tagged with a fluorescent dye. Frozen cryosections were, after thawing, fixed in cold (4°C) 80% ethanol for 10 min and then transferred for another 2 min in 100% aceton (-20°C). The sections were briefly washed in PBS, air dried and staining areas were marked with a hydrophobic pen (PapPen) before

placed in the humidifier chamber. The sections were blocked with 3% BSA in PBS+ solution for 15 min at RT to avoid non-specific binding of the second antibody. Afterwards the first antibody, diluted in the block solution, was incubated for 1h at 37°C and then another 30 min at RT or at 4°C over night. The sections were washed in PBS+ with 0,1% Triton X100 for 5 min and then twice in PBS+ for 5 min. The secondary antibody was also diluted in the blocking solution and incubated for 30 min at 37°C and 30 min at RT. Subsequently the slides were washed as described above with an additional wash at the end for 1 min in ddH_20. The sections were directly covered with a fluorescent mounting medium (DAKO) and a cover slip. The slides were dried for at least 1h at RT and then stored at 4°C.

2.2.4.2 *Hematoxylin and eosin (H&E) - stain*

The hematoxylin and eosin stain (H&E) is a common and most widely used staining in histology to evaluate the morphology of tissue. The hematoxylin is used to visualize the nuclear details (in blue) following by contrast counterstaining with eosin to stain proteins nonspecifically (in pink). The paraffin sections were deparaffinized by incubation in xylene for 8 min twice and then rehydrated by passing the slides through a graded alcohol series (100% ethanol, 96% ethanol, 80% ethanol, 70% ethanol, each 4 min) and finally washed in ddH_20 for 2 min. Subsequently the slides were incubated in hematoxylin for 6 min and then rinsed for 8 min with H_20. The sections were then incubated with eosine for 6 min and again rinsed with H_20 for 6 min. Following this the slides were dehydrated through a series of alcohol in ascending concentrations (70% ethanol, 80% ethanol and 90% ethanol, 100% ethanol) and a short incubation in isopropyl (2 min) and xylene for 2 x 5 min. Finally the slides were mounted with Eukitt mounting medium. The slides were analysed using a microscope (Olympus BX51), Images were taken using a Color view I camera and computer processed using the Olympus software Cell^D.

2.2.5 Molecular biology techniques

2.2.5.1 *RNA Isolation*

To isolate the RNA from small samples the ARCTURUS Pico Pure RNA Isolation Kit (Life Technologies) or RNeasy Mini Kit was used. The protocol was performed according to the manufacturer´s instruction. Additionally all samples were treated with DNaseI for 15 min at RT (RNase-Free DNase Set, Qiagen). The concentration of the RNA was determined with an Agilent 2100 Bioanalyzer (Agilent Technologies GmbH). RNA samples were stored at -80°C.

2.2.5.2 *DNA Isolation*

For the isolation of genomic DNA of cells the QIAamp DNA Mini Kit (Quiagen) was used. The protocol, DNA Purification from Tissues, was performed according to the manufacturer´s instruction.

2.2.5.3 *Reverse Transcriptase*

For the synthesis of cDNA for qRT-PCR the RevertAid H Minus first Strand cDNA Synthesis Kit was used. For each reaction 3µg of total RNA was transcribed according to the manufacturer's instructions. First to the RNA were 2µl oligo $(dT)_{18}$ primer (1 µg/µl) added and mixed with RNase free water to a final volume of 22 µL. The mixture was incubated for 5 min at 70 °C and 5 min at 4 °C. Subsequently 8µl 5x reaction buffer, 2µl RiboLock RNase Inhibitor (20 U/µl), 2 µl of RevertAid H Minus M-MuLV Reverse Transcriptase (200 U/µl) and 4µl dNTP mix (10mM) were added. The mixture was incubated for 60 min at 42 °C and terminated by heating to 70 °C for 10 min. The cDNA in a final volume of 40µL was stored at -20 °C for real-time PCR. For small RNA samples, the RNA samples were send to the microarray unit of the DKFZ "Genomics and Proteomics Core Facility" where the cDNA synthesis was performed with the NuGEN Ovation Pico WTA System.

2.2.5.4 *Real-time PCR*

Quantitative real-time PCR (qRT-PCR) was used for the relative quantification of mRNA expression of different selected genes. The qRT-PCR was performed in a thermal block LightCycler 480-II (Roche) according to the manufacturer's instructions. Each reaction had a total volume of 15µL containing 10µL LC Master probe, 10mM forward/reverse primers and UPL-probe (0.1mM) and nuclease free water. All primers were designed with the Universal Probe Libary software. After pipetting the 15µL into a PCR 96 well plate, 50ng of cDNA dissolved in 5 µL RNase free water was added. For negative control 5µL water was added to the 15µL. The plate was then sealed properly with a LightCycler® 480 sealing foil by pressing it firmly to the plate surface using a sealing foil applicator and centrifuged for 1 min at 1000rpm. Every qRT-PCR was performed in duplicates and a house keeping gene, GAPDH, as an internal reference was measured. The mixture was pre-incubated for 10 min at 95 °C, then 45 cycles were carried out, each composed of 95°C for 10sec and annealing for 30 sec at 60 °C and 1 min at 72°C. After each cycle the fluorescence was measured at 530nm. The reaction ended with a cooling step at 40°C for 10sec. Before beginning all real times experiments with a new set of primers an efficiency test was performed to verify the quality of the primer/probe combination. To obtain a standard curve the cDNA of the target

cells was used in a dilution series of 100, 20, 4, 0.8 and 0.16ng. With the LightCycler® 480 Software and the algorithm “Second Derivative Maximum” the crossing point (CP) of each gene of interest could be determined. This CP values allowed the calculation of the ratio of the relative mRNA expression of control (basal keratinocytes) vs. LRCs, normalized to the housekeeping gene, using the formula of Pfaffl (Pfaffl, 2001), whereas controls were set to 1.

$$\text{ratio} = (E_{target})^{\Delta CP\ target\ (control\text{-}sample)} / (E_{ref})^{\Delta CP\ ref\ (control\text{-}sample)}$$

Since for each test a standard curve of the cDNA was performed, the quality and the efficiency of the PCR reaction could be included into the calculation.

2.2.6 Microarray

For expression profiling microarrays were performed. Therefore RNA samples (small samples) were send to the microarray unit of the DKFZ “Genomics and Proteomics Core Facility”. For the analysis the BeadChip HumanHT-12 v4 was used. For the cDNA synthesis the NuGEN Ovation Pico WTA System was used. The protocols were performed according to the manufacturer´s instruction. For the analysis three replicates from independent experiments were used. From each experiment isolated LRCs were compared to isolated basal keratinocytes from OTCs after a chase period of 6-7 weeks. Data extraction was individual for each bead, whereas the data point was excluded if the median absolute deviation (MAD) was above 2.5.

2.2.7 Analysis of microarray data

The raw data were analysed with Chipster an open source platform (www.chipster.csc.fi). Normalisation was performed with the Illumina- lumi pipeline. Statistical analysis of the microarray data was performed after normalization. For quality control the genes were filtered on the basis of their coefficient of variation (CV), only genes with a CV above 0.95 pass the filter. Statistics were performed by using the Empirical Bayes test with a p-value cut off of 0.05. The two samples Benjamini and Hochberg's (BH) correction was applied for p-value adjustment. A p-value below 0.05 was considered as significant. Annotation was performed with Ingenuity pathway analysis software.

2.2.8 Linear Amplification Mediated (LAM)-PCR

150ng of DNA was used for integration site analysis by 3´LTR-LAM-PCR as described previously (Schmidt et al., 2001; Schmidt et al., 2007) and subsequent Illumina MySeq

sequencing was performed. For linker ligation during LAM PCR procedure, sample specific barcoded linker cassettes were used. LAM restriction digest was performed using MluCl. For sequencing, specific barcoded primers were added to both ends of the LAM-PCR. Analysis of sequenced integration sites was performed as described previously. The sequenced integration sites were valid if the lentiviral LTR was fully present at the vector-genome junction and the genomic DNA flanking the vector integration had a unique sequence match of ≥95% in alignment with the human genome employing Blat. A sequencing validity cut-off was set as described (Dieter et al., 2011). Based on sequencing of clones harboring known integration sites the cut-off was defined at a minimal level below 0.1% of the total sequence counts. Collisions below the cut-off were subsequently removed from the analysis.

3 Results

3.1 Optimization of infection methods for human adult primary keratinocytes with the Tet-Off-H2B-GFP lentiviral vector

Until now the identification of epidermal stem cells in the IFE is still difficult. In the hair follicles and mouse ear epidermis, which lack hair follicles, infrequently dividing, slow-cycling, cells have been described as stem cells (Bickenbach, 1981; Braun et al., 2003; Cotsarelis et al., 1990). For the detection of label-retaining cells (LRC) in the epidermis, the potential stem cells, and the isolation of a pure LRC population gene transfer is a promising tool. With the generation of Tet-off-controlled Histone 2B-GFP (TRE- H2BGFP/K5Tet^{off}) transgenic mice under the control of a keratin promoter it was possible to identify and isolate LRCs from mouse epidermis (Tumbar et al., 2004). Furthermore, with the development of a lentiviral-based Tet-Off-H2B-GFP reporter harboring the Tet-Off regulatory elements and genes with the Histone 2B-GFP (H2BGFP) fusion construct allowed to transduce various cell types in a single step. Using this Tet-Off-H2B-GFP lentiviral reporter it was possible to successfully infect also epidermal cell lines (Falkowska-Hansen et al., 2010). Normal human adult keratinocytes (NHEK) are difficult to infect (Arcasoy et al., 1997; Grubb et al., 1994). Therefore an effective, but sensitive method had to be established to infect NHEKs.

3.1.1 NHEKs can be efficiently infected with a tet-off-H2B-GFP lentiviral vector

Since keratinocytes have a limited lifespan in culture expansion of H2B-GFP positive NHEKs is excluded. Therefore, a highly efficient gene transfer method, for transduction of the majority of keratinocytes without influencing the cell viability, is required. It was shown in other studies that centrifugation with the infectious supernatant, to concentrate the virus particles at the cell surface (spinoculation), can enhance infection rates from 40 to >90% for primary keratinocytes (Gagnoux-Palacios et al., 2005). Additionally, polybrene (Pb), a cationic polymer, was used to increase the efficiency of lentiviral infection of cells (Nead and McCance, 1995; Staedel et al., 1994; Toyoshima and Vogt, 1969). Accordingly, we compared the effect of spinoculation and Pb in our studies for the optimization of lentiviral transduction in NHEKs. Three different types of normal adult keratinocytes from sub-confluent cultures in low-calcium medium were used for the transduction. NHEKs were either incubated over night or spinoculated for 90 min. with the infectious supernatant. FACS analysis of transduced NHEK 48 h after infection without spinoculation showed that the percentage of cells expressing GFP in NHEKs ranged between 0.5% and 15% according to the used virus dilution (Figure 7 A). We confirmed that to significant enhance the transduction efficiency spinoculation is necessary (Figure 7 B). The transduction efficiency

was about 45% increased with spinoculation in all three tested NHEKs with a virus dilution of 1:500 (Figure 7 B). To investigate the effect of Pb, NHEKs were centrifuged in the presence or absence of 8µg/ml Pb during viral infection. As shown in Figure 7 A and B, addition of Pb increased the transduction efficiency in a range between 5% and 29% dependent on the type of NHEKs and used virus dilution (Figure 7 A and B). However, Pb enhances the viral infection rate less than spinoculation.

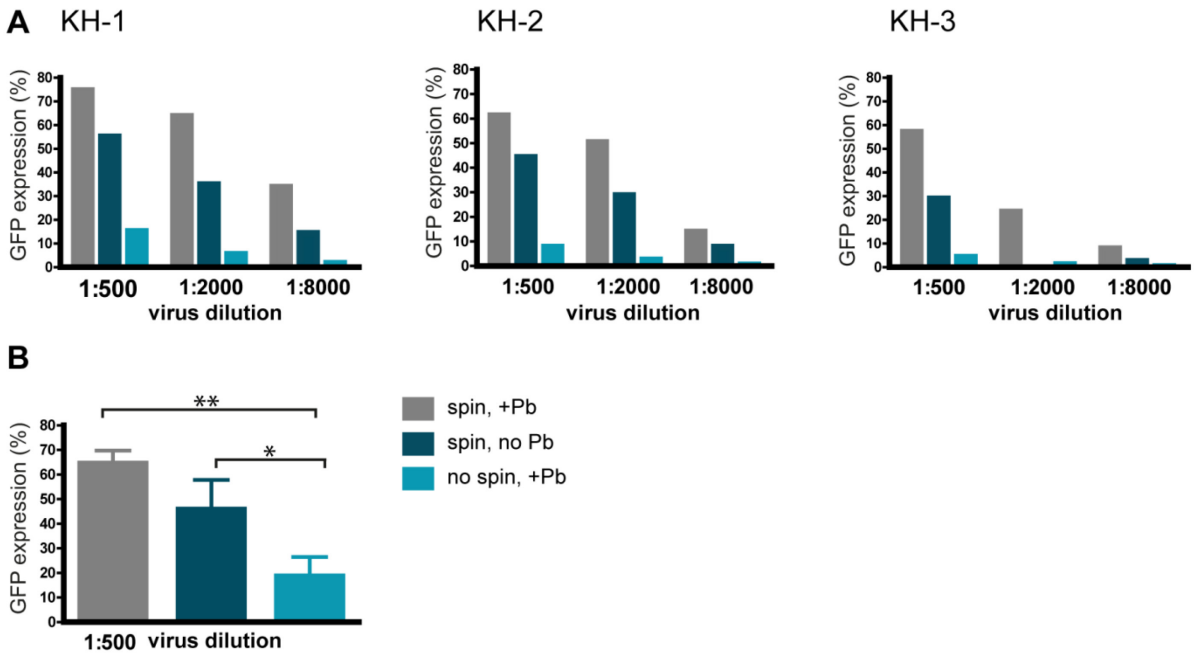

Figure 7: Optimization of infection method for human adult primary keratinocytes with the Tet-Off-H2B-GFP lentiviral vector. (A) Three different types of keratinocytes were tested. Cells were infected with three virus concentrations (1:500, 1:2000, 1:8000) and either spinoculated (spin) or incubated with the virus over night at 37°C (no spin). Polybrene (+Pb) was added to the culture medium (8µg/ml) of 2 groups (spin, +Pb and no spin +Pb). (B) NHEKs were infected with a virus dilution of 1:500 and spinoculated (spin) or infected over night at 37°C with the lentivirus. Cells were cultivated either in the presence or absence of Pb (8µg/ml) during infection. GFP positive cells were assessed by flow cytometric analysis 48 hours after infection. Statistical test: n=3, 1way-ANOVA, Bonferroni's Multiple Comparison Test, * p ≤ 0.05, ** p ≤ 0.01.

Moreover it was shown, that keratinocytes are very sensitive to polybrene at concentrations higher than 5 µg/ml (Nanba et al., 2013). Phase contrast images of transduced NHEKs either in the presence or absence of Pb (8µg/ml) during the infection process showed no morphological differences compared to the non-transduced keratinocytes (Control) (Figure 8 A and B). Therefore, we conclude that keratinocytes tolerate an amount of 8µg/ml (Figure 8 A). This dose was used for all further studies.

Collagen, type I represents a natural ECM component of the skin (Deutzmann R, 2007). Therefore, collagen coating of cell culture plates promotes the adhesion of NHEKs in 2D cultures. To enhance the attachment of NHEKs during the infection process we used collagen type I coated culture dishes. We observed that collagen coating of the cell culture

plates was increasing the rate of infection (Figure 8 C). Using these transduction conditions with higher virus concentrations, for example 1:100, transduction efficiencies up to almost 100% were obtained without damaging the cells (Figure 8 B, lower panel). Both, the control group and the transduced keratinocytes, appeared to be healthy after the virus infection and the treatment with polybrene (Figure 8 A and B).

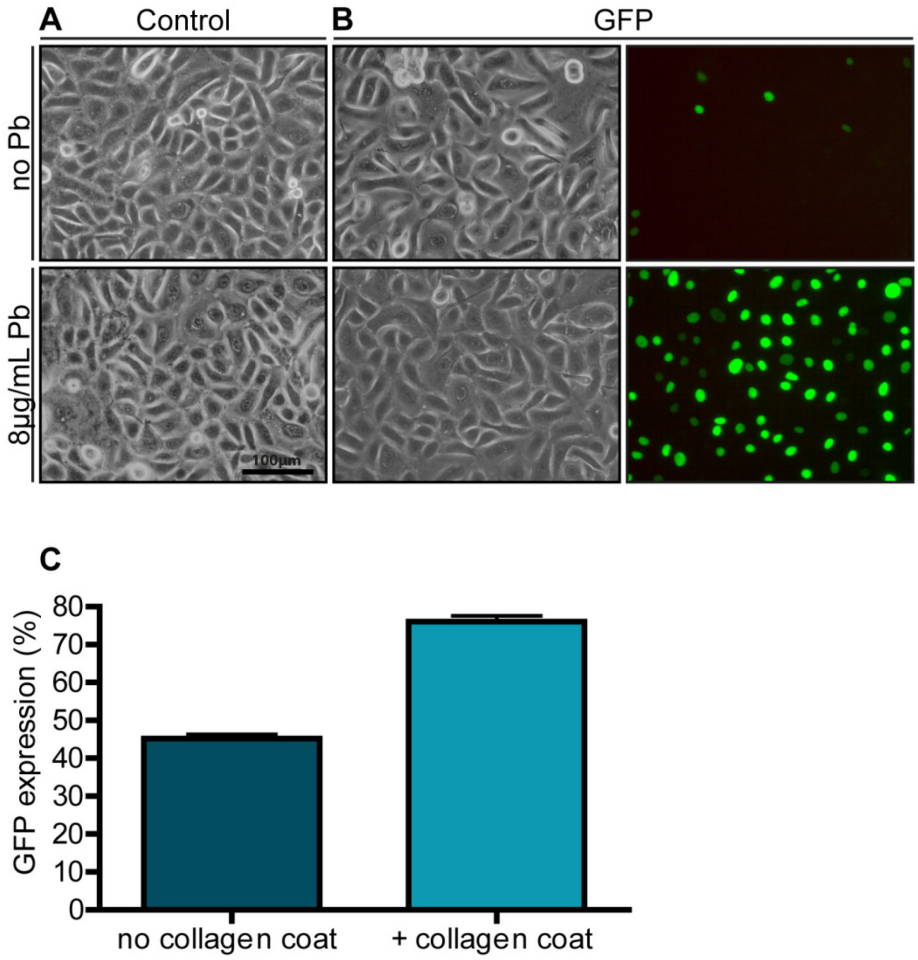

Figure 8: Expression of Tet-Off-H2B-GFP in NHEK 2D cultures (A) Phase contrast images of NHEK non-transduced (Control) or (B) transduced with Tet-Off-H2B-GFP reporter virus (1:100) assessed by fluorescence microscopy. Upper panel: cultivation without Pb, lower panel: cultivation with Pb (8µg/ml) during viral infection. (C) NHEK cultivated on a collagen coated (+ collagen coat) or non-coated (no collagen coat) cell culture dish during viral infection. Numbers of H2B-GFP positive NHEK were analyzed by flow cytometry 48hours after transduction.

In summary we showed, that spinoculation markedly increased the transduction rate. Moreover, the addition of Pb (8µg/ml) and collagen type I coating of the cell culture plates further enhanced the rate of infection. Therefore, we used these conditions for all further studies.

3.2 H2B-GFP expression of NHEKs can be tightly regulated by doxycycline

For the detection of label-retaining cells GFP expression of the reporter has to be turned off in order to detect only slow cycling cells as GFP positive cells. Thus the responsiveness of the reporter plays an essential role to perform pulse-chase experiments. Since we used a

Tet-Off advanced inducible gene expression system, the gene of interest is turned off in the presence the antibiotic, doxycycline (Dox). To evaluate the responsiveness of the reporter construct NHEKs were cultivated under the presence of 1 ng/ml of Dox. The GFP expression was assessed by fluorescence microscopy and flow cytometry. Already one passage after the addition of Dox (Figure 9 A, first arrow) was a strong decline in the number of GFP positive NHEKs, only 5% of the cells were still GFP positive (Figure 9 A, passage 14). No GFP positive cells could be detected anymore two passages after addition of Dox (Figure 9 A, passage 15). To determine the kinetics also for again switching on the H2B-GFP expression, Dox was removed (Figure 9 A, second arrow). Within one passage almost all cells turned on the GFP expression (Figure 9, passage 16). This showed that the H2B-GFP expression was tightly regulated by doxycycline.

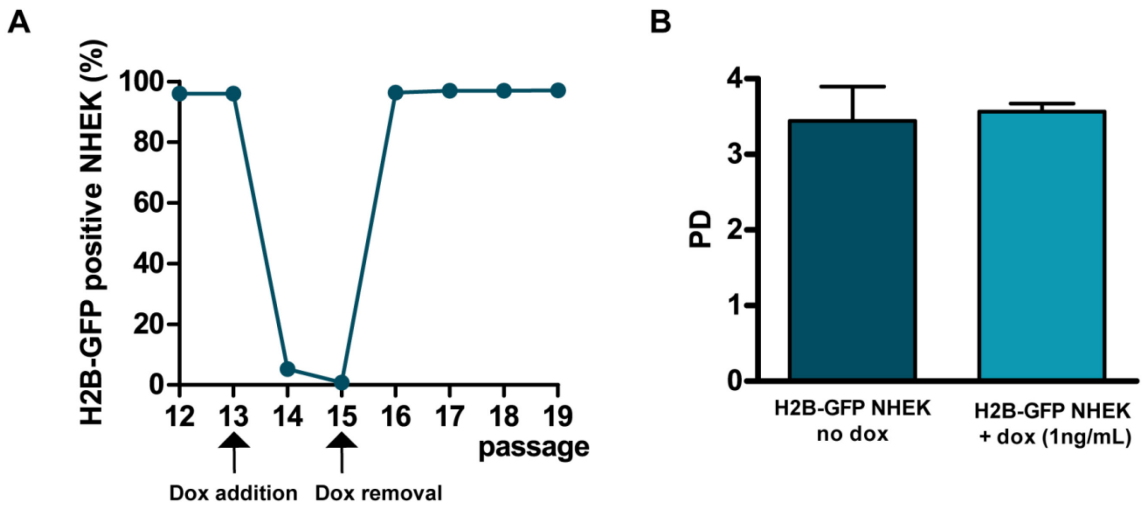

Figure 9: Tight regulation with Dox of the H2B-GFP reporter without influencing the cell viability. (A) NHEKs were cultivated for the indicated passages either in the presence or absence of Dox (1ng/ml) as indicated by the arrows. H2B-GFP positive NHEK were quantified by flow cytometry. (B) Calculation of the population doubling (PD) number of H2B-GFP positive NHEK cultivated with Dox (1ng/ml) or without Dox after each passage. NHEK were cultured for 5 passages.

Moreover, we wanted to examine if Dox has an influence on the cell viability and cell cycle activity. Therefore NHEKs were cultured over several passages under specific conditions (see 2.2.1.5) in the presence or absence of Dox. The population doubling number was determined after each passage (Figure 9 B). The population doubling number of approximately 3.5 per passage was similar whether the cultures were treated with Dox or without Dox. This showed no influence of Dox on the cellular growth.

3.3 Characterization of Tet-Off-H2B-GFP positive NHEKs in 3D OTCs

3.3.1 H2B-GFP transduced NHEKs are able for long-term regeneration in OTCs

For the detection of label-retaining cells in 3D organotypic cultures, long-term homeostasis of the cultures is necessary. The scaffold OTC (sca OTC) model system enables the cultivation of keratinocytes with a healthy and vital epithelium for more than 15 weeks (Muffler et al., 2008). Thus, sca OTCs can establish a microenvironment providing human epidermal stem cells with the ability for epidermal long-term regeneration. In this study, as a second type of organotypic cultures, fdm OTCs were used (Berning et al., 2015). In this setting normal human dermal fibroblasts (NHDF) produce a fibroblast-derived matrix as dermal equivalent to establish long-term homeostasis which provides a similar microenvironment for NHEKs (Berning et al., 2015). Sca OTCs and fdm OTCs were used in this study in order to test if there are any differences between the different 3D models grown with H2B-GFP keratinocytes.

To determine if transduced NHEKs were able to establish regenerative capacity and long-term maintenance, H2B-GFP NHEKs were seeded on dermal equivalents and cultivated air-exposed for 8 weeks. The transduced keratinocytes developed a well organized, stratified and differentiated epithelium after 2 weeks (Figure 10 B, C). Importantly, these cultures were also suitable for long-term regeneration (Figure 10 B, C, 8 weeks). The histological analysis revealed no visible differences between the control groups, the non-transduced keratinocytes and the transduced keratinocytes, irrespective of the treatment with Dox (Figure 10 A, B, C). Also in comparison no differences were seen between fdm OTCs and sca OTCs after 2 and 8 weeks (Figure 10, upper panel vs. lower panel). Taken together, the results demonstrated that neither the tet-off-H2B-GFP vector nor Dox influenced NHEKs in their long-term regeneration ability in 3D tissue cultures.

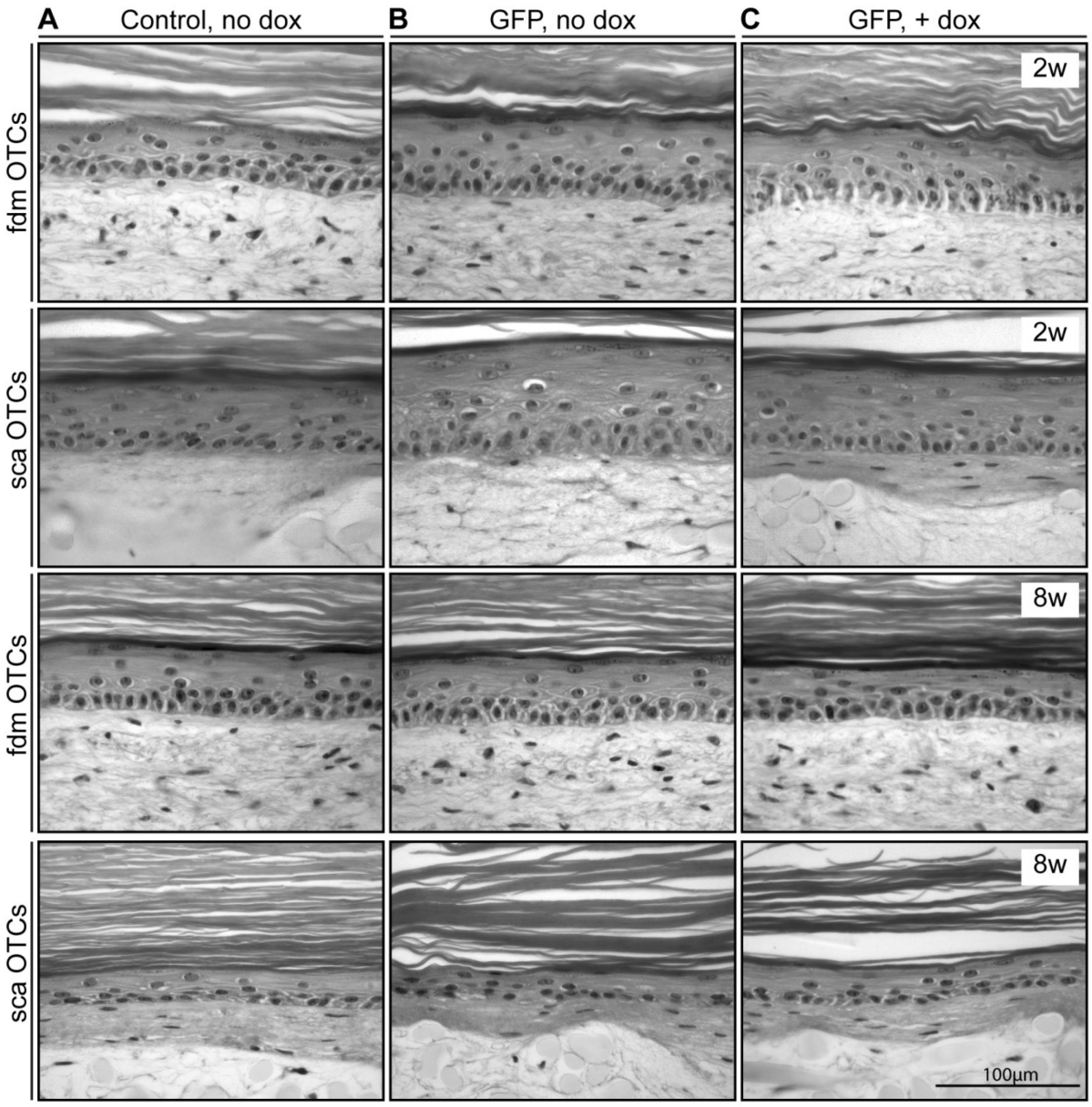

Figure 10: Influence of H2B-GFP expression and Dox on long-term regeneration in OTCs. Paraffin sections of 2-week-old (2w) and 8-week-old (8w) OTCs stained with hematoxylin/eosin to analyze the histological structure. OTCs were either grown from non-transduced NHEK (A) or H2B-GFP transduced NHEK (B+C) and cultivated in the absence (A+B) or presence (C) of Dox.

3.3.2 No influence on the proliferation capacity of transduced NHEKs in OTCs

The histology was very similar between OTCs grown from H2B-GFP NHEKs and non-transduced NHEKs, suggesting that the proliferation was not altered by gene transduction. To test this, the proliferation rate was determined by staining sections of 3D cultures with the proliferation marker Ki67 (Figure 11 A.). There was no difference in the proliferation rate between the control group and OTCs made up from transduced keratinocytes. Proliferation of keratinocytes in 4 week-old epithelia was restricted to the basal cell layer and was about 25% of the basal cells. The addition of Dox into the culture medium had also no effect on cell

proliferation (Figure 11 C.). Furthermore the proliferation rate was similar between fdm OTCs (Figure 11 B) and sca OTCs (Figure 11 C) independent of transduced keratinocytes or non transduced keratinocytes.

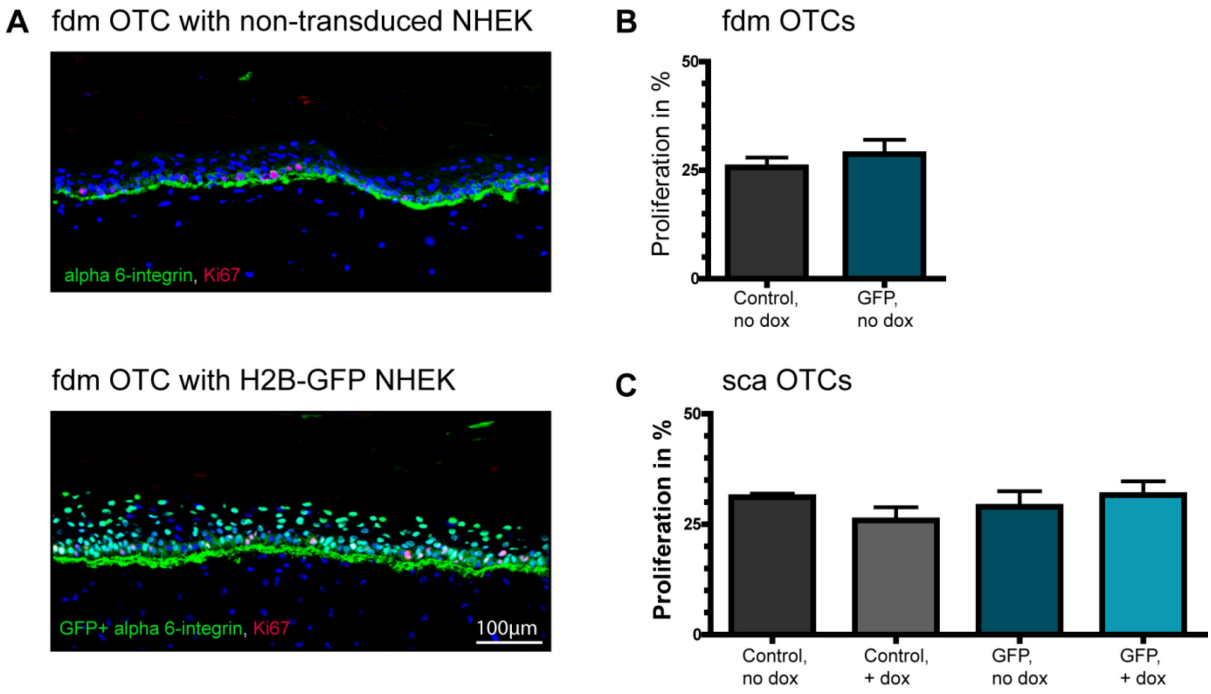

Figure 11: Proliferation of H2B-GFP NHEK compared to non-transduced NHEK in OTCs. (A) Cryosections of fdm OTCs and sca OTCs were stained for the proliferation marker, Ki67 (red) and α6 integrin (green). The nuclei were counterstained with Dapi (blue). Upper picture: fdm OTCs, non-transduced NHEK, lower picture: fdm OTCs, H2B-GFP NHEK. The percentage of Ki67-positive cells compared to the total basal cell number was quantified by microscopy. Two cultures per condition were analyzed either of (B) fdm OTCs or (C) sca OTCs, cultivated in the absence or presence of Dox, grown with transduced or non-transduced NHEK for 4weeks. Images of 4 representative regions per culture were taken using a 20x objective in order to calculate the percentage of Ki67-positive cells normalized to the corresponding number of basal keratinocytes.

3.3.3 Regular epidermal differentiation of transduced keratinocytes in OTCs

For studies on epidermal stem cells, tissue homeostasis including the regular epidermal differentiation and the development of a proper stem cell microenvironment *in vitro* is crucial. To evaluate tissue homeostasis, the regular epidermal differentiation and establishment of a basement membrane as well as intracellular junctions as marker for tissue integrity and stability, were analyzed. Therefore, we seeded H2B-GFP NHEKs on sca OTCs or fdm OTCs and cultivated them air-exposed for 4 weeks. The expression of different markers in the skin were examined in OTCs of transduced keratinocytes (GFP) compared to non-transduced keratinocytes (control), either treated with Dox (GFP, +Dox) or untreated (GFP, no Dox). Desmoglein 1, a typical marker for desmosomes in the epidermis, showing the tight connection between the cells of all vital suprabasal cell layers, was regularly expressed in all transduced and non transduced cultures (Figure 12 A) and independent of the treatment with Dox (Figure 12 A). There was also no difference between sca OTCs and fdm OTCs (Figure

12 A, upper 3 panels vs. lower 3 panels). As a marker of the basement membrane the expression of collagen VII was analyzed. Collagen VII is part of the anchoring fibrils in the *sublamina densa* and a sign of a mature basement membrane. In all epithelia regular Collagen VII expression could be detected in the basement membrane (Figure 12 B) confirmed therefore the development of a proper basement membrane associated with tissue homeostasis. Notably, in sca OTCs, without Dox treatment, the expression of collagen VII was partly fragmented, this was not the case for sca OTCs + Dox treatment. There was also no difference in the expression of keratin 14 in all epithelia (Figure 12 C). Keratin 14 could be detected in the basal layer, slightly lowered within the more apically located layers specifically in the *stratum spinosum* and *stratum granulosum*. An early differentiation marker is involucrin, a component of the cornified envelope, first visible in the upper layers of the stratum spinosum (Rice and Green, 1979). The expression displayed proper differentiation in all cultures (Figure 12 D). The expression of E-cadherin in cultures with transduced and non transduced keratinocytes (Figure 13 A) displayed the development of adherens junctions, important cell-cell contacts in the skin and critical for tissue integrity.

Also differentiation markers like filaggrin which are indicating terminal differentiation (Candi et al., 2005), were observed regularly expressed in all GFP and control groups (Figure 13 B).

Integrins, receptors for cell adhesion to extracellular matrix proteins, play an important role in cell-cell adhesions and act as key player in tissue homeostasis (Hynes, 2002). Moreover, there are also involved in niche formation (Lowell and Mayadas, 2012). In keratinocytes α6 integrin is detected at the basal pole of the basal cell layer and the main component of hemidesmosomes. Irrespective of the H2B-GFP expression the typical distribution for in the basal cell layer could be detected in all cultures (Figure 13 C) and therefore displays a homeostatic epidermis (Hertle et al., 1991).

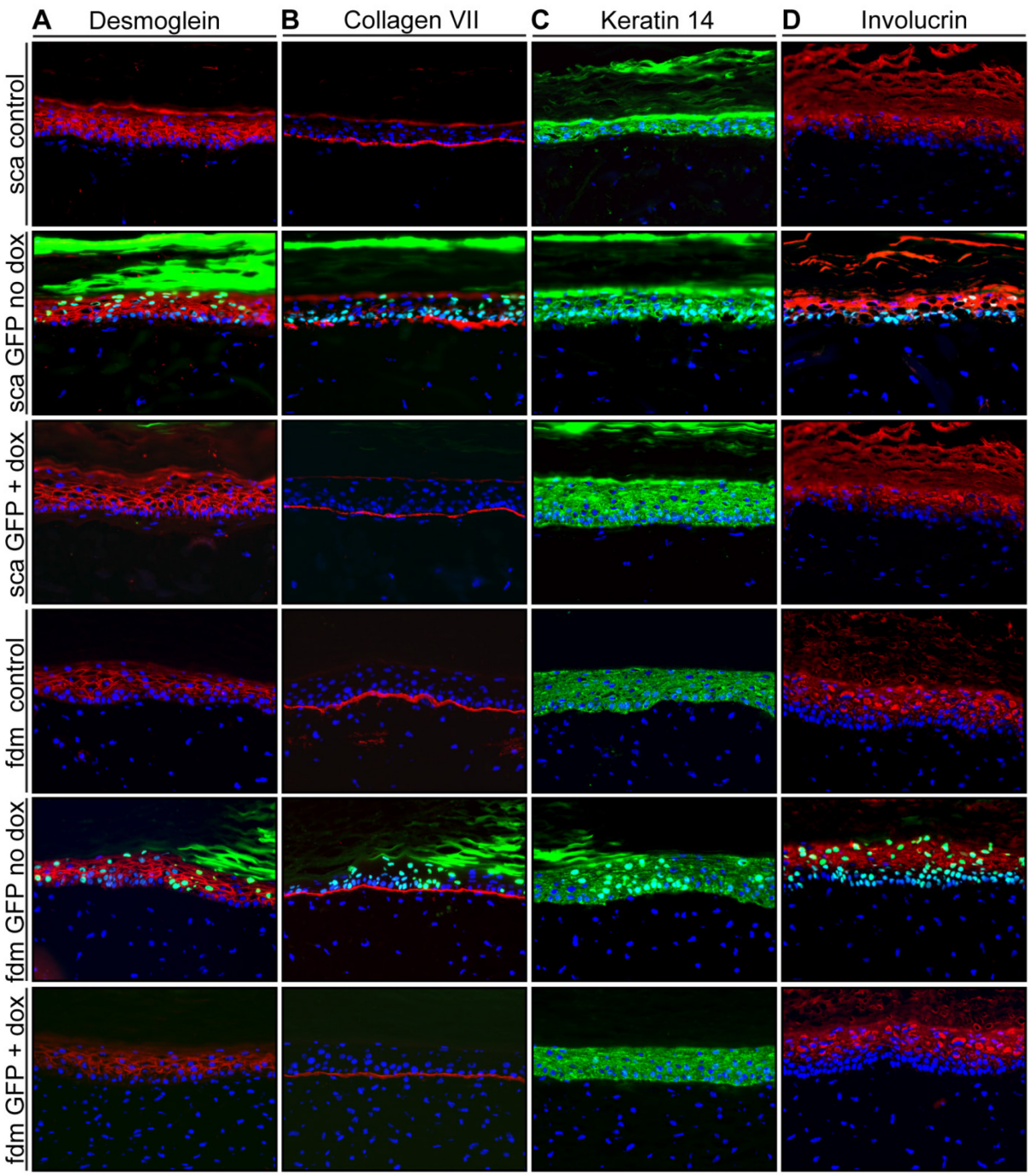

Figure 12: Influence of H2B-GFP expressing NHEK in comparison to non-transduced NHEK on the epidermal differentiation. Cryosections of 6-week-old OTCs (fdm OTCs and sca OTCs) grown from H2B-GFP NHEK and non-transduced NHEK were fixed and then analyzed by immunofluorescence staining for the expression of the epidermal adhesion molecule desmoglein1 (red) (A), the basement membrane marker Collagen VII (red) (B), Keratin 14 (green) (C) and the early differentiation marker Involucrin (D), shown in red. Nuclei were counterstained with Dapi (blue). GFP expression in green. Upper three panels: sca OTCs. Lower three panels: fdmOTCs. Tet-Off-H2B-GFP NHEK were cultivated in the presence or absence of Dox as indicated.

Taken together the immunostaining analysis of typical epidermal marker proteins displayed regular expression and localization of all markers. This reflects a normal epidermal tissue architecture developed by transduced NHEK OTCs. Neither the vector nor Dox seems to influence tissue development in 3D OTCs. Thus, the cultures made with transduced

keratinocytes were suitable to be used for pulse-chase experiments to study epidermal stem cells. Furthermore both dermal equivalents, scaffold-based and fdm-based, are suitable for long-term experiments with H2B-GFP NHEK.

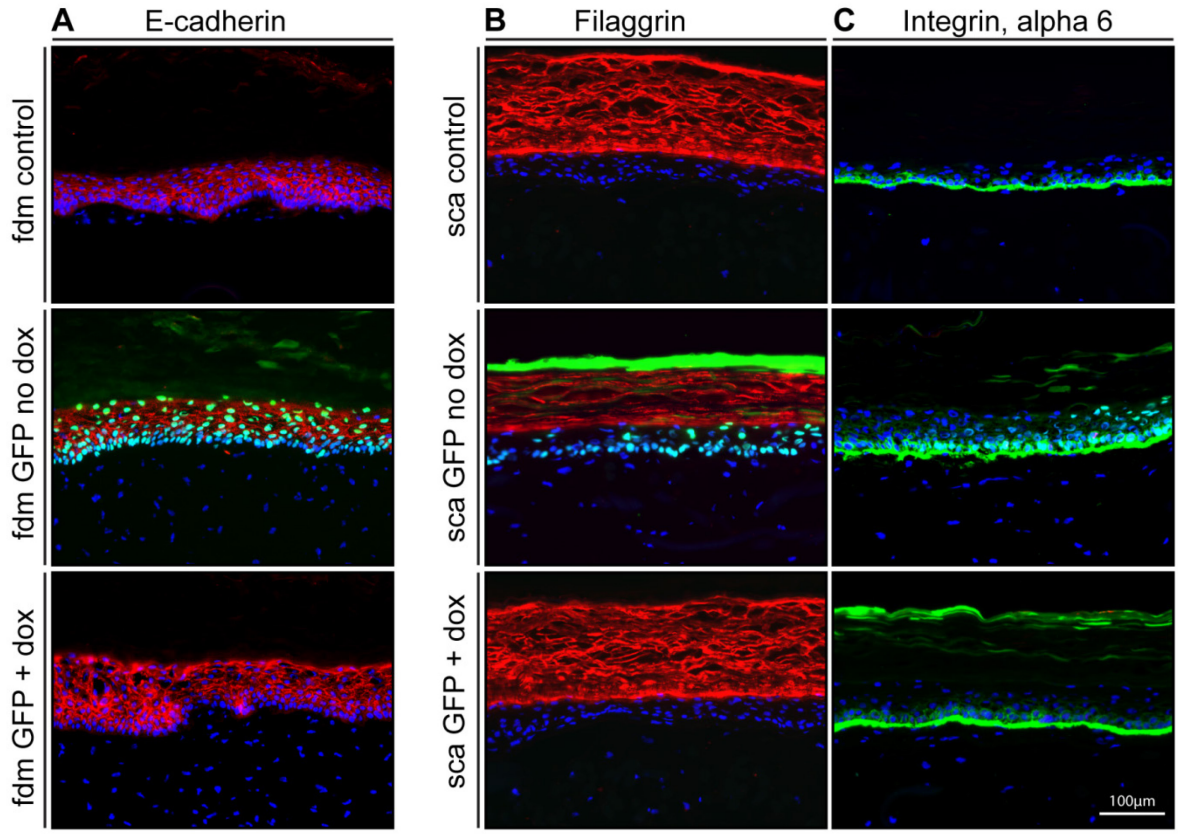

Figure 13: 6 week-old OTCs either fdm OTCs (A) or sca OTCs (B, C) grown with H2B-GFP NHEK or non-transduced NHEKs in the presence or absence of Dox as indicated. Fixed cryosections were stained with specific antibodies in combination with Dapi (blue) as DNA staining. GFP expression is shown in green. Sections were analyzed for the expression of the adhesion molecule E-Cadherin (A), the late differentiation marker Fillagrin (B). Stainings all shown in red. (C) Expression of α6 integrin, a marker for basal cells, is shown in green.

3.3.4 Tight regulation of the Tet-Off-H2B-GFP lentiviral reporter with Dox in OTCs

To ensure the responsiveness of the Tet-Off-H2B-GFP lentiviral reporter the Dox regulation was also tested in OTCs. This is required to avoid false positive cells which could be identified incorrectly as LRCs. Therefore, H2B-GFP expressing NHEKs were seeded on OTCs. The cultures were cultivated for 2 weeks with Dox in the culture medium. After 2 weeks of Dox treatment all cells had turned off the GFP (Figure 14 A), subsequently Dox was removed in order to turn on again the GFP. After a cultivation period of 1 week without Dox the keratinocytes were still GFP negative (Figure 14 B). The GFP signal could be detected in all cells after 4 weeks of cultivation without Dox (Figure 14 C). Taken together, the vector remained responsive to Dox and is also tightly regulated in OTCs.

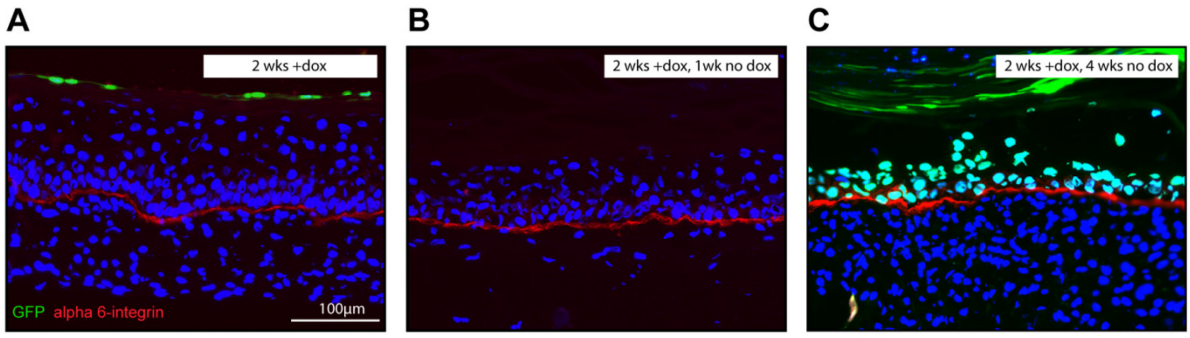

Figure 14: Tight regulation of the H2B-GFP reporter in 3D. Cryosections of OTCs with H2B-GFP transduced NHEK were analyzed for GFP expression and α6 integrin (red) as basal cell marker by immunofluorescence staining. Nuclei were counterstained with Dapi (blue). (A) Tet-Off-H2B-GFP NHEK were cultivated in OTCs in the presence of Dox (1ng/ml) for the first 2 weeks. (B) Thereafter, Dox was removed for one week. (C) Tet-Off-H2B-GFP NHEK cultivated for the first two weeks with Dox followed by the cultivation in the absence of Dox for 4 weeks.

3.3.5 Gene silencing of H2B-GFP positive cells in OTCs

For pulse-chase experiments, H2B-GFP NHEKs were sorted for their GFP expression and seeded on OTCs. Subsequently, the cultures were cultivated in the absence of Dox for the first two weeks (expression of H2B-GFP, pulse period). Analysis of OTCs grown with sorted H2B-GFP NHEKs showed a decline in the GFP signal (10-40%) after 2 weeks cultivation under the absence of Dox (Figure 15) although we sorted the cells for the GFP expression before seeding them on the dermal equivalent. This might be due to gene silencing of the Tet-Off-H2B-GFP reporter. To circumvent this loss of GFP positive cells we conclude to resort the H2B-GFP NHEKs in order to obtain a stable H2B-GFP expressing cell population. Due to the short lifespan of keratinocytes in culture such approaches are under normal cultivation conditions difficult to approach. Therefore we investigated the effect of a Rho-associated protein kinase (ROCK) inhibitor Y-27632, which had been shown to improve the survival of dissociated human embryonic stem cells (Watanabe et al., 2007) as well as the cloning efficiency (Terunuma et al., 2010) and long-term proliferation of human keratinocytes (Chapman et al., 2010). Moreover, it was suggested that the ROCK inhibitor Y-27632 enabled keratinocytes to efficiently bypass senescence and become immortal without detectable cell crisis (Chapman et al., 2010).

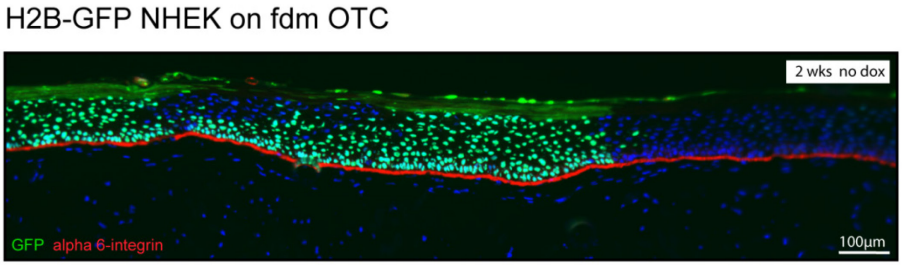

Figure 15: Analysis of cryosection from transduced, FACSorted, H2B-GFP NHEKs grown on OTCs after 2 weeks in the absence of Dox. Scale bar:100µm.

3.4 Long-term cultivation of NHEKs with Rho kinase inhibitor Y-27632

To explore the effect of Rho kinase inhibition on the long-term growth of keratinocytes isolated from adult skin, NHEKs were cultivated in the absence (Control) or presence of 10µM Y-27632 (+Y-27632) in 2D cultures. To bypass senescence it was shown that the presence of feeder cells is required in concert with Y-27632 for foreskin keratinocytes (Chapman et al., 2010). Therefore we also tested whether the co-cultivation with feeder is prerequisite for long-term cultivation of NHEKs in the presence of Y-27632. Already in passage 1, directly after the addition of the Rho kinase inhibitor, the treated cells were growing faster irrespective of being cocultivated with feeder in calcium-containing medium (FAD) or being cultivated in low-calcium, serum-free medium (DermaLife) without feeder cells (Figure 16, passage 1 A-D). In passage 4 the growth of the control cultures slowed down remarkably compared to the Y-27632 treated cultures (Figure 16, passage 4 A-D). In passage 5 signs of senescence, like the enlargement of cells, and increased differentiation in both control cultures, could be observed while the morphology of the Y-27632 treated cultures still resembled undifferentiated early passage NHEKs (Figure 16 B, D). In passage 6 both control cultures cell death occurred (Figure 16, passage 6, A and C, indicated by the cross). Also the Y-27632 treated group cultivated in low-calcium medium without feeder (Figure 16 B, passage 6) showed first morphological signs of senescence, like bigger nuclei (Figure 16 B, passage 6). Beyond passage 6, only NHEKs grown in co-culture with feeder and FAD medium, containing Y-27632, continued to proliferate (Figure 16, D). In passage 22 Y-27632 treated NHEKs still showed the morphology of early passages of NHEKs (Figure 16 D, passage 1 and passage 22). These results demonstrated that NHEKs can be passaged for long-term in 2D by addition of Y-27632 to the culture medium in co-cultivation with feeder.

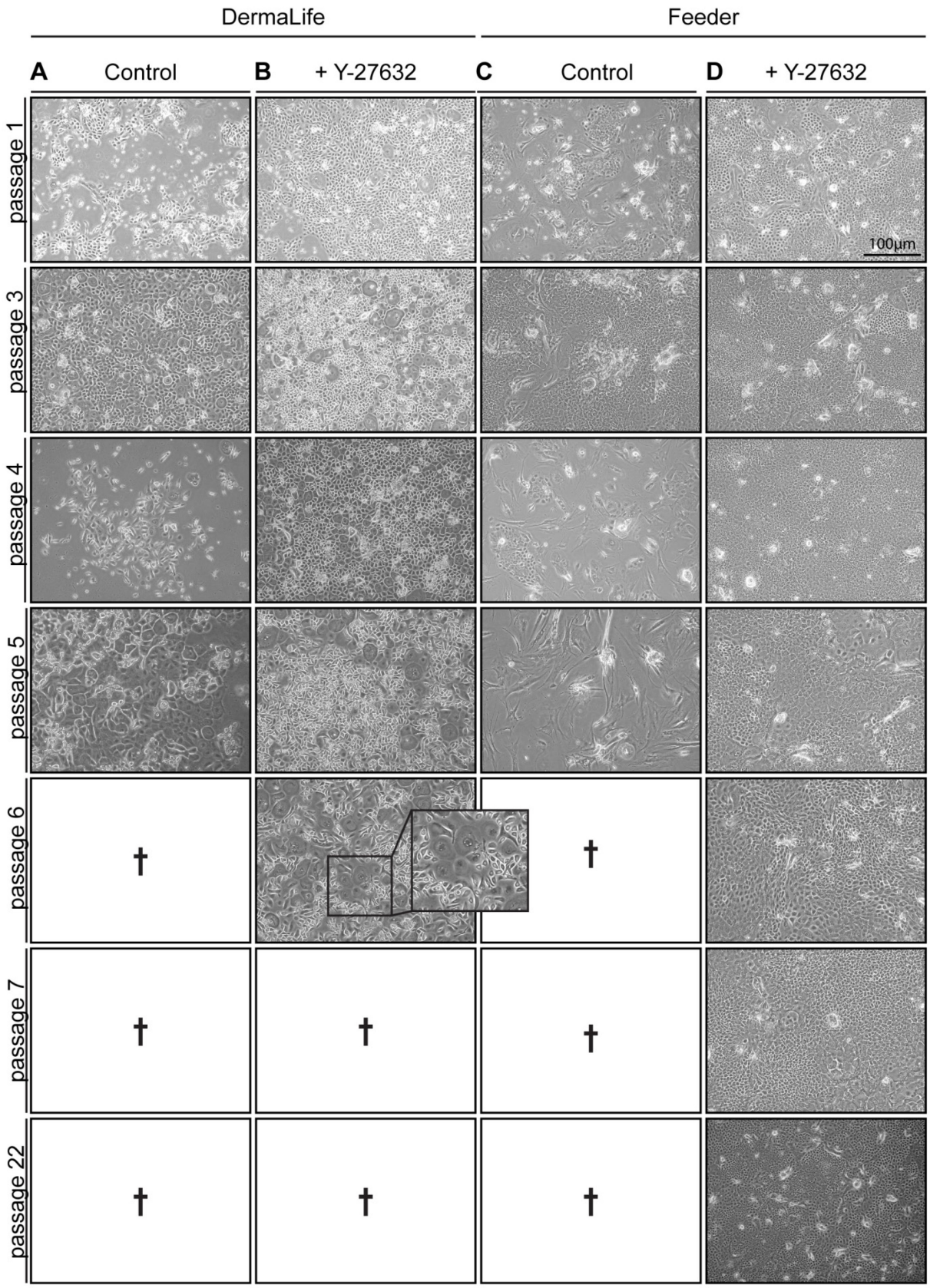

Figure 16: Long-term cultivation of NHEKs with Y-27632 required the co-cultivation with feeder cells. (A) – (D) Phase contrast images of keratinocytes cultivated in low-calcium medium (DermaLife, without feeder) are shown in the first two columns, whereas NHEKs cultivated in feeder co-culture with calcium-containing medium are shown in the last two columns. Passage of NHEKs and treatment with Y-27632 (10µM) as indicated. Cell death is indicated as cross. The magnification in passage 6 shows the enlargement of the cells with bigger nuclei.

3.4.1 Increased proliferation of NHEKs in the presence of Y-27632

To determine whether the proliferation ability of Y-27632 treated NHEKs is higher compared to the control cultures, proliferation assays were performed with Y-27632 treated and non-treated cells. The total cell number was analyzed via SYBR Green staining. The proliferation assay was performed in DermaLife medium without feeder in passage 2. We could confirm that Y-27632 treated NHEKs have a higher proliferation ability compared to the untreated control (Figure 17 A) as it was also shown for neonatal foreskin keratinocytes, for human ectocervical keratinocytes and human vaginal keratinocytes (Chapman et al., 2010).

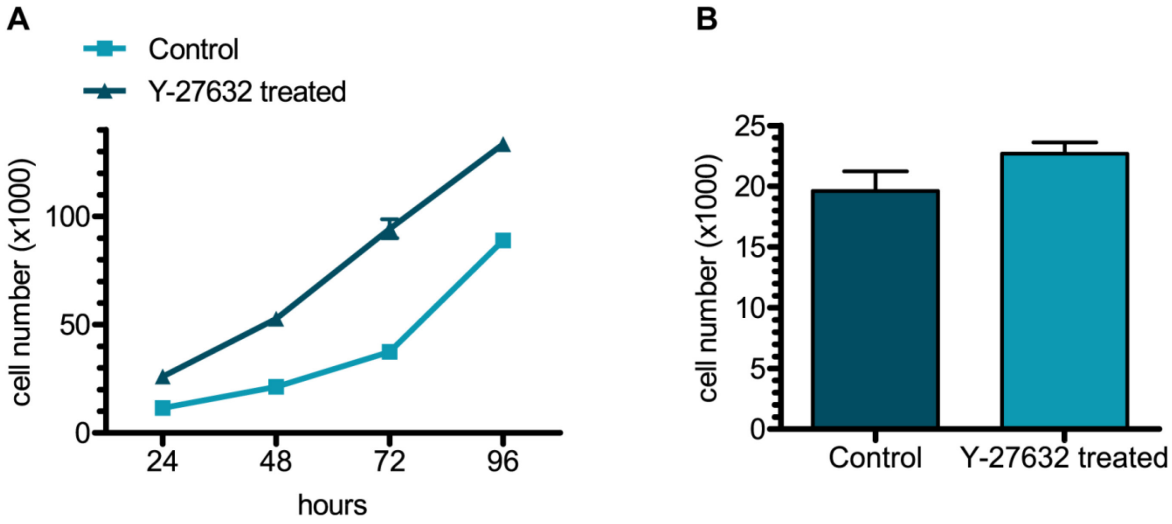

Figure 17: (A) In orders to perform a SYBR Green proliferation assay, defined numbers of NHEK were seeded in 24-well plates. Cells in passage 2 were cultured in the absence or presence of Y-27636 in low-calcium medium (without feeder). Plates were harvested at the indicated time points and the resulting number of cells was quantified by SYBR Green incorporation, compared to a well plate with defined cell numbers. Each measurement was performed in triplicates per time point. (B) Quantification of adherent NHEK in the presence or absence of Y-27632 following plating on collagen for 30 minutes. Cell number was determined via SYBR Green staining. (C) Growth rate of NHEK cultivated in the presence or absence of 10µM Y-27632 cultivated with feeder. The growth rate is measured as population doubling each passage. The proliferation assay was performed twice and one representative experiment is shown.

To support that increased cell numbers in Y-27632 treated cells are due to higher proliferation and not caused by increased attachment to the culture dish after seeding, we performed adhesion assays. Therefore plates were coated with collagen type I, subsequently NHEKs were seeded in DermaLife in the presence or absence of Y-27632, incubated for 30 minutes and washed with PBS.

To examine the total cell number SYBR Green staining was performed. The analysis showed that there was no difference in adhesion (Figure 17 B). Taken together, our results indicate that in the presence of Y-27632 proliferation of NHEKs is increased rather than increased attachment of the cells.

3.4.2 Rho kinase inhibitor suitable to expand H2B-GFP positive NHEKs

The cultivation of NHEKs in the presence of the Rho kinase inhibitor Y-27632 enables the cells for long-term cultivation over several passages. Consequently, the addition of Y-27632 to the culture medium could be used to expand H2B-GFP NHEKs. Therefore transduced H2B-GFP NHEKs, with a transduction efficiency of 90-96%, were sorted 48 hours after transduction for their GFP expression and cultivated in FAD medium with feeder cells in the presence of Y-27632 (1st sort). At a confluence of 80% H2B-GFP NHEKs were trypsinized and resorted for their GFP expression. The second FACSort showed that 90% of the cells were still positive for GFP expression, whereas about 10% of the H2B-GFP positive NHEKs have lost the GFP expression (Figure 18 A, 2nd sort). The resorted H2B-GFP NHEKs were cultivated again in the presence of Y-27632 and harvested at 80% confluency. The third sort revealed that the H2B-GFP expressing cells sustained GFP expression (Figure 18 A, 3rd sort). Furthermore, phase contrast images showed no morphological difference between transduced NHEKs in passage 4 in the presence of Y-27632 (Figure 18 C) compared to the control cells in passage 4 in the presence of Y-27632 (Figure 18 B, non transduced, + Y-27632). The morphology of transduced NHEKs in passage 4 with Y-27632 appeared as homogenous monolayers of small polygonal cells, resembling early passage NHEKs (Figure 18 C). As shown in Figure 4 D, all transduced NHEK, in passage 4, sustained H2B-GFP expression after resorting. Taken together, the expansion of a stable H2B-GFP expressing NHEK population after two times of FACSorting was feasible.

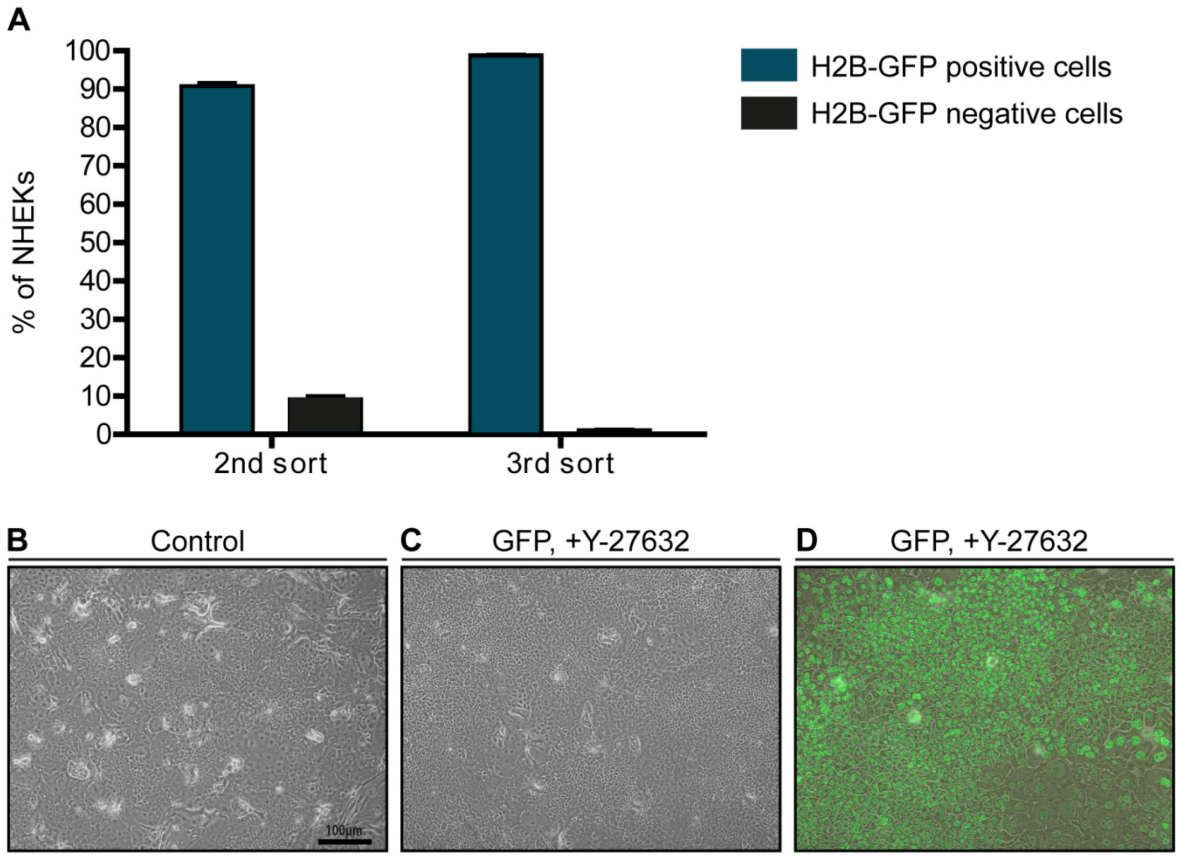

Figure 18: Stable Expression of GFP after second sort in presence of Y-27632. (A) Flow cytometric analysis of H2B-GFP positive population. 2nd sort: 90% of the H2B-GFP positive NHEK were sorted and cultivated in the presence of Dox, trypsinized at confluence and resorted for their GFP expression (3rd sort). Phase contrast images of Y-27632 treated NHEK (B) and Y-27632 treated transduced NHEK (C) in passage 4. (D) Y-27632 treated H2B-GFP positive NHEKs in passage 4 after two times of sorting. Overlay of phase contrast image and GFP expression (green, FITCS/GFP channel). GFP was assessed by fluorescence microscopy. Scale bar: 100µm. The experiment was performed in duplicates.

3.4.3 Rho kinase inhibitor does not support growth of transduced keratinocytes in OTCs

Next we wanted to determine whether H2B-GFP NHEKs in later passages, propagated in the presence of Y-27632, retained their capacity to form a stratified epithelium in OTCs. It was reported that foreskin keratinocytes treated for 18 passages with Y-27632 were able to establish a well differentiated epithelium in organotypic raft cultures (Chapman et al., 2010). However, Chapman et al. showed that differentiation into a stratified tissue of Y-27632 treated keratinocytes is only in the absence of Y-27632 possible (Chapman et al., 2010). Therefore H2B-GFP NHEKs, sorted twice by FACS, that had been cultured up to this point in the presence of Y-27632 were seeded on sca OTCs and cultured air exposed for 8 weeks without Y-27632 in the OTC media. As control cells, non-transduced NHEKs also in passage 4, cultivated in Y-27632 and resorted for two times, were used. As second control, NHEK in passage 2, non- treated with Y-27632, were seeded on sca OTCs. The histological analysis

was done in three independent experiments. There was no remarkable difference in the differentiation capacity between the control group in passage 2 (Figure 19 A) and NHEKs in passage 4, precultivated with Y-27632 and FASorted twice (Figure 19 B). However, H2B-GFP transduced keratinocytes, also in passage 4, previously expanded in the presence of Y-72632 and FACSorted twice, did not grow on OTCs (Figure 19 C). We could exclude that the H2B-GFP transduced NHEKs did not grow because of the sorting process, since the untransduced group pass through the same procedure and was also sorted twice. In summary, the Rho kinase inhibitor (Y-72632) is a valuable tool to expand transduced NHEKs and extend the lifespan of the cells in monoculture. Nevertheless, this method was not suitable to cultivate these cells in OTCs as they did not allow long-term growth in OTCs. Therefore, we performed OTCs with non-sorted transduced NHEKs in an early passage in further experiments.

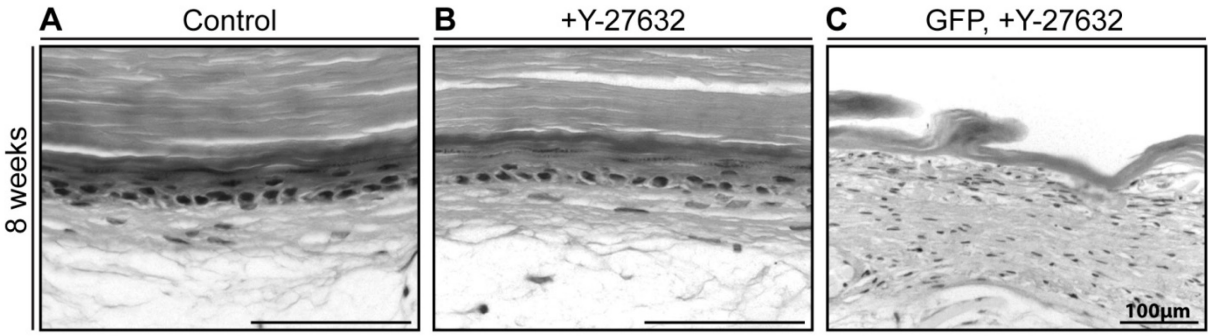

Figure 19: Histological Analysis of NHEKs precultivated with Y-27632 in passage 4 on sca OTCs after 8 weeks. Paraffin sections of these OTCs were fixed and stained with hematoxylin/eosin to visualize the morphology. (A) Control NHEK in passage 2, precultivation was in the absence of Y-27632. (B) NHEK precultivated in 10µM Y-27632 and seeded in passage 4 on OTCs. (C) H2B-GFP positive NHEK precultivated in 10µM Y-27632 and seeded in passage 4 on OTCs. Cultivation medium of OTCs was in all cultures in the absence of Y-27632. Scale bar: 100µm. Three independent experiments were performed and one representative experiment is shown.

3.5 Detection of LRCs in H2B-GFP OTCs

For pulse-chase experiments H2B-GFP keratinocytes were seeded on OTCs. The cultures were cultivated for the first two weeks without Dox (pulse period). This allowed the establishment of a homeostatic epithelium and the maturation of the stem cell niche while H2B-GFP is turned on. Subsequently, after 2 weeks, Dox is added to the culture medium in order to turn off the H2B-GFP (chase period). The H2B-GFP is declining in all cells in a proliferative associated manner; only slow cycling cells (LRCs) are able to keep the H2B-GFP label over time. At the end of the pulse period we detected, as already described under chapter 3.3.5, a decline in H2B-GFP positive cells in OTCs (Figure 20 A). However, after 6 weeks of chase, in the presence of Dox, we were able to detect basal LRCs in OTCs grown from H2B-GFP NHEKs (Figure 20 D, white arrow). Furthermore cluster of LRCs could be

observed after a chase period of 8 weeks (Figure 20 E) as well as after a chase period of 11 weeks (Figure 20 F). Moreover, analysis of OTCs grown with H2B-GFP transduced NHEKs, cultivated in the absence of Dox (expression of H2B-GFP), showed, that most of the cells were labeled in an 8 and 12 week old epithelium (Figure 20 B and C), hence demonstrating that expression was sustained also under 3D conditions.

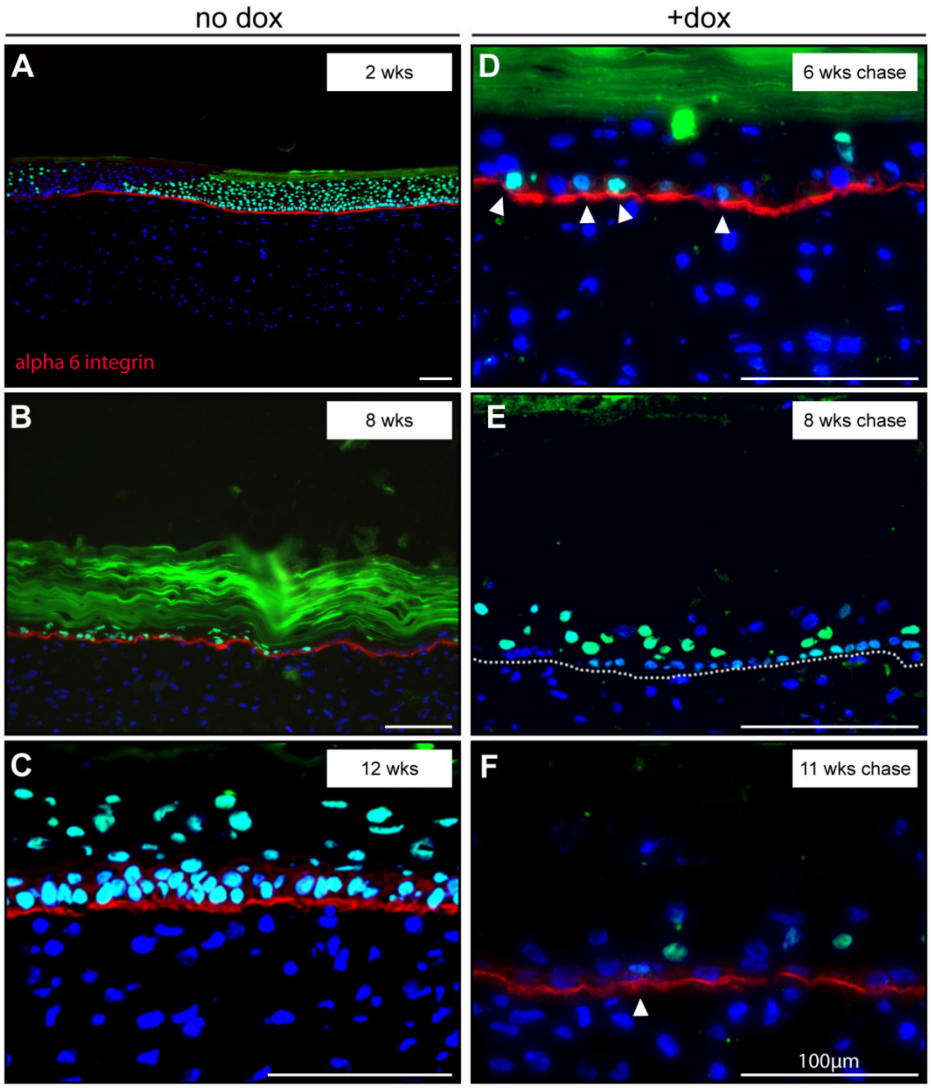

Figure 20: Detection of LRCs in H2B-GFP NHEK cultures. (A) OTCs from H2B-GFP transduced NHEKs were cultivated for two weeks in absence of Dox (expression of H2B-GFP, pulse period). OTCs from H2B-GFP transduced NHEK were cultivated for 8 weeks (8 wks) (B) or 12 weeks (12 wks) (C) in absence of Dox (expression of H2B-GFP). OTCs from H2B-GFP transduced NHEK were cultivated for two weeks in absence of Dox (pulse period) and then for 6 weeks (6 wks) (D) or 8 weeks (8wks) (E) or 11 weeks (11 wks) (F) in the presence of Dox in order to turn off the reporter (chase period) and to detect LRCs. White arrows: H2B-GFP positive LRCs. Cryosections were examined by immunofluorescence staining. Nuclei were stained with Dapi (blue). GFP expressed is shown in green. Basal cells were stained for α6 integrin (red) or the basement membrane is indicated by the dotted white line (E). Scale bar: 100µm. 5 independent experiments were performed and one representative experiment is shown.

3.6 Isolation of basal NHEKs from OTCs

To understand, characterize and assess the regenerative properties of the skin, the isolation of vital LRCs, the potential epidermal stem cells, is necessary. Therefore the aim of this study was to isolate LRCs after a chase period of minimum 6 weeks. It was shown that a chase period of 6 weeks is required to detect LRCs in OTCs (Muffler et al., 2008). The prerequisite to isolate vital LRCs is a single cell suspension of the epithelium. For this purpose a method was needed to obtain single cells from the epidermis of OTCs. To test the isolation method, 8 week-old OTCs grown from non-transduced NHEK were used. To separate the epidermis from the dermal part, OTCs were incubated with Dispase II (1mg/ml) for 2 hours at 37°C. Dispase II is an enzyme from *Bacillus polymyxa* and a gentle agent for the disruption of extracellular matrix of tissues and was shown to successfully separate epidermis from the dermis at the dermo-epidermal basement membrane (Kitano and Okada, 1983). With this enzymatic digestion the epithelium is effectively removed from the dermal part without dissociation of keratinocytes (Figure 21 A). Subsequently, the epithelial sheets were dissociated into single cell suspensions by trypsinization similar to a protocol described by Longley et al. and Okada et al. (Kitano and Okada, 1983; Longley et al., 1991). Notably, we used higher trypsin concentrations (0.4%) and shorter incubation times (3 min., 37°C). To specifically select for basal keratinocytes of the epidermis the cell suspension was stained for α6 integrin, a surface marker for basal keratinocytes. Moreover, the cell suspension was analyzed for the expression of Keratin 10, a marker for early differentiation of keratinocytes. The analysis was performed by flow cytometry. Almost 60% of the isolated cells were α6 integrin positive (Figure 21 B). Only 10% of the isolated cells were Keratin 10 positive (Figure 21 B). Concomitantly, also IIF stainings of cytospin slides of the analyzed experiments showed that mainly basal keratinocytes were isolated, most of the cells were α6 integrin positive (Figure 21 B). Taken together, with this approach it was possible to obtain a single cell suspension from the epidermis of OTCs. This should be a suitable method to select for GFP-positive basal LRCs.

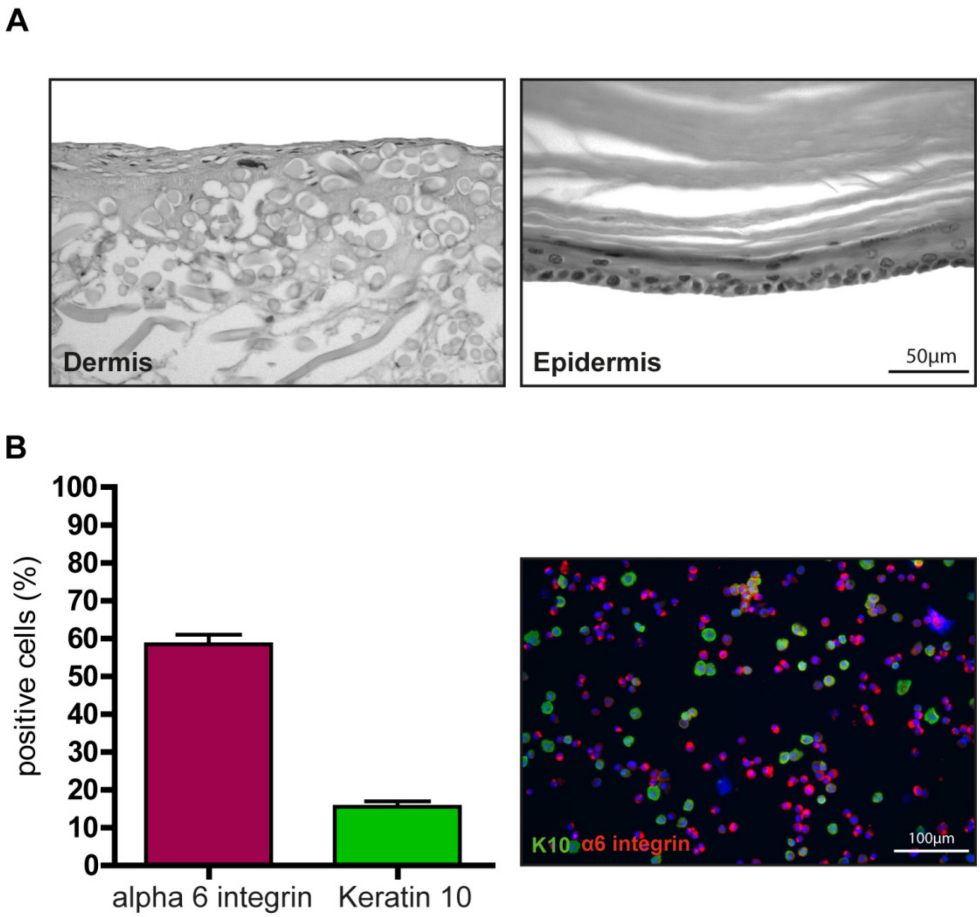

Figure 21: (A) Paraffin section of 8-week-old OTC grown from NHEK treated with Dispase II (1mg/ml) for 2 hours at 37°C. First images displayed the dermal part, the second image the epidermis. Sections were fixed and stained with hematoxylin/eosin. (B) Single cell suspension of the dissociated epidermal sheet was analyzed by flow cytometry. Epidermal suspensions were labeled with antibodies to α6 integrin, a marker for basal cell (shown in red) and Keratin 10, a marker for differentiated cells (in green). (C) Single cell suspension of an 8 week-old Epithelium on a cytospin slide. For Cytospin slides, single cell suspensions are spun onto a microscope slide by use of a cytocentrifuge. Nuclei are stained with Dapi (blue), α6 integrin, a marker for basal cell, is shown in red and Keratin 10, a marker for differentiated cells in green. The experiment was performed three times. One representative experiment is shown.

3.7 Isolation of vital LRCs

Having demonstrated that we were able to successfully isolate basal epidermal cells from OTCs we next aimed at isolating LRCs from OTCs. For this purpose keratinocytes, transduced with H2B-GFP, were cultivated in OTCs 2 weeks under the absence of Dox (expression of H2B-GFP, pulse period). In order to turn the H2B-GFP reporter, Dox was added to the culture medium during the following 6–8 weeks of cultivation (chase period). Only slow cycling cells kept their H2B-GFP expression and could be detected as LRCs. The epidermis of these OTCs was separated from the dermal equivalent using Dispase II, followed by trypsination as described in chapter 3.6.

The separation was checked for every experiment by histological analysis. To select for basal keratinocytes and in particular for the GFP-positive basal LRCs, the cell suspension was stained for α6 integrin. For the purification of vital LRCs FACSorting was performed. The cell suspension was sorted for α6 integrin positive basal cells and α6 integrin- GFP double positive cells (LRCs). The FACS analysis showed three distinct populations; α6 integrin positive cells (basal cells), α6 integrin GFP double positive cells (basal LRCs) and α6 integrin negative cells (suprabasal cells) (Figure 22 A). The range of isolated LRCs compared to the cell number of isolated basal cells from 7 independent experiments was between 1%-7,4%, with an mean value of 5% (Figure 22 B). By this method LRCs could be isolated even after 20 weeks of chase (Figure 22 B, experiment 7). Differences in the total amount of isolated basal cells and LRCs (Figure 22 B, 2nd and 3rd row) were due to different amounts of OTCs for the isolation (Figure 22 B, last row). Taken together, LRCs could successfully be purified from 7 independent preparations.

A

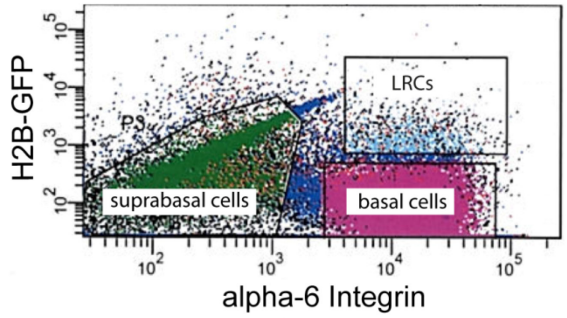

B

experiment #	absolute cell number basal cells	absolute cell number LRCs	% of isolated LRCs	chase in weeks	number of OTCs
1	321.000	21.000	6.5	7	11.5
2	432.000	32.000	7.4	6.5	18
3	160.000	10.000	6.3	6	8
4	1.346.900	30.900	2.3	6	32
5	35.500	2.500	7	8	6
6	4.638.000	52.000	1.1	7	35.5
7	54.563	563	1	20	4

Figure 22: (A) Illustration of the flow cytometric fractionation of single cell suspension of H2B-GFP NHEKs grown for 8 weeks on sca OCTs with a chase period of 6 weeks. The epidermal suspension was stained for α6 integrin, a marker for basal keratinocytes. Three distinct populations could be detected by flow cytometry. Population 1 (LRCs): α6 integrin positive and GFP positive. Population 2 (basal cells): α6 integrin positive and GFP negative. Population 3 (suprabasal): α6 integrin negative. (B) Overview about the fractionated isolations. LRCs making up between 1-7.4% of isolated basal cells. The isolated cell numbers of LRCs were between 563 cells and 52.000 cells. Cell numbers for basal cells were between $0.054x10^6$ and $4.6x10^6$. Chase period is shown in the fifth column. The number of OTCs which were used for the experiment is shown in the last row.

3.8 Global gene expression analysis of isolated LRCs compared to isolated basal cells of OTCs

To further characterize the isolated LRCs, a global gene expression analysis was performed. The expression profile of isolated LRCs, derived from OTCs after a chase period of 6-7 weeks, was compared to isolated basal cells (α6 integrin positive and GFP-negative) of the same preparation. The microarray analysis were carried out by the DKFZ “Genomics and Proteomics Core Facility” using Ilumina BeadChip HumanHT-12 v4 which allows to analyze the expression level of 31.000 annotated genes. The analysis was run with biological triplicates. The raw data were analyzed with Chipster (software for high throughput data) and further analyzed with Ingenuity pathway analysis (IPA) software. The cut off for the p-value was 0.05. Non-metric multidimensional scaling (NMDS), a method to display a multidimensional data in fewer dimensions, calculates euclidean distances between the samples in the dataset. These distances are visualized using a 2D-plot. Therefore increasing distances between sample points equates to more dissimilarity. In Figure 23 A the NDMS showed that samples LRC #2 and #3 as well as the control #1, #2 and #3 were clustering whereas the sample LRC #1 was located at a different position (Figure 23 A). Therefore LRC #1 was excluded from further analysis. The analysis with chipster, considering the statistical tests (see method), revealed that 102 genes were significantly differentially regulated (Table 5, appendix). The scatterplot in Figure 23 B is visualizing the differential analysis. Each dot represents the expression value of a gene, genes with equal expression values line up on the diagonal, whereas points below the diagonal represent genes with higher expression in the sample plotted on the x-axis (LRCs) and genes above have higher expression values in the sample plotted on the y-axis (control) (Figure 23 B). The further away the point is from the diagonal the larger is the expression difference. The scatter plot illustrated that there are more genes higher differentially expressed in LRCs than in basal cells (control) (Figure 23 B). The heatmap image of the statistically processed data is another method to visualize grouping of samples and showing the differentially regulated genes. The gene is colored according to its expression level in the data, red is overexpressed and blue underexpressed. This clarified the similarities of expression levels within the groups (LRCs vs. Control) (Figure 22 C).

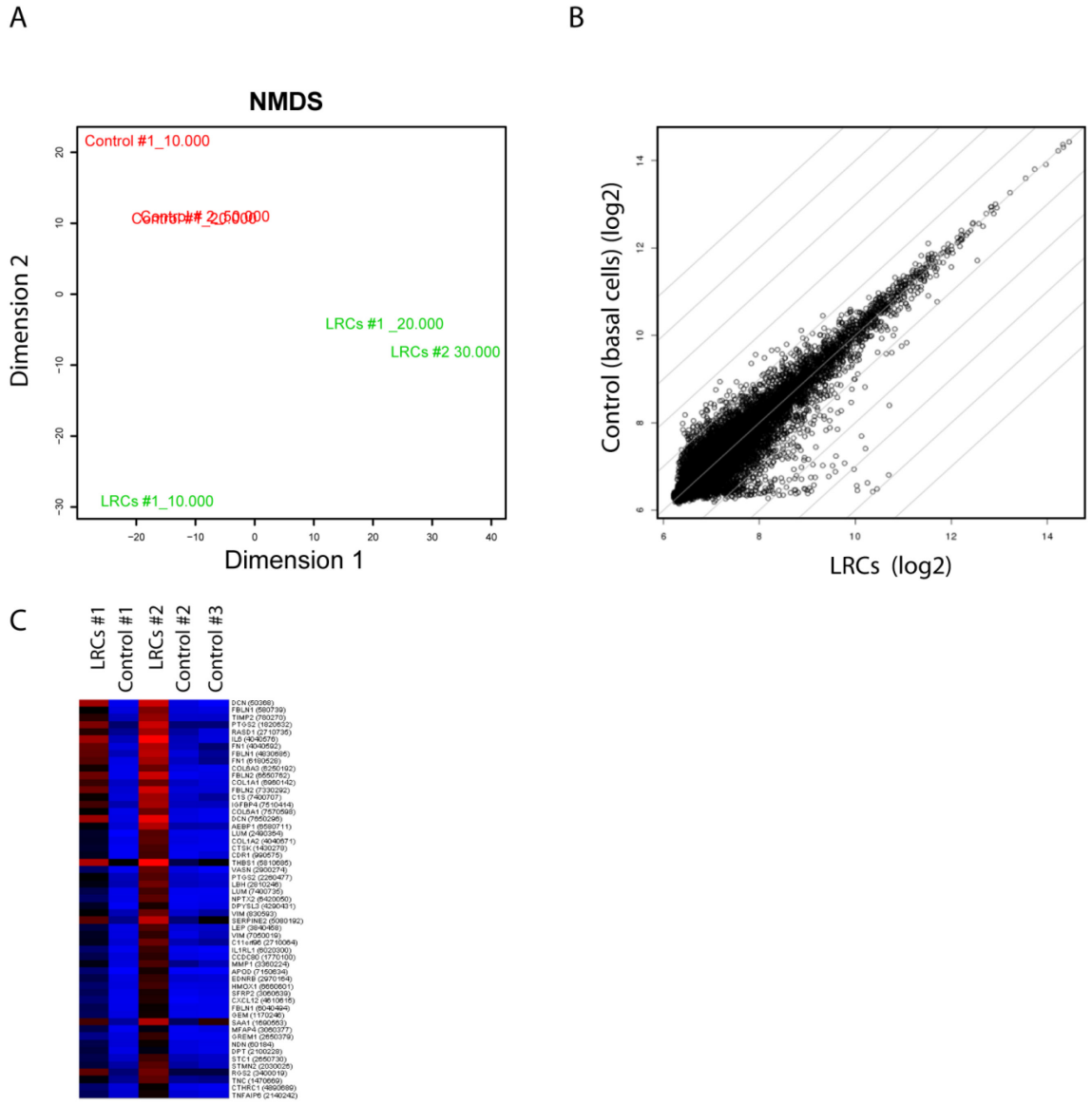

Figure 23: (A) Non-metric multidimensional scaling (NMDS) comparison of the different samples. LRCs (triplicates) are depicted in green, basal cells (triplicates) in red. NMDS was performed by chipster. (B) Differential analysis of the gene expression profiles. Fold changes and p-values of LRCs against controls. Each dot represents a gene and is differentially expressed if it is not located on the diagonal. Scatter plot was created by chipster. (C) Chipster software was used to visualize the grouping of samples as a heatmap image. Genes are colored according to their expression level in the dataset. Differentially overexpressed genes are colored in red or underexpressed genes in blue.

Table 2 shows the 20 top upregulated genes and the top 6 downregulated genes with the highest foldchange. The complete list with all 102 differentially regulated genes can be found in the appendix. A selection of differentially regulated genes, which are classified in different clusters, is summarized in table 3. Clustering was performed with Chipster using Reactome which creates gene lists for over-represented pathways. Notably, the most over-represented pathways were pathways regarding the ECM composition, ECM interaction and cell adhesion (Table 3).

A

	gene symbol	gene	foldchange
1	**DCN**	**decorin**	**22,40631251**
2	**IL6**	**interleukin 6 (interferon, beta 2)**	**19,27065005**
3	**FBLN2**	**fibulin 2**	**16,42134054**
4	**FN1**	**fibronectin 1**	**9,741653484**
5	**IGFBP4**	**insulin-like growth factor binding protein 4**	**9,285631315**
6	**TIMP2**	**TIMP metallopeptidase inhibitor 2**	**8,534657944**
7	**COL6A1**	**collagen, type VI, alpha 1**	**8,0556444**
8	**COL1A1**	**collagen, type I, alpha 1**	**7,981537412**
9	C1S	complement component 1, s subcomponent	7,754318535
10	RASD1	RAS, dexamethasone-induced 1	7,498835972
11	AEBP1	AE binding protein 1	7,34451216
12	**FBLN1**	**fibulin 1**	**7,279749911**
13	PTGS2	prostaglandin-endoperoxide synthase 2	6,700025873
14	CTSK	cathepsin K	6,415966756
15	**LUM**	**lumican**	**6,190259974**
16	**THBS1**	**thrombospondin 1**	**5,958709852**
17	VASN	vasorin	5,769048265
18	NPTX2	neuronal pentraxin II	5,540437872
19	DPYSL3	dihydropyrimidinase-like 3	5,502167273
20	**VIM**	**vimentin**	**5,256733755**

B

	gene symbol	gene	foldchange
1	DUSP6	dual specificity phosphatase 6	0,40
2	**HIST1H2BG**	**histone cluster 1, H2bg**	**0,39**
3	**HIST1H4H**	**histone cluster 1, H4h**	**0,39**
4	GOLGA7B	golgin A7 family, member B	0,38
5	CXCL14	chemokine (C-X-C motif) ligand 14	0,38
6	**KRT14**	**keratin 14**	**0,37**

Table 2: (A) Overview about the genes with the highest fold change. A selection of 20 genes found to be most differentially upregulated in LRCs compared to basal cells. (B) Overview with the top 6 downregulated genes. In bold are the genes which were validated by qRT-PCR.

Pathway	Genes mapped
Extracellular matrix organization	MMP1; DCN; FBLN1; FBLN2; COL1A2; NID1; LUM; ITGB4; COL1A1; COL4A1; LOXL4; COL3A1; FN1; TNC; THBS1; COL6A1; COL6A3; TIMP2; MFAP4; CTSK; KLK7; COL5A1
Collagen formation	MMP1; COL1A2; LOXL4; ITGB4; COL1A1; COL4A1; COL3A1; COL6A1; COL6A3; COL5A1
Collagen biosynthesis and modifying enzymes	COL5A1; COL1A1; COL6A1; COL4A1; COL6A3; COL3A1; COL1A2
Assembly of collagen fibrils and other multimeric structures	MMP1; ITGB4; COL6A1; COL6A3; COL4A1; LOXL4
Scavenging by Class A Receptors	COL3A1; COL1A2; COL1A1; COL4A1
Binding and Uptake of Ligands by Scavenger Receptors	COL1A1; SAA1; COL3A1; COL1A2; COL4A1
Degradation of the extracellular matrix	MMP1; DCN; CTSK; KLK7; TIMP2; NID1
Integrin cell surface interactions	THBS1; LUM; COL4A1; TNC; FN1
Syndecan interactions	ITGB4; THBS1; TNC
Molecules associated with elastic fibres	MFAP4; FBLN1; FBLN2

Table 3: Functional classification of differentially regulated genes. Clustering was performed with chipster using Reactome which creates gene lists for over-represented pathways. Shown are the top 10 hits.

Further analysis was done with Ingenuity pathway analysis (IPA) which is mapping data to biological processes and pathways as well as creating and modifying biological networks. The analysis showed a high involvement of genes associated with cellular assembly, organization and movement, cell death, survival, growth and proliferation (Table 4, Box A). Moreover the analysis predicted upstream regulators (Table 4, Box B). Particularly TGFβ was predicted to be upregulated and many upregulated genes from the dataset could be mapped to the TGFβ pathway (Table 4, Box C).

A

Top Bio Functions: Molecular and Cellular Functions		
Name	p-value	# Molecules
Cellular Movement	3.70E-22 - 6.75E-03	54
Cell Death and Survival	9.77E-10 - 6.75E-03	44
Cellular Growth and Proliferation	3.46E-09 - 6.08E-03	53
Cellular Assembly and Organization	4.81E-09 - 5.99E-03	23
Cellular Function and Maintenance	4.81E-09 - 5.99E-03	31

B

Top Upstream Regulators		
Upstream Regulator	p-value of overlap	Predicted Activation State
TNF	1.20E-14	
NEUROG1	1.88E-13	
TGFB1	1.03E-12	Activated
IL1A	7.73E-11	Activated
CTNNB1	1.32E-10	

C

TGFB1 pathway			
Genes in dataset	Prediction	Fold Change	Findings
VIM	Activated	2.555	Upregulates (18)
TNC	Activated	1.970	Upregulates (11)
SERPINA3	Activated	1.590	Upregulates (2)
PTGS2	Activated	2.935	Upregulates (3)
IL6	Activated	4.140	Upregulates (9)
HMOX1	Activated	2.160	Upregulates (10)
FN1	Activated	3.615	Upregulates (35)
COL6A3	Activated	3.095	Upregulates (1)
COL5A1	Activated	1.485	Upregulates (2)
COL3A1	Activated	1.810	Upregulates (1)
COL1A2	Activated	2.725	Upregulates (13)
COL1A1	Activated	2.915	Upregulates (25)
BGN	Activated	1.275	Upregulates (5)
THBS1	Inhibited	2.695	Downregulates (4)
MMP1	Inhibited	2.230	Downregulates (4)
FBLN1	Affected	3.630	Regulates (6)
IL1RL1	Affected	2.290	Regulates (1)
S100A4	Affected	1.680	Regulates (6)

Table 4: (A) Summary of the Ingenuity pathway analysis (IPA) which is mapping data to biological processes and pathways as well as creating and modifying biological networks. (B) Top Upstream Regulators predicted by Ingenuity pathway analysis (IPA). (C) Genes in the dataset which could be mapped to the TGFβ pathway. TGFβ is predicted to be up- or downregulated or affected, calculated on the fold change of genes in the dataset compared to the data in the literature (Findings).

3.9 Validation of Gene Array data by Real-Time-quantitative-PCR

From the genes that showed an increased expression level in basal LRCs compared to GFP-negative basal cells, 12 candidates were selected (Table 2, in bold) and their expression was validated by Real-Time-quantitative-PCR (qRT-PCR) (Figure 24). For the validation, RNA from four experiments was used; LRCs and the GFP-negative basal cells (referred as control) were evaluated. Two were identical to those of the microarray analysis and two were achieved from two other independent experiments.

3.9.1 Upregulation of ECM genes in LRCs

The global gene expression analysis of fractionated LRCs revealed that the top upregulated genes and associated networks were ECM components, the assembly of ECM as well as adhesion to the ECM via the major class, integrins (Table 3). This was an unexpected result, since those genes are generally expressed in fibroblasts in the dermal part. However, regarding the stem cell niche the ECM plays an essential role and can profoundly influence cell fate and the maintenance of stem cell homeostasis (Brizzi et al., 2012; Hall, 1989; Lu et al., 2012). Decorin, an important member of the ECM in the skin, was shown to be most highly upregulated (22.4 fold change) in the LRCs analyzed by the microarray. This could be also confirmed by qRT-PCR, in all tested samples the relative mRNA expression was highly increased (3300 fold) (Figure 24 A, third bar), however there was a high variance between the expression levels within the analyzed groups (between 36 fold and 5600 fold increased expression). Also other components of the ECM, like fibronectin, different collagens, fibulin 1 and fibulin 2 had elevated gene expression in LRCs analyzed by the mircroarray. The verification with qRT-PCR for collagen, type I, alpha 1 (COL1A1), confirmed enriched mRNA levels (700 fold) (Figure 24 A, second bar). Validation by qRT-PCR for fibulin 1 expression showed a 1000 fold upregulation. Likewise here we detected high variances between the expression levels within the analyzed groups (between 150 fold and 3200 fold increased expression). Fibronectin was about 40 fold increased (Figure 24 A), except of one group were the upregulation was only 2.4 fold. The relative mRNA expression of fibulin 2 in the analyzed LRCs was 7800 fold upregulated (Figure 24 A). Also here the expression levels had a high variance within the samples and were from 4 to 23.400. Lumican, a class II small leucine-rich proteoglycan, which also plays a key role in ECM organization (Schaefer and Iozzo, 2008), was shown to be 1.100 fold upregulated in LRCs (Figure 24 B) with expression levels between 11 and 4.230 fold within the analyzed groups.

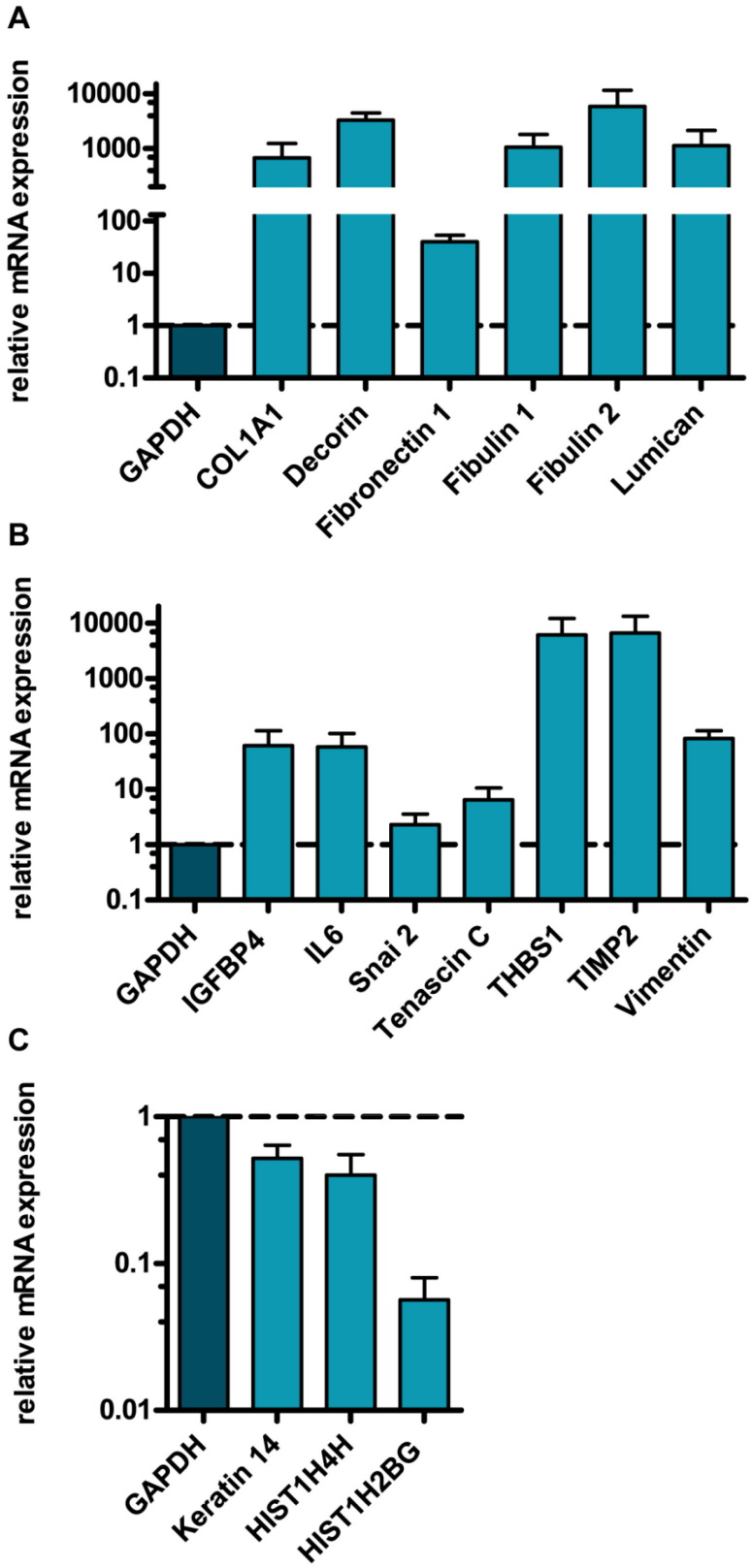

Figure 24: qRT-PCR confirmed microarray data. Two LRCs and basal cells from OTCs analyzed in the BeadChip HumanHT-12 v4 gene expression array and two independent LRCs and basal cells from OTCs not analyzed in the BeadChip HumanHT-12 v4 gene expression array were used. The relative mRNA expression of selected genes, which were upregulated in the mircroarray, were validated with qRT-PCR. The mRNA expression of the tested genes were normalized to the control and the housekeeping gene GAPDH, as described (Pfaffl, 2001). Controls were set to 1 (dashed line). Results are the mean of the four experiments.

Surprisingly, vimentin, an intermediate filament protein, which is primarily found in mesenchymal cells and a marker for fibroblasts (Franke et al., 1979b) was also upregulated in LRCs. The mRNA expression of vimentin was 90 fold upregulated confirmed by qRT-PCR, whereas also here in one group the upregulation was only 2.4 fold (Figure 24 B).

Thrombospondin-1 (THBS1) is a glycoprotein in the ECM that takes part in the cell-to-matrix communication through different pathways (Bornstein, 2001; Lawler, 2000; Sage and Bornstein, 1991; Taraboletti et al., 1990; Taraboletti et al., 1987) and is able to bind to fibronectin, laminins, collagens and other ECM proteins (Lahav et al., 1982). The microarray analysis revealed THBS1 as a 6 fold upregulated LRC transcript (Table 2). However, verification by qRT-PCR could not confirm the upregulation, since in two analyzed groups THBS1 expression was downregulated (0.06 fold and 0.002 fold). The mean value of THBS1 expression was 6.000 fold increased (Figure 24 B) because the expression was in the two other LRCs between 212 fold and 24.200 fold increased.

IGFB4 was shown to be highly upregulated (9 fold) in the microarray analysis (Table 2). IGFBP4 is an interesting target gene, since it binds and sequesters insulin growth factors and is thereby an inhibitor of the insulin pathway. The overexpression in LRCs may ensure that LRCs do not respond to IGF, a potent stimulant of epithelial proliferation (Bennett et al., 2003; Sadagurski et al., 2006; Vasioukhin et al., 2001) and therefore regulate the quiescent replicative arrest. This assumption is supported by the fact that IGFBPs were also found to be upregulated in quiescent fibroblasts (Goldstein et al., 1991), mouse hair follicle stem cells (Morris et al., 2004) and quiescent human foreskin keratinocytes (Schluter et al., 2011). Particularly IGFBP4 can also bind to the canconcial Wnt receptors, frizzled and LRP6, thereby block signal transduction by Wnt (Cruciat and Niehrs, 2013). Therefore, also the inhibition of Wnt could play a role in LRCs. However, the analysis by qRT-PCR could not confirm increased transcription in all LRCs, in two groups we detected an upregulation (between 22 and 220 fold), while in two groups we detected no regulation or a downregulation (0.7 fold) (Figure 24 B).

Tenascin c, also a member of ECM proteins and enriched in hair follicle stem cells (Morris et al., 2004) and bulge LRCs (Tumbar et al., 2004), was confirmed to be upregulated in LRCs (9 fold) determined by qRT-PCR (Figure 23 B).

In summary, we could confirm the upregulation of COL1A1, decorin, fibulin 1, fibulin 2, fibronectin, lumican, tenascin C and vimentin. Whereas, the upregulation of IGFBP4 and THBS1 was not confirmed by qRT-PCR.

3.9.2 Degradation of ECM possibly inhibited in LRCs

The microarray analysis revealed that LRCs expressed higher levels of TIMP2, a tissue inhibitor of metalloproteases (MMPs). MMPs are enzymes which are able to degrade all kinds of extracellular matrix proteins. Interestingly, TIMP2 was also upregulated in mouse hair follicle stem cells (Morris et al., 2004). The verification by qRT-PCR showed that the mean expression value of TIMP2 was 6.600 fold increased (Figure 24 B). Notably, also here the analyzed LRCs had a high variance in the mRNA expression levels, TIMP 2 was compared to the control cells between 9 and 26.500 fold upregulated. Our results indicate, that the upregulation of TIMP2 in LRCs could prevent the degradation of ECM proteins by MMPs.

3.9.3 No EMT in LRCs

Snai2 did not show up in the differentially regulated genes of the microarray, nevertheless there were hints that LRCs have phenotypic characteristics towards a more undifferentiated, mesenchymal phenotype e.g. the upregulation of vimentin (Figure 24 A). Since vimentin is also a marker for epithelial to mesenchymal transition (EMT) we wanted to exclude EMT of the LRCs. Therefore we tested the expression of Snai2 an inducer of EMT (De Craene and Berx, 2013). Interestingly, it was also shown that Snai2 can promote the transition of differentiated luminal cells to mammary stem cells (Mani et al., 2008). In addition Snai2 expression was detected in the nucleus of basal cells in the human IFE and depletion of Snai2 leads to enhanced Keratin 10 expression, a differentiation marker. It was suggested that Snai2 can bind to differentiation promoting transcription factors and thereby regulate the undifferentiated state of basal keratinocytes (Mistry et al., 2014). Therefore, Snai2 was an interesting target and the expression of snai2 was analyzed. The mean gene expression of snai2 in LRCs was slightly upregulated (3 fold) (Figure 24 B). However, since in two groups of LRCs the expression was either not regulated (1.1 fold) or even downregulated (0.44 fold) we could not verify a specific upregulation of snai2 by qRT-PCR. Summarizing that we have no indication that snai2 does play a role in the state of LRCs nor we have EMT in the isolated LRCs.

3.9.4 Upregulation of the cytokine IL6 in LRCs

Interleukin 6, IL6, mRNA was the second highest upregulated gene in the analyzed LRCs (19 fold) by the microarray (Table 2). IL6 acts as a multifunctional cytokine and regulates a broad range of inflammatory processes and stimulates immune responses (Kishimoto, 1989). Nonetheless, it was shown that IL6 expression in the skin has no direct prooinflammatory

activity (Turksen et al., 1992). Instead, it was demonstrated that IL6 expression did not enhance epidermal proliferation but was responsible for increased thickening of the stratum corneum (Turksen et al., 1992) and is an important regulator of the epidermal barrier (Wang et al., 2004). Moreover, it was proposed that IL6 regulates the survival and self-renewal in hematopoietic stem cells and early progenitors (Bernad et al., 1994). IL6 was confirmed to be upregulated by qRT-PCR with a mean fold change of 75 (Figure 24 B). Whereas the expression levels in the analyzed groups ranged from 11 to 189. However, the role of increased expression levels of IL6 in LRCs of the IFE is elusive and needs further investigations.

3.9.5 Downregulation of Keratin 14 and histone clusters indicate reduced proliferation of LRCs

Keratin 14, a marker of basal cells (Byrne et al., 1994; Coulombe et al., 1989), was downregulated in LRCs analyzed by the microarray. This result was verified by qRT-PCR, where Keratin 14 was downregulated with a fold change of 0.5 (Figure 24 C). It was suggested that downregulation of Keratin 14 results in reduced cell proliferation and that Keratin 14 expression plays a role in the maintenance of cell proliferation in the basal layer (Alam et al., 2011). Therefore, downregulation of Keratin 14 could also lead to a reduced proliferation of LRCs.

Interestingly, mRNA transcripts for different histone clusters were also downregulated, revealed by the microarray analysis (table 2). It was shown that cells which progress from G1 to S phase have an increased rate of histone gene transcription (Harris et al., 1991; Marzluff and Duronio, 2002). The Expression of the histone cluster 1, H4h (HIST1H4H) (0.4 fold change) and the histone cluster 1, H2bg (HIST1H2BG) (0.05 fold change) was downregulated confirmed by qRT-PCR (Figure 24 C) in LRCs. Therefore this could be a hint for a reduced cell proliferation in LRCs.

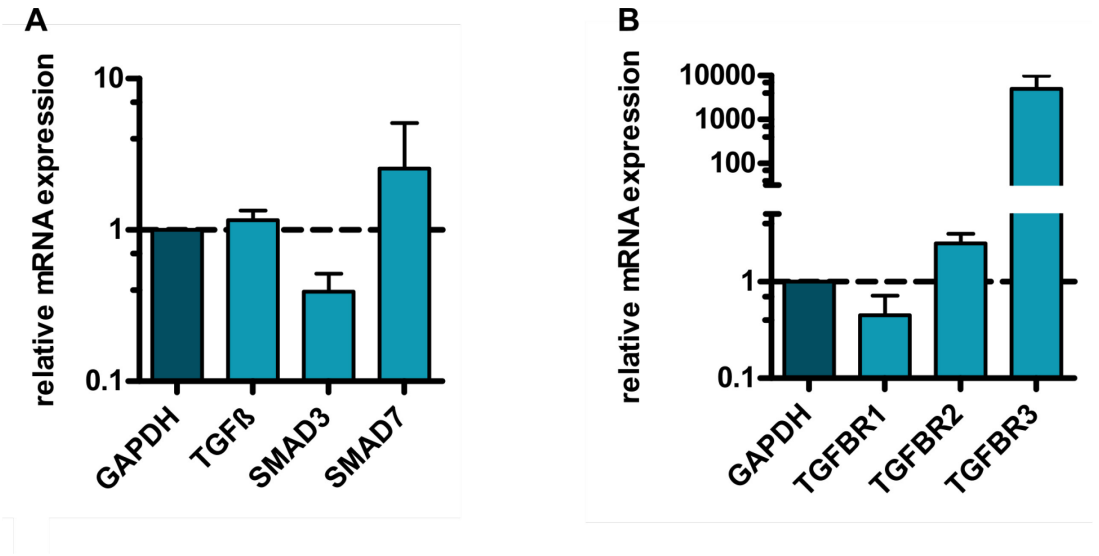

Figure 25: qRT-PCR revealed upregulated of TGFβ receptor 3. One sample of LRCs and basal cells from OTCs analyzed in the BeadChip HumanHT-12 v4 gene expression array and two independent LRCs and basal cells from OTCs, not analyzed in the microarray, were used. The relative mRNA expression of TGFβ, Smad3, Smad7, TGFβ receptor 1 (TGFβR1), TGFβR2 and TGFβR3 were validated with qRT-PCR. The mRNA expression of the tested genes were normalized to the control and the housekeeping gene GAPDH, as described (Pfaffl, 2001). Controls were set to 1 (dashed line). Results are the mean of the three experiments.

3.10 Role of TGFβ in LRCs

Although transforming growth factor-β (TGFβ) did not show up in the list of differentially regulated genes in the expression array analysis, the ingenuity pathway analysis (IAP) revealed TGFβ as one of the top upstream activators (Table 4). TGFβ signaling is known to be essential for the regulation of cell growth, development, and stem cell renewal and differentiation (Massagué and Chen, 2000; Patterson and Padgett, 2000; Ten Dijke et al., 2002, 2009, Miyazono). Moreover it was shown that TGFβ signaling inhibits the proliferation of keratinocytes (Massague andWeinberg,1992). Thus, TGFβ may be an interesting target as it may regulate the slowly cycling of the LRCs. Accordingly, the expression of TGFβ, the TGFβ receptors and Smad3 and Smad7 was analyzed. Smad proteins, like Smad3, are mediating signals from the cell membrane to the nucleus (Derynck et al., 1998; Massagué, 1998), whereas Smad7 acts as an endogenous Smad pathway inhibitor. We did not find differences in the expression level of TGFβ (Figure 25 A). Smad3 was slightly downregulated (0.4 fold change). Furthermore, the mean expression of Smad7 was upregulated (5 fold) (Figure 24 A), but was strongly downregulated (0,002 fold) in one group. Taken together, there were no differences in the expression of TGFβ or Smad3 and Smad7.

The TGFβ receptor type I showed a slight down-regulation (0.6 fold change) whiles the TGFβ receptor type II was slightly upregulated (2.5 fold) in the LRCs (Figure 25 B). Interestingly, the TGFβ receptor type III (TGFβR3) was strongly upregulated (5.000 fold) (Figure 25 B).

TGFβR3, also named as betaglycan, is located at the cell surface and was shown to bind all three TGFβ isoforms with high affinity (Kaname and Ruoslahti, 1996). Betaglycan presents TGFβ to the TGFβR2 and promotes the binding of TGFβ, thereby regulating the availability of TGFβ to the cell. Betaglycan can serve as reservoir for TGFβ (Blobe et al., 2001; Lopez-Casillas et al., 1991). However, betaglycan has no intrinsic TGFβ signaling activity (Andres et al., 1991; Cheifetz et al., 1987). Notably, there were observations that also other members of the TGFβ superfamily, like the bone morphogenetic proteins BMP-2 and BMP-7 are able to bind to betaglycan which is increasing the binding of BMPs to the their receptors (Kirkbride et al., 2008). Taken together, the qRT-PCR results do not support an upregulation of the TGFβ pathway, whereas increased betaglycan expression could indicate higher availability of TGFβ.

3.11 No increased ECM protein expression of LRCs

As a first attempt to investigate whether RNA upregulation was also effective for protein expression of selected target genes with elevated mRNA expression, indirect immunofluorescence (IIF) stainings were performed. For the staining, sections of OTCs from the analyzed isolated LRCs were used. There was a strong expression of fibronectin in the dermal part and the basement membrane (Figure 26 A). However, with conventional detection methods no apparent difference of protein expression in LRCs (Figure 26 A, white arrows) and basal cells equally in the inherent underlying basement membrane was seen. This was also for thrombospondin-1, vimentin and decorin the case (Figure 26 B, C, D). Nevertheless, since this was only a first attempt to investigate the protein expression of ECM components in LRCs more effort has to be taken to explore this further.

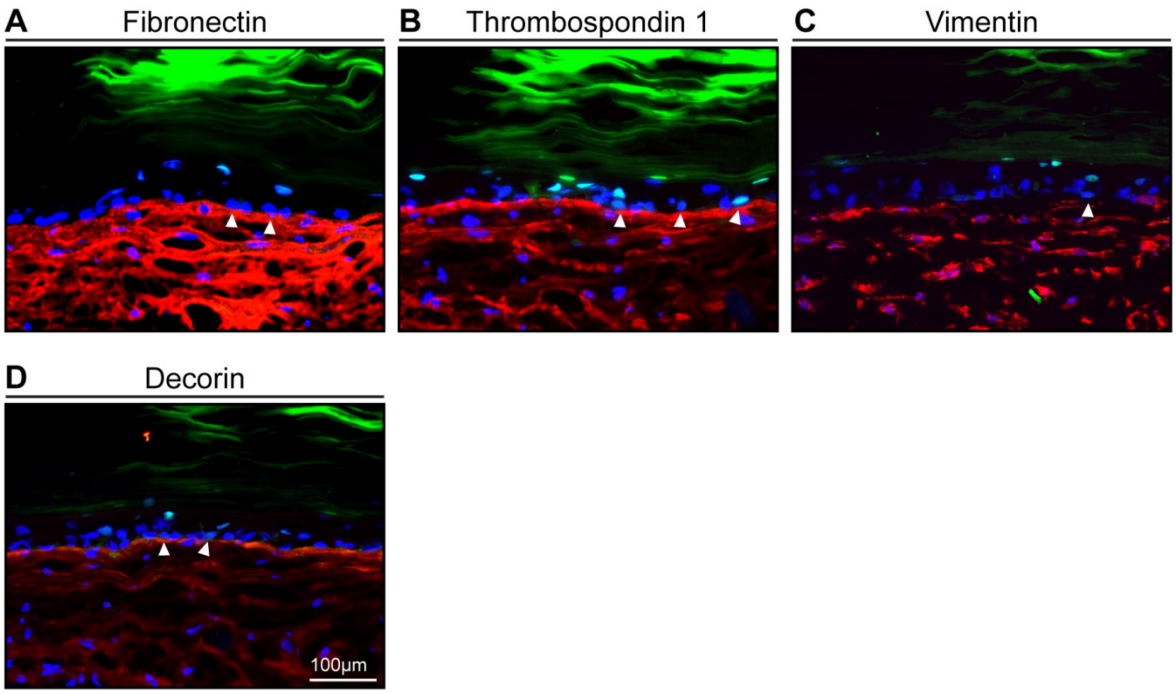

Figure 26: Protein expression of ECM molecules and vimentin in LRCs vs. basal cells. Cryosections of 8-week-old OTCs (sca OTCs with 6 weeks chase) grown from H2B-GFP NHEK used for the microarray were fixed and then analyzed by immunofluorescence staining for the expression of (A) Fibronectin and (B)Thrombospondin-1 (Thbs1) and (C) Vimentin as well as (D) Decorin. Stainings all shown in red. GFP is shown in green. Nuclei were counterstained with Dapi. LRCs: white arrows. Scale bar: 100µm.

3.12 Induction of a LRC phenotype *in vitro* by TGFβ stimulation

The ingenuity pathway analysis (IAP) associated many genes, which were upregulated in the microarray analysis, to the TGFβ pathway (Table 4 C). Moreover, our results showed an increased TGFβR3 (betaglycan) expression (Figure 25 B), which was shown to enhance the TGFβ dependent signaling by increasing the affinity of the ligand to TGFβR2 (Lopez-Casillas et al., 1993; Sankar et al., 1995). Therefore, we wanted to test if TGFβ can induce the expression of target genes, found in the microarray, in NHEKs in 2D cultures. It was already shown that TGFβ can induce a more mesenchymal phenotype with higher vimentin and fibronectin expression (Miettinen et al., 1994). NHEKs were cultivated in low-calcium medium (DermaLife) and treated either with 1ng/ml or 5ng/ml TGFβ-1 for up to 7 days. Gene expression was analyzed after 8 and 48 hours as well as 3 and 4 days. First results showed, that there was an early induction of vimentin (2.2 fold), thrombospondin-1 (THBS1) (2.3 fold), fibronectin (3.4 fold), Interleukin 6 (IL6) (2.6 fold), collagen, type I, alpha 1 (COL1A1) (3 fold) and tenascin C (3.3 fold) 8 hours after TGFβ treatment (Figure 27). After 2 days the relative mRNA expression of vimentin, THBS1, fibronection and IL6 decreased slightly, whereas the expression of COL1A1 (fold change 1.1) was not regulated or for tenascin C even slightly downregulated (0.9 fold, Figure 27). After 4 days of treatment with 1ng/ml TGFβ-1 vimentin

was 3 fold increased, also fibronectin, IL6 and COL1A1 were slightly upregulated while there was no difference in the expression levels of THBS1 and tenascin C between 48 hours and 4 days (Figure 27). However, there was increased expression of vimentin (5.4 fold), THBS1 (2.8 fold), fibronectin (20.5 fold), Il6 (22.6 fold), COL1A1 (4.3 fold) and Tenascin c (3.3 fold) in NHEKs after treatment with 5ng/ml after 3 days (Figure 27). There was no difference in the expression level of fibulin 1 independent of the time and concentration of TGFβ treatment (Figure 27). Even though there were indications that for instance in human airway smooth muscle cells TGFβ induced Fibulin1C mRNA expression (Lau et al., 2010). Taken together, it was possible to slightly induce genes, which had elevated expression levels in LRCs, by TGFβ stimulation, whereas treatment with higher TGFβ-1 concentrations (5ng/ml) seems to be required.

To determine if TGFβ-1 stimulation also causes a downregulation of the histone clusters, as seen in LRCs, we also analyzed the expression of histone Cluster 1, H2bg (HIST1H2BG) in TGFβ treated NHEKs. We could determine a slight upregulation of HIST1H2BG (1.8 fold) in NHEKs stimulated with 5ng/ml TGFβ for 3days (Figure 27). Therefore, stimulation with TGFβ-1 did not lead to a decrease in histone cluster expression.

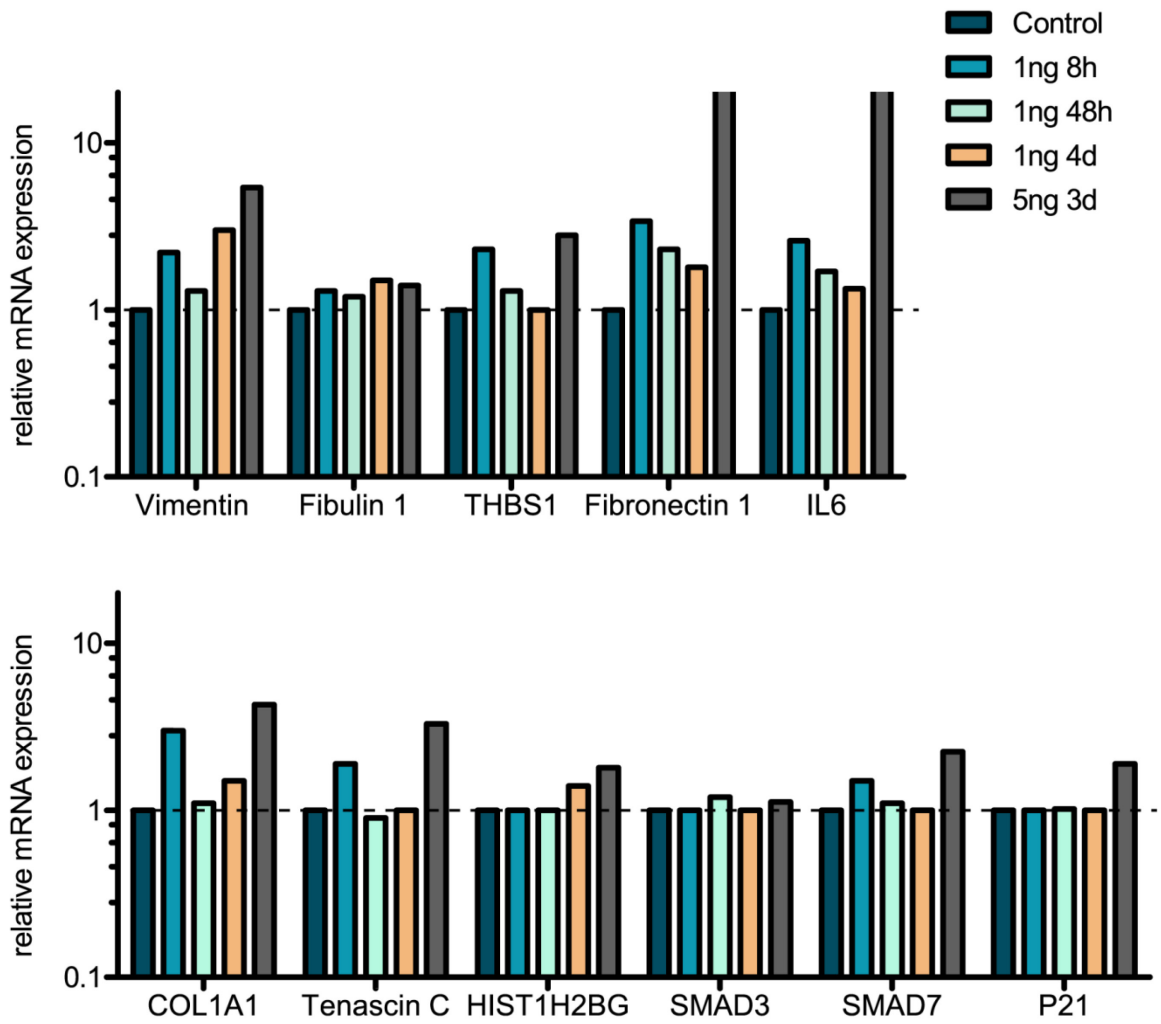

Figure 27: To characterize the effect of TGFβ stimulation NHEKs were cultivated in DermaLife without feeder for 8h, 48h and 4days with 1ng/ml TGFβ-1 or for 4days in 5ng/ml TGFβ-1 in 2D. Cells were harvested for total RNA-isolation and were subjected to qRT-PCR using primers specific for Vimentin, Fibulin 1, Thrombospondin-1 (THBS1), Fibronectin, Interleukin 6 (IL6), collagen, type I, alpha 1 (COL1A1), Tenascin C, Histone Cluster 1, H2bg (HIST1H2BG), SMAD3, SMAD7 and Cyclin-Dependent Kinase Inhibitor 1A (P21) to quantify relative mRNA expression. The mRNA expression of TGFβ stimulated samples was normalized to the unstimulated control and the housekeeping gene GAPDH, as described by (Pfaffl, 2001). Controls were set to 1 (dashed line).

3.13 TGFβ pathway is activated upon stimulation with high concentrations of TGFβ in NHEKs cultivated in low-calcium medium

In order to analyze if the TGFβ pathway is activated in NHEKs treated with different TGFβ concentrations in 2D, we looked for the expression of Smad3, Smad7 and the cell cycle inhibitor P21 by qRT-PCR. TGFβ was shown to induce the expression of cell cycle inhibitors, like Cyclin-Dependent Kinase Inhibitor 1A (P21) and cyclin-dependent kinase inhibitor 2B (P15) (Buschke et al., 2011; Datto et al., 1995; Hannon and Beach, 1994; Massague, 2000; Reynisdottir et al., 1995). We detected only a slight increase of P21 expression (2 fold) after treatment with 5ng/ml TGFβ for 3days (Figure 27). Furthermore there was no upregulation of SMAD3 in stimulated NHEKs (Figure 27). The expression of the endogenous Smad pathway

inhibitor, SMAD7, is induced by TGFβ (Buschke et al., 2011; Itoh et al., 2000; Massague and Chen, 2000; Moustakas et al., 2001). Smad7 was slightly upregulated (2.2 fold) after TGFβ stimulation for 3 days with 5ng/ml (Figure 27). In summary, these data do not support an activation of the TGFβ pathway in NHEKs treated with TGFβ-1 in monoculture.

Therefore, we determined the phosphorylation status of the intracellular mediators of TGFβ signaling, Smad3, in response to TGFβ treatment in NHEKs by IIF. Expression of phospho-Smad3 was detected partially in NHEKs in response to 5ng/ml TGFβ (for 48 hours) whereas upon treatment with 10ng/ml (for 48 hours) a strong phosphorylation of Smad3 was observed compared to the untreated control cells (Figure 28 A). This demonstrated that upon treatment with 5ng/ml TGFβ-1, the TGFβ pathway was not activated in all cells, whereas this was the case upon treatment with 10ng/ml TGFβ-1.

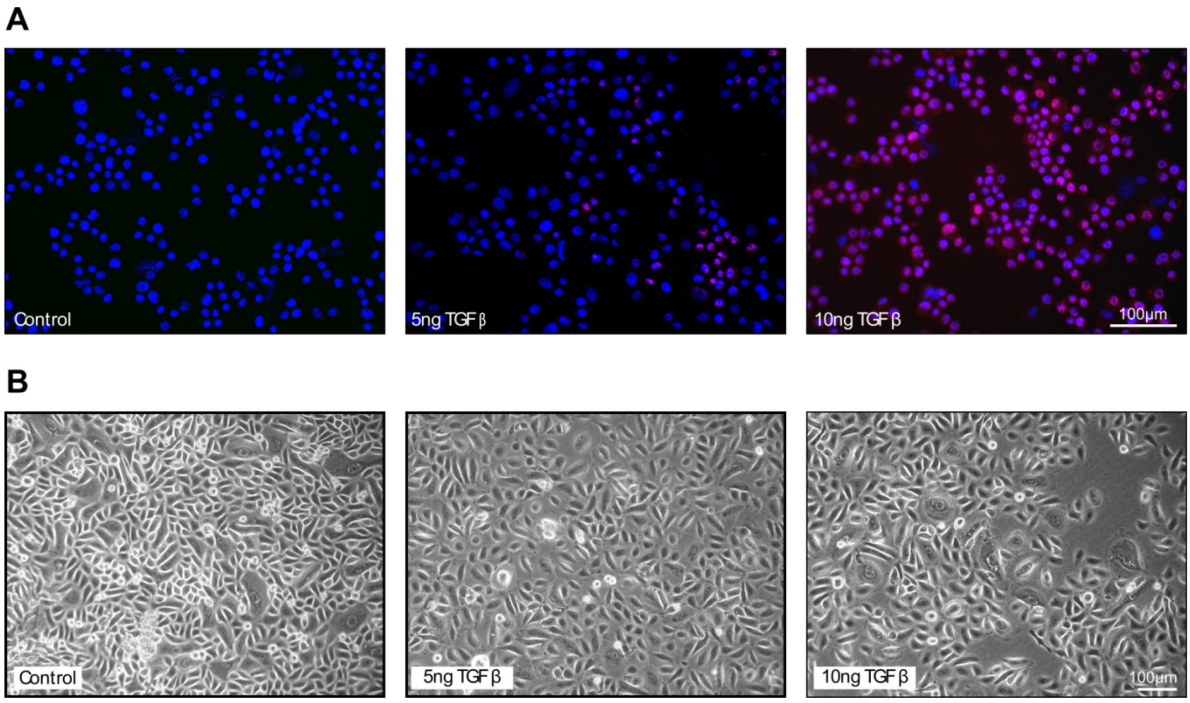

Figure 28 (A) Single cell suspension of NHEKs treated for 48h with 5ng/ml or 10ng/ml TGFβ or the unstimulated Control on a cytospin slide. Nuclei are stained with Dapi (blue), Phospho-Smad3 staining is shown in red. (B) Phase contrast images of NHEKs in passage 2 treated with 5ng/ml or 10ng/ml TGFβ for 3days compared to the unstimulated Control. Scale bar: 100µm.

3.14 Influence of TGFβ on the proliferation of NHEKs in low-calcium medium

TGFβ is known for the inhibition of the proliferation of keratinocytes in 2D cultures (Massague and Weinberg, 1992). To confirm that also NHEKs used for our 3D experiments are sensitive to TGFβ-dependent growth inhibition, NHEKs were supplied with 10pg to 1ng/ml TGFβ-1 in monolayer cultures for up to 7 days. Counting cell numbers showed that the presence of TGFβ in a concentration up to 1ng/ml had no influence on the proliferation of

keratinocytes in low-calcium medium (Figure 29 A). Only treatment with a concentration of 5ng/ml led to decreased proliferation (30%) already after 24 hours (Figure 29 B). NHEKs treated from passage 2 over several passages with low concentrations (1ng to 1pg/ml) showed decreased proliferation (Figure 29 C), this effect became even more pronounced in the presence of 1ng/ml (Figure 28 C).

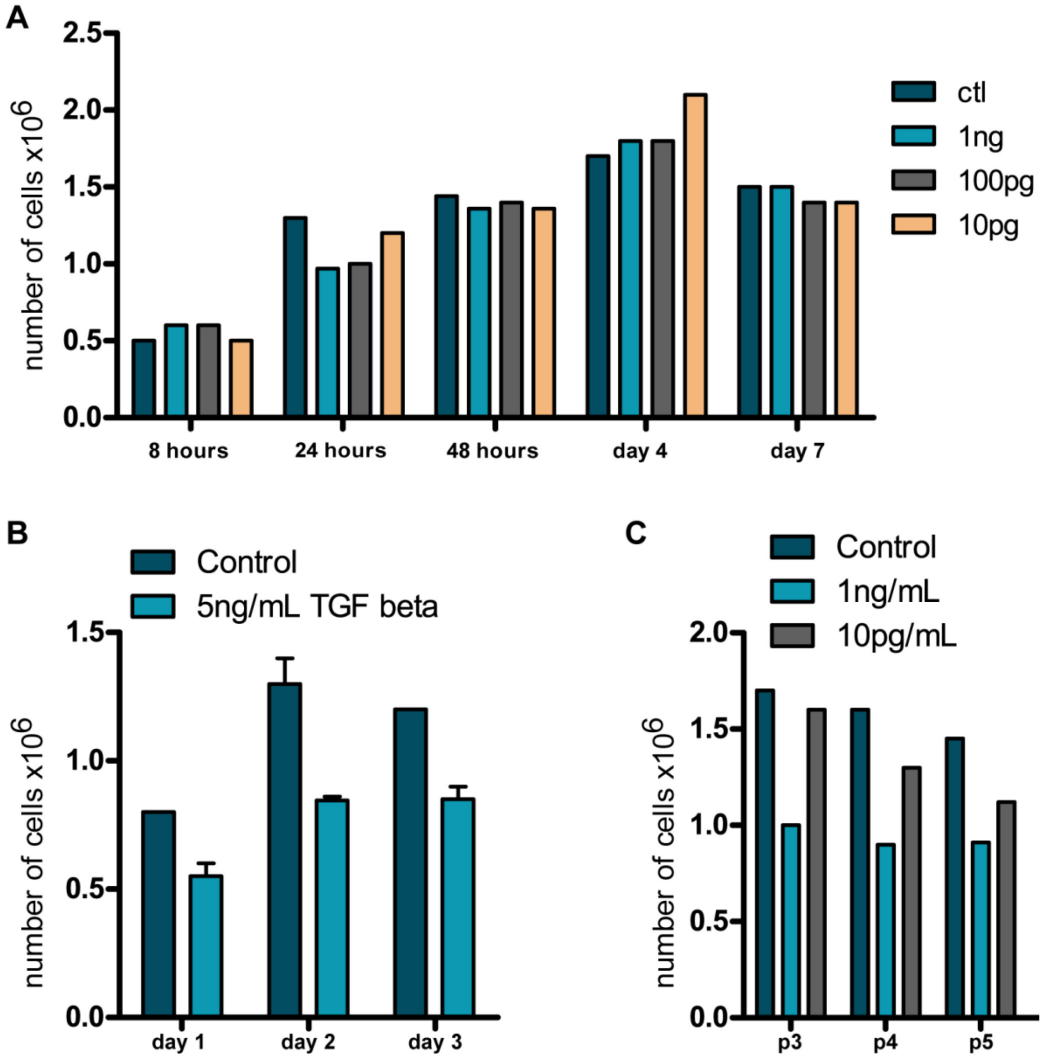

Figure 29: (A) NHEK in passage 2 cultivated in low-calcium medium (without feeder) were stimulated for 8h, 24h, 48h, 4days and 7days either with 10pg/ml, 100pg/ml or 1ng/ml TGFβ and compared to the unstimulated Control. Cells were trypsinized and counted at each timepoint. (B) NHEK in passage 2 cultivated in low-calcium medium (without feeder) were stimulated for 1, 2 and 3days with 5ng/ml TGFβ and compared to the unstimulated Control. Cells were trypsinized and counted at each timepoint. Cell counting was performed in duplicates per time point. (C) NHEK in passage 3 (p3), p4, p5 and p6 were cultivated in low-calcium medium (without feeder) and were stimulated from passage 2 continuously either with 10pg/ml or 1ng/ml TGFβ and compared to the unstimulated Control. Cells were trypsinized and counted at each timepoint

Phase contrast images of NHEKs treated with 5ng/ml or 10ng/ml showed upon treatment of 5ng/ml only a slight effect on the proliferation (Figure 28 A), whereas treatment with 10ng/ml of TGFβ-1 had an enhanced inhibiting effect on the proliferation of NEHK (Figure 28 B). These data clearly demonstrated that TGFβ-1 stimulation with low concentrations (1ng to 1pg/ml) for up to 7 days did not influence the proliferation of NHEKs. Inhibition of proliferation is achieved only upon stimulation over several passages with low concentration or treatment with higher TGFβ-1 concentrations (5-10ng/ml) in low-calcium medium.

3.15 TGFβ stimulation increased ECM protein expression in 2D cultures

To analyze protein expression of target genes which are involved in TGFβ signaling and were shown to be upregulated after stimulation with TGFβ-1 in NHEKs (Figure 27), indirect immunofluorescence (IIF) staining was performed. Therefore, NHEKs were harvested after 3 days of treatment with 5ng/ml TGFβ-1. Single cell suspensions of these NHEKs are spun onto a microsc*ope* slide and IIF stainings were performed. There was a strong upregulation in protein expression of decorin after treatment with TGFβ for 3 days with 5ng/ml (Figure 30 A). Furthermore increased expression of fibronectin and vimentin was observed after stimulation with TGFβ-1 (Figure 30 B, C). These data confirmed increased protein expression in NHEKs after stimulation with TGFβ-1 of target genes shown in the microarray.

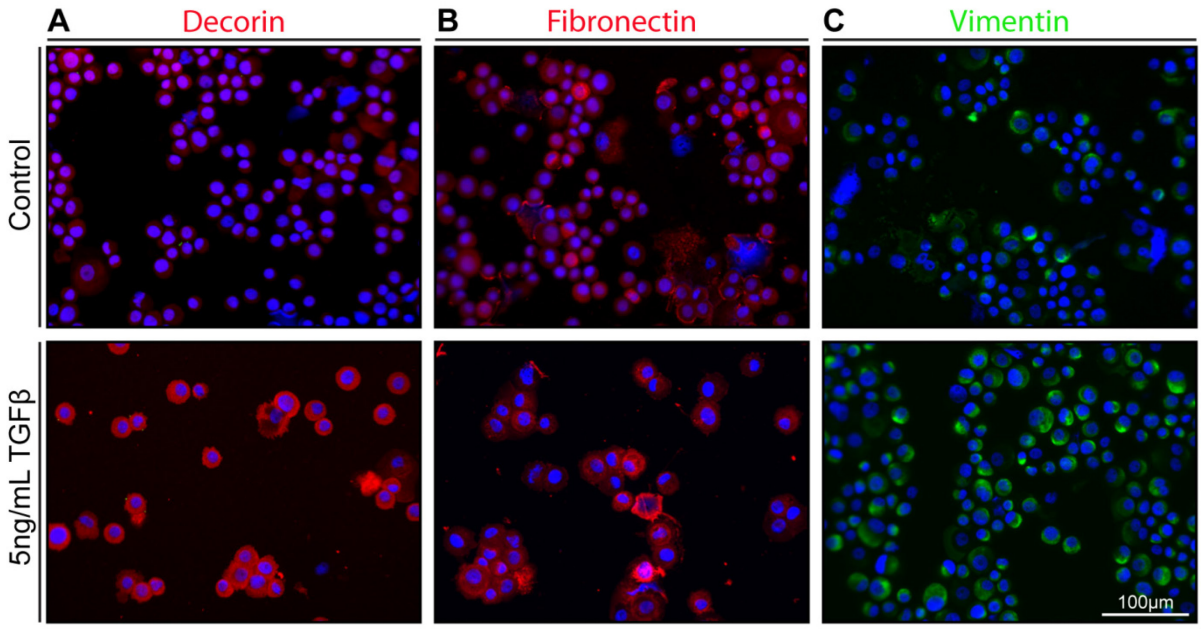

Figure 30: Single cell suspension of NHEK treated for 3days with 5ng/ml TGFβ (lower panel) or the unstimulated Control (upper panel) on a cytospin slide. Nuclei are stained with Dapi (blue), Decorin and Fibronectin staining is shown in red. Vimentin staining is shown in green. Scale bar: 100µm.

3.16 Clonal Analysis in OTCs

Several studies suggested that 1-10% of the basal cells are stem cells (reviewed in (Kaur, 2006)). We wanted to investigate how many stem cells in OTCs are required to maintain the epidermis long-term. Linear amplification-mediated PCR (LAM-PCR) is a powerful tool to study cell kinetics in OTCs. With LAM-PCR it is possible to identify the integration site of lentiviral vectors in the cellular genome (Schmidt et al., 2007; Schmidt et al., 2009). This integration site serves as a unique molecular marker for each transduced cell and its clonal progeny. Using H2B-GFP transduced NHEKs allows tracking of individual vector integration sites and studying the clonal distribution in OTCs. For the analysis, H2B-GFP NHEKs were FACSorted for their GFP expression, expanded in 2D and seeded on fdm OTC. After 2, 6, 9 and 12 weeks, respectively, the epidermis was separated from the dermis and the DNA of the epidermis was isolated. LAM-PCR was performed by the group of Prof. Hanno Glimm (DKFZ, Heidelberg). After 2 weeks of cultivation 186 individual clones could be detected (Figure 31). After 6 weeks, we saw a strong decline of the number of detected clones, only 22 clones could be found. After 9 weeks 4 clones could be detected on average which maintain the entire epithelium of the OTCs. After a cultivation period of 12 weeks, only a single clone is responsible for maintaining the epidermis of the OTC. Although this approach did not provide any information about the average size of the clones during the cultivation in OTCs, these studies revealed that the number of clones progressively decreased in OTCs over time which confirmed studies in the mouse tail skin epidermis (Clayton et al., 2007). Moreover, our data suggest that only a single stem cell is able to maintain epidermal regeneration of the entire OTC.

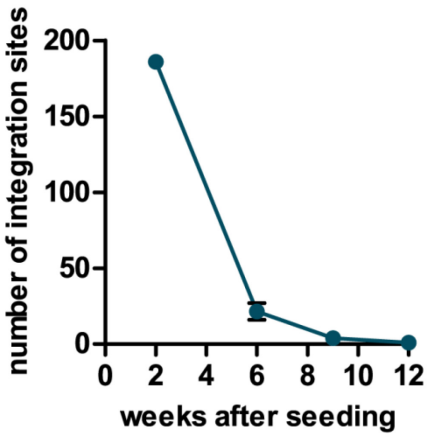

Figure 31: Clonal analysis of OTCs. LAM-PCR performed of fdm OTCs grown from H2B-GFP NHEK after 2, 6, 9 and 12 weeks. DNA was isolated from the epithelium of the OTCs and then analyzed by LAM-PCR for the individual integration sites of the viral vector. n= 2. A sequencing validity cut-off was set as described (Dieter et al., 2011). Collisions below the cut-off were removed from the analysis. Graph of the individual integrations site after the indicated timepoints.

4 Discussion

The aim of this study was the isolation and characterization of label-retaining cells, the potential epidermal stem cells. The purification and molecular characterization of vital label-retaining cells (LRCs) is a key feature to understand the role of LRCs in long-term regeneration of the epidermis. Since there are no distinct markers, the identification of stem cells in the human interfollicular epidermis is still difficult. Studies of the human IFE revealed heterogeneous proliferation of the keratinoctyes within the epidermis (Potten, 1974; Potten and Morris, 1988; Rowe and Dixon, 1972). Because it is thought that stem cells rarely divide, LRCs were designated as stem cells (Bickenbach, 1981). However, using DNA labels like 5´-iodo-2´-deoxyuridine (IdU) or 5´-bromo-2´-deoxyuridine (BrdU) for the detection of LRCs does not allow the isolation of living slow-cycling cells due the required fixation methods. A new pulse-chase strategy based on the Tet-Off controlled expression of a Histone2B-GFP fusion protein was used by Tumbar et al. (Tumbar et al., 2004) to detect LRCs in living young mice and to isolate vital LRCs from mouse epidermis. A major benefit of this labeling method is the constant expression of H2B-GFP without affecting chromosomal structures (Kanda et al., 1998) and a slow turnover of the H2B-GFP fusion protein (Brennand et al., 2007; Tumbar et al., 2004). To study and isolate LRCs in the human system, we used organotypic cultures (OTCs). OTCs grown from human normal keratinocytes (NHEK) can be cultured for several weeks and thereby permit the development of a stem cell niche (Muffler et al., 2008). Moreover, the establishment of LRCs in the basal layer was shown (Muffler et al., 2008). Therefore, OTCs as a 3D *in vitro* model of the human skin, provide an excellent experimental tool to study epidermal stem cells (Muffler et al., 2008; Stark et al., 2006; Stark et al., 2004).

4.1 H2B-GFP lentiviral reporter for the detection of LRCs

The generation of a Tet-Off-H2B-GFP lentiviral reporter could be used to infect various cell types, like HeLa cells, murine pancreatic ductal adenocarcinoma (mPDAC) cells, Neuroblastoma cell lines, Medulloblastoma cell lines, Hepatocarcinoma cell lines and epidermal cell lines (Falkowska-Hansen et al., 2010). Moreover, it offers a new method for the detection of LRCs in 3D tissue culture systems (Falkowska-Hansen et al., 2010). The identification of LRCs in OTCs grown from H2B-GFP transduced human malignant keratinocytes was reported by Falkowska-Hansen et al. Our first goal was to successfully infect normal human keratinocytes (NHEK) with the same lentiviral vector. Since epithelial cells, like primary keratinocytes, are difficult to infect with adenoviral or lentiviral vector systems (Arcasoy et al., 1997; Grubb et al., 1994) the transduction method was optimized. With a modified infection method, like spinoculation and the addition of polybrene, transduction could be significantly improved and reached infection rates up to 90%. The

spinoculation procedure was also shown in other studies to increase transduction rates from 40 to >90% for primary keratinocytes without influencing cell viability (Gagnoux-Palacios et al., 2005). The addition of 8µg/ml polybrene increased the infection rate by 20-30% (Figure 1), confirming previous works (Nanba et al., 2013). However, Nanba et al. showed a reduction of keratinocyte proliferation at polybrene concentrations higher than 5µg/ml (Nanba et al., 2013). Notably, in these studies keratinocytes were exposed to polybrene over night, which could have negative effects. With our infection method NHEKs were incubated with the virus and polybrene for only 90 minutes and we could not observe any toxicity on the cells. This was in agreement with studies from Kuhn et al. where the cells were exposed to polybrene for 4 hours and no toxic effects were reported (Kuhn et al., 2002).

To perform pulse-chase experiments with this reporter system, it is important to reliably turn off the GFP expression in keratinocytes. Therefore, the responsiveness of the reporter to Dox is crucial. For the detection of LRCs in OTCs, H2B-GFP is expressed in all cells for the first 2 weeks in the absence of Dox (pulse period). Subsequently, Dox is added to the culture medium and thus the expression of the reporter is turned off. The H2B-GFP is diluted in all proliferating cells (chase period), only slow-cycling cells are able to keep the label and can be detected as LRCs. If the reporter is not reliably turned off in all cells after addition of Dox, H2B-GFP positive cells could be identified as false positive LRCs after the chase period. NHEKs in 2D cultures showed a tight regulation of the reporter without toxicity. This was consistent with studies done in human malignant keratinocytes (HaCaT-ras II4) (Falkowska-Hansen et al., 2010). The tight control of the vector could be also demonstrated in 3D cultures, showing that GFP expression after the chase period is a result of a long-lived, stable protein and not *de novo* expression in the presence of Dox (Figure 12).

However, when analyzing OTCs with H2B-GFP NHEK in the absence of Dox, we detected a decline of H2B-GFP positive cells (10-30%) already after 2 weeks of cultivation even though the culture contained 100% GFP positive cells at the beginning of the experiment. Notably, long-term transgene expression was still sustained in most of the cells even after 8 weeks in the absence of Dox. This demonstrated that the H2B-GFP expression is not turned off in all cells over time (in the absence of Dox) and there was no growth advantage of the H2B-GFP negative cells. The decline of H2B-GFP cells could be due to transcriptional silencing which can occur with lentiviral infection (He et al., 2005). Other studies did not observe such findings, only aberrant expression of H2B-GFP reporter in transgenic mice was reported (Challen and Goodell, 2008) or possible insertion of the H2B-GFP transgene into sites of permanently silenced chromatin (Fuchs E., 2005, Patent WO2005054445A8).

Moreover, we wanted to ensure that the expression of the H2B-GFP protein in NHEKs does not influence the epidermal homeostasis. It was shown that tissue homeostasis is maintained by the interplay between stem cells and its surrounding cells (Moore and Lemischka, 2006). Therefore it was of major importance to achieve tissue integrity and long-term epidermal regeneration with H2B-GFP transduced NHEKs. BrdU can be toxic for human skin keratinocytes (Muffler et al., 2008). Interestingly, treatment of HSCs with BrdU caused an injury response leading to increased proliferation of HSCs (Wilson et al., 2008). In our study we could not detect any influence of H2B-GFP on the proliferation of NHEKs neither in 2D nor in 3D (Figure 9 and 11). Keratinocytes transduced with the H2B-GFP lentiviral vector were capable of generating a well-organized epithelium positive for epidermal differentiation markers and markers for a mature basement membrane and cell-cell contacts (Figure 13 and 14). In summary, the Tet-Off-H2B-GFP lentiviral vector can maintain long-term gene expression without toxicity in NHEK grown on OTCs.

4.2 OTCs to study stem cells in the human epidermis

To test if there are differences in the growth of H2B-GFP keratinocytes between different 3D models we used two types of OTCs, scaffold-based OTCs (sca OTCs) and fibroblast-derived matrix OTCs (fdm OTCs) in our studies. Sca OTCs can support epidermal tissue regeneration of NHEKs for 15 weeks or longer (Boehnke et al., 2007; Stark et al., 2004) and are therefore a suitable tool to study LRCs. Moreover, LRCs labeled with IdU could be identified in sca OTCs (Muffler et al., 2008). For fdm OTCs, normal human dermal fibroblasts (NHDF) were used to generate a fibroblast-derived matrix as dermal equivalent, called fdmDE. By using fdm OTCs, an epidermis with normal tissue morphology was maintained for up to 24 weeks (Berning et al., 2015). Furthermore, an improved matrix with a high density of assembled collagen fibrils and a dermal ECM which largely displays the dermal ECM architecture in the human skin was demonstrated (Berning et al., 2015). There is growing evidence that the ECM is crucial for the establishment of the stem cell niche by directly or indirectly regulating the maintenance, proliferation, self-renewal and differentiation of cells (Lu et al., 2012). We therefore also used fdm OTCs. Histological stainings and analysis of typical epidermal marker proteins, like Desmoglein, E-Cadherin, Keratin 14 or α6 integrin did not reveal any differences between H2B-GFP NHEKs grown on sca OTCs or fdm OTCs. In both culture approaches, the cells followed a normal differentiation process and established a basement. Thus, there was no evidence for an advantage of the fdm OTCs compared to sca OTCs. Since the precultivation time is significantly shorter in sca OTCs compared to fdm OTCs, we used sca OTCs for all further co-culture experiments.

4.3 Influence of the Rho kinase inhibitor Y-27632 on NHEKs

It was shown that treatment with Y-27632 successfully immortalized human foreskin keratinocytes, human ectocervical keratinocyte and human vaginal keratinocytes (Chapman et al., 2010). Gene expression analysis performed by Chapman et al. revealed downregulation of many genes which are expressed during keratinocyte differentiation as an effect of rho kinase inhibition. It is believed that inhibition of differentiation and stratification is one of the key causes for the long-term keratinocytes proliferation mediated by ROCK inhibition (Chapman et al., 2014). Supporting this, Notch1, an inducer of keratinocyte differentiation (Watt et al., 2008), was suggested as upstream regulator for ROCK1. Interestingly, it was suggested that the activation of ROCK is mediated by signal transduction and not on transcriptional level (Yugawa et al., 2013). Rho kinases are targeting the phosphoproteome rather than the transcriptome (Chapman et al., 2014). Nonetheless, the precise mechanism of Y-27632–mediated long-term proliferation of keratinocytes is still elusive. With the addition of Y-27632, we were able to passage NHEKs for several months (Figure 16). Moreover, we showed that cocultivation with feeder fibroblasts is indispensable for long-term subculturing of NHEK in the presence of Y-27632 (Figure 16) as described by Chapman et al. (Chapman et al., 2010). As demonstrated by several other studies (Chapman et al., 2010; McMullan et al., 2003; Terunuma et al., 2010) proliferation of NHEKs in the presence of Y-27632 was increased in our experiments. Previous studies have also shown that keratinocytes that had been cultured with Y-27632 for up to 18 passages kept their ability to differentiate after removal of Y-27632 and formed a stratified epithelium in organotypic cultures after 17 days (Chapman et al., 2010). Here, we found that NHEKs, precultivated in Y-27632, maintained their capacity to form a stratified epithelium. However, H2B-GFP transduced NHEKs retained their proliferation potential over several passages in the presence of Y-27632 in 2D, but did not form a stratified epidermis long-term in OTCs. In contrast to our results, van den Bogaard et al. showed even enhanced epidermal morphology of OTCs generated from transduced, Y-27632- treated keratinocytes with Y-27632 present during the submerged phase of the OTCs (van den Bogaard et al., 2012). However, this study did not consider long-term regeneration since the OTCs were harvested after 10 days (van den Bogaard et al., 2012). Therefore, we suggest that long-term regeneration cannot be achieved with transduced NHEKs precultivated in the presence of Y-27632 grown on OTCs. Consequently, we could not perform repeated FACSoring in order to select for a stable H2B-GFP population. Such approaches are under normal culture conditions restricted owed to the limited life span of NHEKs. All subsequent studies were done with H2B-GFP NHEKs, which were not expanded in Y-27632 and a decline of H2B-GFP expression during the pulse period has to be taken into account with the possible consequence, that less LRCs than present could be detected after the chase period.

4.4 Detection and Isolation of LRCs in OTCs

One assay to study epidermal stem cells in the absence of distinct cell surface markers is to functionally identify stem cells as label-retaining cells. Stem cells are believed to divide rarely and can therefore be identified as label-retaining cells (LRCs) (Arai and Suda, 2007; Bickenbach, 1981; Bickenbach et al., 1986; Cotsarelis et al., 1990; Morris and Potten, 1999; Orford and Scadden, 2008). Evidence for this could be also found in the interfollicular epidermis where it was shown that slow cycling cells *in vivo* are those cells with the highest self-renewal capacity *in vitro* (Jones et al., 1995). LRCs could also be detected in the in the HF bulge (Braun et al., 2003; Cotsarelis et al., 1990). The way in which stem cells balance tissue maintenance in the IFE is still elusive and is controversially debated. Therefore, there is a strong need to isolate and characterize LRCs of the human IFE in order to investigate the role of LRCs in tissue homeostasis and to find new markers for their identification. In our studies, we were able to detect LRCs after chase periods up to 11 weeks (Figure 20). Intriguingly, LRCs were detected mostly in clusters. This clustered distribution was also reported for the permanent portion of the hair follicle and cornea limbus (Braun et al., 2003). In OTCs of human skin LRCs were observed more individual, nonclustered cells (Muffler et al., 2008). Accordingly in the interfollicular epidermis of mouse back and tail skin (Braun et al., 2003) and in the sweat gland of mice LRCs were also detected in a scattered pattern. However, we could not detect any uniform pattern of the LRC distribution which would indicate the presence of epidermal proliferative units suggested by previous studies (Mackenzie, 1970; Morris et al., 1985; Potten, 1974). Different patterns of LRCs could be due to differences in mouse and human skin and different labeling methods. Notably, LRC detection in OTCs was done by labeling with IdU (Muffler et al., 2008). A main disadvantage of labeling with IdU is the harsh condition to visualize the label which could degrade the structure of tissue (Salic and Mitchison, 2008). Moreover, the antibody detection of IdU could be less sensitive than the detection of GFP without any fixation or antibody staining. This could explain different patterns of LRCs in OTCs. The LRC cluster could be a result of differences in the proliferative manner of individual LRCs. It was reported that individual quiescent LRCs were able to proliferate and could be detected as Ki67-positive in OTCs at all time points, even after 10-week chase (Muffler et al., 2008). Additionally Ki67- positive cells were detected close to LRCs (Muffler et al., 2008). Clusters of LRCs could indicate that not only LRCs are occasionally proliferating, but also the progeny of these LRCs are slow-cycling cells.

In our study, we were able to isolate LRCs in a range between 1% and 7.4% of basal cells (Figure 21 B). The results are in agreement with *in vivo* experiments of the murine interfollicular epidermis (Morris et al., 1985; Morris and Potten, 1994). In another study

performing limiting dilutions experiments, different ratios of GFP-positive keratinocytes and GFP-negative keratinocytes of the murine IFE were mixed in order to study long-term repopulating cells transplanted on the fascia of mice. The results proposed that only 0.01% of the basal cells are stem cells (Schneider et al., 2003). However, it is likely that the suggested stem cell numbers could differ depending on the methodology of detection (*in vivo* vs. *in vitro* vs. transplantation studies) and model system (murine vs. human IFE).

4.5 Molecular characterization of LRCs

With the aim to find different gene expression patterns and new markers to identify LRCs we performed global gene expression analysis of the isolated LRCs.

The previously suggested epidermal stem cell marker of the human IFE, such as expression of β1 integrin^{high}, the Notch-ligand delta-like 1 (DLL1), the melanoma chondroitin sulfate proteoglycan (MCSP), the transmembrane protein LRIG1 and the transmembrane glycoprotein CD46 (Jensen and Watt, 2006; Jones and Watt, 1993; Legg et al., 2003; Lowell et al., 2000; Tan et al., 2013), could not be recapitulated in our analysis. Notably, single cell expression profiling of human keratinocytes did not always show an overlap of expression of these suggested marker (Jensen and Watt, 2006). Moreover, although cells isolated on the basis of these markers had a greater colony forming efficiency in 2D (Tan et al., 2013), little is known about the contribution of these cells to the homeostasis of the IFE due to the lack of further characterization by transplantation assays. Furthermore, it was already shown that in OTCs grown from NHEKs some but not all LRCs co-expressed MCSP, and some MCSP-positive clusters lacked LRCs altogether (Muffler et al., 2008). Other suggested markers are high expression of α_6 integrin and low expression of the transferrin receptor CD71 in quiescent keratinocytes (Li et al., 1998). These cells showed in transplantation studies greater intrinsic tissue-regenerative capacity (Li et al., 2004; Schluter et al., 2011). Interestingly, cells with α_6^{bri} and CD71^{dim} expression were detected at the bottom part of the rete ridges in human IFE, whereas cells expressing MCSP, DLL1 and β1 integrin^{high} were located at the opposite site (Muffler et al., 2008). The Wnt inhibitor WIF1 was also suggested as marker for quiescent stem cell in the IFE and LRCs in OTCs showed co-expression of WIF1 (Schluter et al., 2013). The heterogeneous expression of stem cell markers could display a functional heterogeneity of stem cells in the IFE. Heterogenic expression could be also due to body-site specific variances in the structure of the IFE, for example there are rete ridge-poor parts in human skin, like e.g. human breast skin. However, in our microarray analysis of isolated LRCs we did not detect any upregulation of the suggested marker.

In our study, differential analysis of the gene expression profiles clearly showed a high correlation of gene expression within the isolated LRCs and basal cells, reflecting a homogeneous population of analyzed cells (basal keratinocytes) (Figure 23 B). However, the transcriptional profiling of isolated LRCs revealed a group of 102 genes which were differentially expressed (Table 2, and Table 6 in the appendix). The microarray analysis unexpectedly revealed that especially ECM genes were highly upregulated in LRCs. There is growing evidence that particularly the ECM provides an essential niche component for stem cells in various tissues (Hall and Watt, 1989; Scadden, 2006; Spradling et al., 2001; Watt and Hogan, 2000). Also in the human skin several hints can be found for the important role of the ECM in the regulation of epidermal stem cells. Strikingly, ECM and integrin expression seems to differ among different regions of the human skin (Watt, 2002). Furthermore, variations of ECM components and integrins play a role during development. For example, it was suggested that neonatal keratinocytes and neonatal fibroblasts maintain a higher integrin expression (Cho et al., 2004; Choi et al., 2015). Moreover, the differential expression of ECM components can modulate tissue specificity (Votteler et al., 2010; Watt and Fujiwara, 2011). It was also suggested that increased level of integrin expression, which mediates cell binding to the ECM, can be used as marker to enrich epidermal stem cells (Jones et al., 1995; Jones and Watt, 1993; Stingl et al., 2006; Wagers and Weissman, 2006; Watt and Jones, 1993) and make them more adhesive to the ECM (Jones et al., 1995). Accordingly, the loss of contact with the ECM or reduced integrin expression leads to the differentiation of epidermal cells (Grose et al., 2002; Watt, 2002). Importantly, microarray analysis of epidermal mouse label-retaining cells and Keratin-15-positive mouse hair follicle stem cells revealed that these cells also showed increased expression of ECM genes (Morris et al., 2004; Tumbar et al., 2004).

Our findings support a functional role for ECM components for stem cell regulation. We could show increased expression in LRCs for collagen, type I, decorin, fibronectin-1, fibulin 1, fibulin 2 and lumican, which are all important members of the ECM. Decorin, a small leucine rich proteoglycan, is abundant in the ECM of the human skin (Carrino et al., 2011; Seidler, 2012). Decorin is binding to type 1 collagen which is necessary for proper collagen fibril assembly and prevents the cleavage by MMPs (Ruhland et al., 2007; Stuart et al., 2011). Interestingly, decorin and collagen, type 1 were identified as quiescins. Quiescins are genes which were found to be upregulated in quiescent cells, for example W138 human embryo lung fibroblasts, compared to actively cycling cells (Coppock et al., 1993). Decorin was also shown to influence the induction of quiescence. Transfected CHO cells, which overproduce decorin, had a decrease in their growth rate (Ruoslahti, 1989). Moreover, decorin might play a role in the regulatation of cell growth since it can bind and sequester TGFβ, demonstrated in chinese hamster ovary cells (Yamaguchi et al., 1990). Thus, decorin could be also

involved in TGFβ binding and sequestering in the microenvironment of LRCs. Other components of the ECM that seem to play a role were Fibulin 1 and Fibulin 2. Both were shown here to be upregulated in LRCs. Fibulin 1 and Fibulin 2 are secreted glycoproteins and support ECM stability (Lau et al., 2010). They build a tight connection with fibronectin and a number of other ECM proteins like laminin and fibrinogen (Tran et al., 1997). In addition, Fibulin 2 is an important factor for the basement membrane integrity (Longmate et al., 2014). Fibulin 1 was also enriched in the stem cell niche of the bulge (Fujiwara et al., 2011) and also upregulated in hair follicle stem cells (Morris et al., 2004). Our findings suggest that these ECM components could be important for the integrity and regulation of LRCs.

Notably, not only ECM components were upregulated, but also the tissue inhibitor of metalloproteinase, TIMP2, was upregulated. This is a hint towards a decreased degradation of ECM molecules. An upregulation of TIMP2 was also shown in label-retaining cells of the hair follicle (Tumbar et al., 2004) and Keratin-15-positive mouse hair follicle stem cells (Morris et al., 2004), thus confirming that TIMP2 could play a role in stem cells.

Interestingly, we did not find any downregulation of genes which are related to cell cycle progression, suggesting that slow cycling of the LRCs is not necessarily regulated on transcriptional level. The expression profile, as mentioned above, could indicate a different regulation of quiescence of the LRCs. A hint for a quiescent phenotype of the isolated LRCs was the downregulation of histone clusters. Histone clusters are upregulated in actively cycling cells which progress from G1 to S phase (Harris et al., 1991; Marzluff and Duronio, 2002). The downregulation of histone clusters confirmed may therefore represent the G0 status of the LRCs. Other indications came from the downregulation of Keratin 14 in LRCs. Keratin 14 is a marker of basal keratinocytes (Alam et al., 2011; Byrne et al., 1994; Coulombe et al., 1989). Keratin 14 knockdown in HaCaT cells was shown to lead to decreased cell proliferation and to a delay in cell cycle progression, but also to the induction of keratinocyte differentiation (Alam et al., 2011). Since we saw a downregulation in LRCs, it is conceivably that moderate downregulation of Keratin 14 also leads to decreased proliferation in LRCs.

Surprisingly, vimentin, an intermediate filament protein which is usually expressed in mesenchymal cells and a marker for fibroblasts was also upregulated in LRCs. Vimentin can be detected transiently in non-mesenchymal cells, like epithelial cells, during embryonic development, especially during cell migration processes (Bignami et al., 1982; Kasper et al., 1989; Lane et al., 1983). Moreover, vimentin is upregulated in keratinocytes at the migratory

tongue during wound healing in the skin (Yan et al., 2010). Vimentin was found to be also expressed in NHEKs cultivated in 2D under low-calcium conditions (Franke et al., 1979a; Franke et al., 1979b). A different study showed a vimentin-expressing population located at the migratory/proliferative rim of growing colonies also under normal calcium growth conditions. A small fraction of these vimentin positive NHEKs showed high levels of α5β1 integrin and integrin α6 (Castro-Munozledo et al., 2015), which were suggested as epidermal stem cell markers (Hotchin et al., 1993; Jones et al., 1995). Silencing of vimentin in keratinocytes leads to smaller colonies, suggesting a role for vimentin for a migratory phenotype of NHEKs and colony growth (Castro-Munozledo et al., 2015). Interestingly, β1 integrin, a suggested epidermal stem cell marker, was also shown to be involved in migration (Grose et al., 2002); since β1 integrin-null keratinocytes showed not only impaired adhesion but also to a less migratory phenotype (Grose et al., 2002). Therefore, the unexpected upregulation of vimentin in LRCs could indicate a more motile phenotype.

In summary, we could show that LRCs in the IFE express unique ECM genes different from those of the bulk of the basal cells. Supporting this, the molecular characterization of Keratin-15-positive mouse hair follicle stem cells revealed also an upregulation of ECM genes, like different collagens, fibulin 1, Tenascin C, TIMP2 among others. Similar results were revealed by expression analysis of mouse epidermal label-retaining cells. The functional importance of the different ECM is still elusive. There are indications that increased levels of ECM components not only allow for better adherence of the stem cells in the niche, it may also play a role for the binding, distribution and activity of polypeptide growth factors (Mooradian et al., 1989). This is also known from other cell types, like endothelial cells which produce bFGF and incorporate it into the local niche where it may regulate autocrine endothelial cell growth (Gordon et al., 1987; Vlodavsky et al., 1987). Studies from Mooradian et al. and others demonstrated that TGFβ can interact with different ECM proteins and may be released by extracellular matrices as consequence (Mooradian et al., 1989; Streuli et al., 1993). Thereby the ECM could serve as a reservoir for growth factors, such as TGFβs, and could generate stable gradients of these (reviewed in (Fuchs, 2008), (Zhu and Clark, 2014)). The expression of different ECM components could also lead to different responses to the same growth factor (reviewed in (Zhu and Clark, 2014)). We propose that LRCs might retain at least in part their stem cell character by expressing differential ECM components that influence the immediate surroundings of LRCs.

4.6 A role for TGFβ signaling in LRC regulation?

Transforming growth factor (TGF)-β family signaling has been reported to be involved in the development and maintenance of stem cells in various organs. For example it was shown that TGFβ plays an important role in the maintenance of embryonic stem cell identity (summarized in (Mishina et al., 2002; Sirard et al., 1998; Watabe and Miyazono, 2009)). Molecular characterization of LRCs of the bulge in the hair follicle also showed involvement of TGFβ. It was shown that LRCs had elevated transcripts for Latent TGF-beta binding protein (LTBP-1), which activates latent TGFβ (Unsold et al., 2001), and TGFβ target genes as well as Smad interacting genes (Tumbar et al., 2004). TGFβ activation was also indicated by increased phospho-Smad2 expression in the bulge compared to the progeny (Tumbar et al., 2004). Moreover, studies revealed that the proliferation of keratinocytes is inhibited by TGFβ signaling (Massague and Weinberg, 1992), which could be also involved in regulating the slow cycling of LRCs. However, in hair follicle stem cells loss of TGFβ receptor type II does not influence the quiescent state (Guasch et al., 2007). Studies performed in OTCs with human adult HaCaT variants, like Smad7-overexpressing HaCaT, demonstrated that active TGFβ/Smad signaling is essential for epidermal differentiation (Buschke et al., 2011). Notably, it was demonstrated that diminished TGFβ signaling in the anal epithelium of mice result in increased proliferation but epidermal homeostasis was maintained regulated by increased apoptosis (Guasch et al., 2007). In our study, the results of the IAP analysis from isolated LRCs indicated that TGFβ could be involved in the regulation of LRCs, though direct evidence is still elusive. We could not detect differences in expression levels of TGFβ, Smad3, Smad7 and the TGFβ receptor type I and II determined by qRT-PCR. Since we hypothesize that the concentration of TGFβ in the local environment of LRCs is increased similar mRNA expression levels of TGFβ between LRCs and basal cells were not surprising. However, we did not test the activation of TGFβ/phopho-Smad proteins in LRCs. Hints for enhanced TGFβ activation in isolated LRCs could be shown by higher expression of TGFβ receptor type III. The TGFβ receptor type III, Betaglycan, can also serve as reservoir for TGFβ and regulate access of TGFβ to the cell (Blobe et al., 2001; Lopez-Casillas et al., 1991). This could indicate a higher availability of TGFβ in LRCs.

4.7 Induction of LRC-like phenotype by TGFβ-1

To further analyze the role of TGFβ signaling in LRCs we tested if we can induce the expression of different target genes through TGFβ-1 stimulation of keratinocytes in 2D monoculture. TGFβ was shown to induce higher vimentin, fibronectin and collagen expression and promote their incorporation into the ECM (Ignotz and Massague, 1986;

Miettinen et al., 1994). It was also reported that the expression of collagens, tenascin, proteoglycans and their transmembrane receptor integrins is controlled by TGFβ (Pearson et al., 1988; Roberts et al., 2006). In addition, it was suggested that TGFβ might be an important regulator of IL6 production in fibroblasts (Elias et al., 1991). Therefore, we asked if TGFβ stimulation can also upregulate IL6 in keratinocytes. In a first attempt we could detect an upregulation of fibronectin (20 fold) and IL6 (22.6 fold) and vimentin (5.4 fold) in the presence of higher TGFβ-1 concentrations (5ng/ml). Our results indicate that high concentrations are required, since we could detect only a slight upregulation of TGFβ-associated genes, like vimentin, THBS1, fibronectin, IL6, COL1A1 and tenascin C with low TGFβ-1 concentrations (10pg-1ng/ml). However, the activation of the TGFβ pathway in the treated keratinocytes is questionable since the expression of the endogenous Smad pathway inhibitor, Smad7, which is induced by TGFβ (Itoh et al., 2000; Massague and Chen, 2000; Moustakas et al., 2001) was only slightly upregulated. This was also the case for the cyclin-dependent kinase inhibitor p21, which is rapidly induced by TGFβ-1 (Datto et al., 1995; Hannon and Beach, 1994; Reynisdottir et al., 1995). Phospho-Smad3 stainings from NHEKs treated with 5ng/ml TGFβ-1 for 3 days showed phosphorylation of Smad3 only in few cells (Figure 28 A); whereas upon treatment with 10ng/ml TGFβ-1 phosphorylation of Smad3 was observed in all cells (Figure 28 A). This confirmed that activation of TGFβ pathway in NHEKs, cultured in low-calcium medium, requires high concentrations of TGFβ-1 and further experiments should be performed with such concentrations. This was also shown in other studies where high TGFβ-1 concentrations (20ng/ml) were used to induce e.g. higher fibronectin secretion in keratinocytes (Hashiro et al., 1991).

Confirming this, inhibition of proliferation was only observed with TGFβ-1 concentrations of 5ng/ml or higher. Interestingly, the long-term treatment over several passages with low concentrations led to decreased proliferation (Figure 29 C). It is important to note that the growth inhibitory effect in adult human HaCaT keratinocytes, cultivated in serum and calcium containing medium ((Yang et al., 1996), Dissertation Susanne Buschke 2008) was much more apparent than in our studies with human keratinocytes cultivated in low-calcium medium. It was shown that high Ca^{2+} can inhibit keratinocyte growth similar to TGFβ by activating p21 (Sakaguchi et al., 2004). Studies have shown that S100C/A11, a Ca^{2+}-binding protein, is mediating a pathway which is crucial for the growth inhibition of keratinoctyes induced by high Ca^{2+} and TGFβ (Figure 32) (Sakaguchi et al., 2004). It was demonstrated in keratinocytes that the protein kinase PKCα phosphorylates the protein S100C/A11 after stimulation with TGFβ or Ca^{2+}. This in turn induces the activation of Sp1, which is regulating together with activated Smads the induction of p21 (Figure 32) (Sakaguchi et al., 2004; Sakaguchi et al., 2003). The activation of Sp1 was shown to be important for the growth

inhibition of keratinocytes (Sakaguchi et al., 2004). In another study, it was also suggested that for TGFβ activation physiological concentrations of Ca^{2+} are necessary. It was shown that under low-calcium conditions in conditioned media of growing keratinocytes TGFβ was present in the latent form in contrast to conditioned medium with physiological Ca^{2+} concentrations where the active form was restored (Kato et al., 1995). Therefore, it is conceivable that the presence of TGFβ together with calcium is enhancing the growth inhibitory effect.

The increased expression of ECM proteins determined by immunostaining, like fibronectin and decorin, in NHEKs after TGFβ-1 stimulation in 2D could indicate a role for TGFβ in LRCs. Interestingly, increased fibronectin secretion was suggested to be a specific result of TGFβ-1 stimulation, since stimulation with other growth inhibitory substances did not lead to a change in fibronection secretion (Hashiro et al., 1991). However, we have to carefully evaluate further experiments before making a definite statement on the role of TGFβ in LRCs.

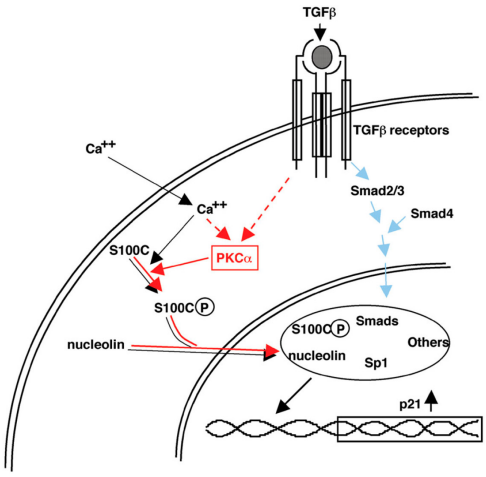

Figure 32: Suggested Signaling pathways for high Ca^{2+} and TGFβ 1-induced inhibition of proliferation in keratinoctyes. Blue arrows, known from the results of studies by others; black arrows, shown in (Sakaguchi et al., 2003); red arrows, shown in (Sakaguchi et al., 2004). Figure from (Sakaguchi et al., 2004). Activtion of PKCα through calcium or TGFβ 1 leads to the phosphorylation of S100C which is translocated to the nucleus and is releasing Sp1 which can transcriptional activate p21, like TGFβ via Smad signaling.

Taken together the transcriptional profiling of the isolated LRCs revealed that LRCs are characterized by a unique set of expressed genes. Our data suggest that LRCs might be able to create their own niche by the autocrine secretion of ECM proteins. This could not only serve for better adherence of the cells but rather it may play a role in regulating signaling pathways, for example to increase the local bioavailability of growth factors and therefore

control the quiescent state of LRCs. It is tempting to speculate that especially TGFβ is involved in the regulation of LRCs. However, one can assume that TGFβ signaling alone is certainly not sufficient to regulate the maintenance of LRCs. Also other signaling pathways could be involved. It was shown that activation of the mitogen-activated protein kinase (MAPK) cascade mediated by the epidermal growth factor receptor (EGFR) is critical for epidermal homeostasis in order to balance proliferation and differentiation (Sotiropoulou and Blanpain, 2012; Zhu et al., 1999). Interestingly, the microarray analysis revealed downregulation of dual specificity phosphatase 6, DUSP6, which is known to negatively regulate members of the mitogen-activated protein (MAP) kinase superfamily (Li et al., 2007; Ramos, 2008). This aspect needs to be addressed in future studies. The functional significance of the individual ECM composition of LRCs is still elusive and further investigations are needed. Moreover, the functional role of LRCs in epidermal homeostasis cannot be sufficient determined from the data presented here. Whether the isolated LRCs possess stem cell properties remains an open question for further studies.

4.8 Clonal kinetics in the IFE

To study the clonal kinetics of H2B-GFP NHEKs grown on fdm OTCs we performed linear amplification-mediated (LAM)-PCR from the epithelium at different time points. Lentiviral vector integration in the cellular genome can be used as unique molecular marker for each transduced cell and allows tracking the distinct clonal progeny (Schmidt et al., 2009). Starting from week 2, we detected 186 individual clones, after 6 weeks the clone number fell to 22 clones and to 4 clones after 9 weeks. Only one clone persisted after 3 months. Notably the analyzed cells contained both basal and suprabasal cells. Thus, we could show that the number of surviving clones gradually diminished as was demonstrated in experiments performed in mouse tail epidermis (Blanpain and Simons, 2013; Clayton et al., 2007). To prove that a constant clone number is approached at later time points, experiments exceeding 12 weeks need to be performed. So far, we observed that as little as 1 clone is able to maintain epidermal regeneration of the entire OTC. The stem/TA cell hypothesis implies that epidermal stem cells divide asymmetrically into a stem cell and a differentiated transit-amplifying (TA) cell which divides for several rounds until exiting the cell cycle thereby creating epidermal proliferating units (EPU). Consequently, in the EPU model each compartment is maintained by a single slow cycling stem cell surrounded by transit-amplifying cells (Mackenzie, 1970; Potten, 1974; Potten, 1981). The stem/TA cell model would predict that the clone-size distribution has to become constant at some average value over time (Blanpain and Simons, 2013; Clayton et al., 2007). In contrast, it was shown by inducible genetic labeling in tail mouse skin that the average clone size was increasing (Blanpain and Simons, 2013; Clayton et al., 2007) which suggests a single-proliferative

compartment during IFE homeostasis correlating with the so called stochastic model. This model predicts that all basal cells follow a stochastically balanced fate, generating either two cycling daughters, or two non-cycling daughters or one of each (Blanpain and Simons, 2013; Clayton et al., 2007; Doupe and Jones, 2012). However, with our approach, we cannot draw any conclusions regarding the stem cell hierarchy prevalent in human IFE. From the LAM-PCR results we can derive the clone number but not the average clone size. Both parameters are required to gain deeper insights into the question how tissue homeostasis is maintained.

4.9 Conclusion

In this study we investigated label-retaining cells, the potential stem cells, in OTCs of human epidermis. It was possible to effectivly transduce normal human keratinocytes with a tet-off controlled H2B-GFP lentiviral vector. Moreover, we were able to expand a stable H2B- GFP positive keratinocyte population in the presence of the rho-kinase inhibitor Y-27632, which prolongs the life span of adult human keratinocytes. However, Y-27632 treated H2B-GFP NHEKs lost their ability for long-term regeneration in 3D, rendering this method unsuitable to detect LRCs. Therefore, non-treated H2B-GFP NHEKs were used in long-term OTCs. Although we observed a decline of GFP positive cells during the 2 weeks of pulse period, LRCs could be detected after chase periods of up to 11 weeks. Subsequently, we were able to isolate LRCs from OTCs. Microarray analysis of LRCs compared to basal cells of the same OTC revealed 102 genes which were differentially regulated. Several genes of those genes were highly upregulated; particularly ECM components were upregulated which could be confirmed by qRT-PCR for most of the genes. To verify differential ECM protein expression in LRCs, further characterization on protein level is necessary. However, the results indicate that LRCs influence their local microenvironment by the autocrine secretion of unique ECM components. Thereby, the ECM could serve not only as anchor for LRCs in the niche but also as a reservoir for growth factors and by that regulate cell signaling. LRCs could be kept in a quiescent state indirectly by local availability of growth factors in their environment. Our studies suggest that TGFβ signaling could be involved in the regulation of LRCs. We have first hints which show the upregulation of genes upon TGFβ stimulation of NHEKs in 2D cultures which were also highly upregulated in LRCs. This was confirmed also on protein level in 2D. Moreover, the proliferation inhibiting capacity of TGFβ was also shown in NHEKs in 2D at least with high TGFβ-1 concentrations (10ng/ml) or long-term stimulation.

Interestingly, the range of isolated LRCs compared to the cell number of isolated basal cells was between 1-7,4% after 6-8 weeks of chase as suggested in the literature (Morris et al., 1985; Morris and Potten, 1994). The detection of individual clones via LAM-PCR revealed

that the epithelium is maintained by 3-11% of individual clones after 6 to 9 weeks, compared to the initial number of clones. At present, it remains elusive if LRCs reflect these clones and are responsible for maintaining tissue homeostasis in OTCs.

5 Literature

Alam, H., L. Sehgal, S.T. Kundu, S.N. Dalal, and M.M. Vaidya. 2011. Novel function of keratins 5 and 14 in proliferation and differentiation of stratified epithelial cells. *Mol Biol Cell*. 22:4068-4078.

Alcolea, M.P., and P.H. Jones. 2013. Tracking cells in their native habitat: lineage tracing in epithelial neoplasia. *Nat Rev Cancer*. 13:161-171.

Allen, T.D., and C.S. Potten. 1974. Fine-structural identification and organization of the epidermal proliferative unit. *J Cell Sci*. 15:291-319.

Andres, J.L., L. Ronnstrand, S. Cheifetz, and J. Massague. 1991. Purification of the transforming growth factor-beta (TGF-beta) binding proteoglycan betaglycan. *J Biol Chem*. 266:23282-23287.

Arai, F., and T. Suda. 2007. Maintenance of quiescent hematopoietic stem cells in the osteoblastic niche. *Ann N Y Acad Sci*. 1106:41-53.

Arcasoy, S.M., J.D. Latoche, M. Gondor, B.R. Pitt, and J.M. Pilewski. 1997. Polycations increase the efficiency of adenovirus-mediated gene transfer to epithelial and endothelial cells in vitro. *Gene Ther*. 4:32-38.

Barker, N., M. Huch, P. Kujala, M. van de Wetering, H.J. Snippert, J.H. van Es, T. Sato, D.E. Stange, H. Begthel, M. van den Born, E. Danenberg, S. van den Brink, J. Korving, A. Abo, P.J. Peters, N. Wright, R. Poulsom, and H. Clevers. 2010. Lgr5(+ve) stem cells drive self-renewal in the stomach and build long-lived gastric units in vitro. *Cell Stem Cell*. 6:25-36.

Barker, N., J.H. van Es, J. Kuipers, P. Kujala, M. van den Born, M. Cozijnsen, A. Haegebarth, J. Korving, H. Begthel, P.J. Peters, and H. Clevers. 2007. Identification of stem cells in small intestine and colon by marker gene Lgr5. *Nature*. 449:1003-1007.

Barrandon, Y., and H. Green. 1987. Three clonal types of keratinocyte with different capacities for multiplication. *Proc Natl Acad Sci U S A*. 84:2302-2306.

Bell, E., H.P. Ehrlich, D.J. Buttle, and T. Nakatsuji. 1981. Living tissue formed in vitro and accepted as skin-equivalent tissue of full thickness. *Science*. 211:1052-1054.

Bennett, W.R., T.E. Crew, J.M. Slack, and A. Ward. 2003. Structural-proliferative units and organ growth: effects of insulin-like growth factor 2 on the growth of colon and skin. *Development*. 130:1079-1088.

Bernad, A., M. Kopf, R. Kulbacki, N. Weich, G. Koehler, and J.C. Gutierrez-Ramos. 1994. Interleukin-6 is required in vivo for the regulation of stem cells and committed progenitors of the hematopoietic system. *Immunity*. 1:725-731.

Berning, M., S. Pratzel-Wunder, J.R. Bickenbach, and P. Boukamp. 2015. Three-Dimensional In Vitro Skin and Skin Cancer Models Based on Human Fibroblast-Derived Matrix. *Tissue Eng Part C Methods*.

Bickenbach, J.R. 1981. Identification and behavior of label-retaining cells in oral mucosa and skin. *J Dent Res*. 60 Spec No C:1611-1620.

Bickenbach, J.R., and E. Chism. 1998. Selection and extended growth of murine epidermal stem cells in culture. *Exp Cell Res*. 244:184-195.

Bickenbach, J.R., J. McCutecheon, and I.C. Mackenzie. 1986. Rate of loss of tritiated thymidine label in basal cells in mouse epithelial tissues. *Cell Tissue Kinet*. 19:325-333.

Bignami, A., T. Raju, and D. Dahl. 1982. Localization of vimentin, the nonspecific intermediate filament protein, in embryonal glia and in early differentiating neurons. In vivo and in vitro immunofluorescence study of the rat embryo with vimentin and neurofilament antisera. *Dev Biol*. 91:286-295.

Blanpain, C., W.E. Lowry, A. Geoghegan, L. Polak, and E. Fuchs. 2004. Self-renewal, multipotency, and the existence of two cell populations within an epithelial stem cell niche. *Cell*. 118:635-648.

Blanpain, C., and B.D. Simons. 2013. Unravelling stem cell dynamics by lineage tracing. *Nat Rev Mol Cell Biol*. 14:489-502.

Blobe, G.C., W.P. Schiemann, M.C. Pepin, M. Beauchemin, A. Moustakas, H.F. Lodish, and M.D. O'Connor-McCourt. 2001. Functional roles for the cytoplasmic domain of the type III transforming growth factor beta receptor in regulating transforming growth factor beta signaling. *J Biol Chem*. 276:24627-24637.

Boehnke, K., B. Falkowska-Hansen, H.J. Stark, and P. Boukamp. 2012. Stem cells of the human epidermis and their niche: composition and function in epidermal regeneration and carcinogenesis. *Carcinogenesis*. 33:1247-1258.

Boehnke, K., N. Mirancea, A. Pavesio, N.E. Fusenig, P. Boukamp, and H.J. Stark. 2007. Effects of fibroblasts and microenvironment on epidermal regeneration and tissue function in long-term skin equivalents. *Eur J Cell Biol*. 86:731-746.

Bornstein, P. 2001. Thrombospondins as matricellular modulators of cell function. *J Clin Invest*. 107:929-934.

Braun, K.M., C. Niemann, U.B. Jensen, J.P. Sundberg, V. Silva-Vargas, and F.M. Watt. 2003. Manipulation of stem cell proliferation and lineage commitment: visualisation of label-retaining cells in wholemounts of mouse epidermis. *Development*. 130:5241-5255.

Brennand, K., D. Huangfu, and D. Melton. 2007. All beta cells contribute equally to islet growth and maintenance. *PLoS Biol*. 5:e163.

Brizzi, M.F., G. Tarone, and P. Defilippi. 2012. Extracellular matrix, integrins, and growth factors as tailors of the stem cell niche. *Curr Opin Cell Biol*. 24:645-651.

Burns, T., Breathnach, S., Cox, N., and Griffiths, C. . 2004. Anatomy and Organization of Human Skin. Blackwell Science Ltd.

Buschke, S., H.J. Stark, A. Cerezo, S. Pratzel-Wunder, K. Boehnke, J. Kollar, L. Langbein, C.H. Heldin, and P. Boukamp. 2011. A decisive function of transforming growth factor-beta/Smad signaling in tissue morphogenesis and differentiation of human HaCaT keratinocytes. *Mol Biol Cell*. 22:782-794.

Byrne, C., M. Tainsky, and E. Fuchs. 1994. Programming gene expression in developing epidermis. *Development*. 120:2369-2383.

Candi, E., R. Schmidt, and G. Melino. 2005. The cornified envelope: a model of cell death in the skin. *Nat Rev Mol Cell Biol*. 6:328-340.

Carrino, D.A., A. Calabro, A.B. Darr, M.T. Dours-Zimmermann, J.D. Sandy, D.R. Zimmermann, J.M. Sorrell, V.C. Hascall, and A.I. Caplan. 2011. Age-related differences in human skin proteoglycans. *Glycobiology*. 21:257-268.

Castro-Munozledo, F., C. Velez-DelValle, M. Marsch-Moreno, M. Hernandez-Quintero, and W. Kuri-Harcuch. 2015. Vimentin is necessary for colony growth of human diploid keratinocytes. *Histochem Cell Biol*. 143:45-57.

Challen, G.A., and M.A. Goodell. 2008. Promiscuous expression of H2B-GFP transgene in hematopoietic stem cells. *PLoS One*. 3:e2357.

Chapman, S., X. Liu, C. Meyers, R. Schlegel, and A.A. McBride. 2010. Human keratinocytes are efficiently immortalized by a Rho kinase inhibitor. *J Clin Invest*. 120:2619-2626.

Chapman, S., D.H. McDermott, K. Shen, M.K. Jang, and A.A. McBride. 2014. The effect of Rho kinase inhibition on long-term keratinocyte proliferation is rapid and conditional. *Stem Cell Res Ther*. 5:60.

Cheifetz, S., J.A. Weatherbee, M.L. Tsang, J.K. Anderson, J.E. Mole, R. Lucas, and J. Massague. 1987. The transforming growth factor-beta system, a complex pattern of cross-reactive ligands and receptors. *Cell*. 48:409-415.

Cho, H.J., I.H. Bae, H.J. Chung, D.S. Kim, S.B. Kwon, Y.J. Cho, S.W. Youn, and K.C. Park. 2004. Effects of hair follicle dermal sheath cells in the reconstruction of skin equivalents. *J Dermatol Sci*. 35:74-77.

Choi, H.R., S.Y. Byun, S.H. Kwon, and K.C. Park. 2015. Niche interactions in epidermal stem cells. *World J Stem Cells*. 7:495-501.

Chu, D.H. 2008. Overview of biology, development, and structure of skin. K. Wolff, L.A. Goldsmith, S.I. Katz, B.A. Gilchrest, A.S Paller, & D.J. Leffell, New York: McGraw-Hill.

Clayton, E., D.P. Doupe, A.M. Klein, D.J. Winton, B.D. Simons, and P.H. Jones. 2007. A single type of progenitor cell maintains normal epidermis. *Nature*. 446:185-189.
Coppock, D.L., C. Kopman, S. Scandalis, and S. Gilleran. 1993. Preferential gene expression in quiescent human lung fibroblasts. *Cell Growth Differ*. 4:483-493.
Cotsarelis, G. 2006. Gene expression profiling gets to the root of human hair follicle stem cells. *J Clin Invest*. 116:19-22.
Cotsarelis, G., T.T. Sun, and R.M. Lavker. 1990. Label-retaining cells reside in the bulge area of pilosebaceous unit: implications for follicular stem cells, hair cycle, and skin carcinogenesis. *Cell*. 61:1329-1337.
Coulombe, P.A., R. Kopan, and E. Fuchs. 1989. Expression of keratin K14 in the epidermis and hair follicle: insights into complex programs of differentiation. *J Cell Biol*. 109:2295-2312.
Cruciat, C.M., and C. Niehrs. 2013. Secreted and transmembrane wnt inhibitors and activators. *Cold Spring Harb Perspect Biol*. 5:a015081.
DasGupta, R., and E. Fuchs. 1999. Multiple roles for activated LEF/TCF transcription complexes during hair follicle development and differentiation. *Development*. 126:4557-4568.
Datto, M.B., Y. Li, J.F. Panus, D.J. Howe, Y. Xiong, and X.F. Wang. 1995. Transforming growth factor beta induces the cyclin-dependent kinase inhibitor p21 through a p53-independent mechanism. *Proc Natl Acad Sci U S A*. 92:5545-5549.
De Craene, B., and G. Berx. 2013. Regulatory networks defining EMT during cancer initiation and progression. *Nat Rev Cancer*. 13:97-110.
Denecker, G., P. Ovaere, P. Vandenabeele, and W. Declercq. 2008. Caspase-14 reveals its secrets. *J Cell Biol*. 180:451-458.
Deutzmann R, B.-T.L., and Bruckner P. 2007. Binde- und Stützgewebe. Springer, Heidelberg. pp. 461-469 pp.
Dieter, S.M., C.R. Ball, C.M. Hoffmann, A. Nowrouzi, F. Herbst, O. Zavidij, U. Abel, A. Arens, W. Weichert, K. Brand, M. Koch, J. Weitz, M. Schmidt, C. von Kalle, and H. Glimm. 2011. Distinct types of tumor-initiating cells form human colon cancer tumors and metastases. *Cell Stem Cell*. 9:357-365.
Doupe, D.P., and P.H. Jones. 2012. Interfollicular epidermal homeostasis: dicing with differentiation. *Exp Dermatol*. 21:249-253.
Doupe, D.P., A.M. Klein, B.D. Simons, and P.H. Jones. 2010. The ordered architecture of murine ear epidermis is maintained by progenitor cells with random fate. *Dev Cell*. 18:317-323.
El Ghalbzouri, A., S. Commandeur, M.H. Rietveld, A.A. Mulder, and R. Willemze. 2009. Replacement of animal-derived collagen matrix by human fibroblast-derived dermal matrix for human skin equivalent products. *Biomaterials*. 30:71-78.
Elias, J.A., V. Lentz, and P.J. Cummings. 1991. Transforming growth factor-beta regulation of IL-6 production by unstimulated and IL-1-stimulated human fibroblasts. *J Immunol*. 146:3437-3443.
Falkowska-Hansen, B., J. Kollar, B.M. Gruner, M. Schanz, P. Boukamp, J. Siveke, A. Rethwilm, and M. Kirschner. 2010. An inducible Tet-Off-H2B-GFP lentiviral reporter vector for detection and in vivo isolation of label-retaining cells. *Exp Cell Res*. 316:1885-1895.
Franke, W.W., E. Schmid, D. Breitkreutz, M. Luder, P. Boukamp, N.E. Fusenig, M. Osborn, and K. Weber. 1979a. Simultaneous expression of two different types of intermediate sized filaments in mouse keratinocytes proliferating in vitro. *Differentiation*. 14:35-50.
Franke, W.W., E. Schmid, S. Winter, M. Osborn, and K. Weber. 1979b. Widespread occurrence of intermediate-sized filaments of the vimentin-type in cultured cells from diverse vertebrates. *Exp Cell Res*. 123:25-46.
Fritsch, P. 2009. Dermatologie und Venerologie für das Studium. Springer Medizin Verlag Heidelberg, Heidelberg.
Fuchs, E. 2008. Skin stem cells: rising to the surface. *J Cell Biol*. 180:273-284.
Fuchs, E., T. Tumbar, and G. Guasch. 2004. Socializing with the neighbors: stem cells and their niche. *Cell*. 116:769-778.

Fujiwara, H., M. Ferreira, G. Donati, D.K. Marciano, J.M. Linton, Y. Sato, A. Hartner, K. Sekiguchi, L.F. Reichardt, and F.M. Watt. 2011. The basement membrane of hair follicle stem cells is a muscle cell niche. *Cell*. 144:577-589.

Fusenig, N.E., D. Breitkreutz, M. Lueder, P. Boukamp, J. Hornung, and P.K.M. Worst. 1980. Keratinization and Structural Organization in Epidermal-Cell Cultures. *European Journal of Cell Biology*. 22:389-389.

Gagnoux-Palacios, L., C. Hervouet, F. Spirito, S. Roques, M. Mezzina, O. Danos, and G. Meneguzzi. 2005. Assessment of optimal transduction of primary human skin keratinocytes by viral vectors. *J Gene Med*. 7:1178-1186.

Garrod, D.R., A.J. Merritt, and Z. Nie. 2002. Desmosomal cadherins. *Curr Opin Cell Biol*. 14:537-545.

Ghazizadeh, S., and L.B. Taichman. 2001. Multiple classes of stem cells in cutaneous epithelium: a lineage analysis of adult mouse skin. *EMBO J*. 20:1215-1222.

Goldstein, S., E.J. Moerman, R.A. Jones, and R.C. Baxter. 1991. Insulin-like growth factor binding protein 3 accumulates to high levels in culture medium of senescent and quiescent human fibroblasts. *Proc Natl Acad Sci U S A*. 88:9680-9684.

Gomez, C., W. Chua, A. Miremadi, S. Quist, D.J. Headon, and F.M. Watt. 2013. The interfollicular epidermis of adult mouse tail comprises two distinct cell lineages that are differentially regulated by Wnt, Edaradd, and Lrig1. *Stem Cell Reports*. 1:19-27.

Gordon, M.Y., G.P. Riley, S.M. Watt, and M.F. Greaves. 1987. Compartmentalization of a haematopoietic growth factor (GM-CSF) by glycosaminoglycans in the bone marrow microenvironment. *Nature*. 326:403-405.

Grose, R., C. Hutter, W. Bloch, I. Thorey, F.M. Watt, R. Fassler, C. Brakebusch, and S. Werner. 2002. A crucial role of beta 1 integrins for keratinocyte migration in vitro and during cutaneous wound repair. *Development*. 129:2303-2315.

Grubb, B.R., R.J. Pickles, H. Ye, J.R. Yankaskas, R.N. Vick, J.F. Engelhardt, J.M. Wilson, L.G. Johnson, and R.C. Boucher. 1994. Inefficient gene transfer by adenovirus vector to cystic fibrosis airway epithelia of mice and humans. *Nature*. 371:802-806.

Guasch, G., M. Schober, H.A. Pasolli, E.B. Conn, L. Polak, and E. Fuchs. 2007. Loss of TGFbeta signaling destabilizes homeostasis and promotes squamous cell carcinomas in stratified epithelia. *Cancer Cell*. 12:313-327.

Gudjonsson, J.E., and J.T. Elder. 2006. Mouse models: psoriasis: an epidermal disease after all? *Eur J Hum Genet*. 14:2-4.

Hall, P.A. 1989. What are stem cells and how are they controlled? *J Pathol*. 158:275-277.

Hall, P.A., and F.M. Watt. 1989. Stem cells: the generation and maintenance of cellular diversity. *Development*. 106:619-633.

Hannon, G.J., and D. Beach. 1994. p15INK4B is a potential effector of TGF-beta-induced cell cycle arrest. *Nature*. 371:257-261.

Hardy, M.H. 1992. The secret life of the hair follicle. *Trends Genet*. 8:55-61.

Harris, M.E., R. Bohni, M.H. Schneiderman, L. Ramamurthy, D. Schumperli, and W.F. Marzluff. 1991. Regulation of histone mRNA in the unperturbed cell cycle: evidence suggesting control at two posttranscriptional steps. *Mol Cell Biol*. 11:2416-2424.

Hashiro, M., K. Matsumoto, K. Hashimoto, and K. Yoshikawa. 1991. Stimulation of fibronectin secretion in cultured human keratinocytes by transforming growth factor-beta not by other growth inhibitory substances. *J Dermatol*. 18:252-257.

He, J., Q. Yang, and L.J. Chang. 2005. Dynamic DNA methylation and histone modifications contribute to lentiviral transgene silencing in murine embryonic carcinoma cells. *J Virol*. 79:13497-13508.

Hertle, M.D., J.C. Adams, and F.M. Watt. 1991. Integrin expression during human epidermal development in vivo and in vitro. *Development*. 112:193-206.

Horsley, V., D. O'Carroll, R. Tooze, Y. Ohinata, M. Saitou, T. Obukhanych, M. Nussenzweig, A. Tarakhovsky, and E. Fuchs. 2006. Blimp1 defines a progenitor population that governs cellular input to the sebaceous gland. *Cell*. 126:597-609.

Hotchin, N.A., N.L. Kovach, and F.M. Watt. 1993. Functional down-regulation of alpha 5 beta 1 integrin in keratinocytes is reversible but commitment to terminal differentiation is not. *J Cell Sci*. 106 (Pt 4):1131-1138.

Hsu, Y.C., L. Li, and E. Fuchs. 2014. Emerging interactions between skin stem cells and their niches. *Nat Med*. 20:847-856.

Hynes, R.O. 2002. Integrins: bidirectional, allosteric signaling machines. *Cell*. 110:673-687.

Ignotz, R.A., and J. Massague. 1986. Transforming growth factor-beta stimulates the expression of fibronectin and collagen and their incorporation into the extracellular matrix. *J Biol Chem*. 261:4337-4345.

Ito, M., Y. Liu, Z. Yang, J. Nguyen, F. Liang, R.J. Morris, and G. Cotsarelis. 2005. Stem cells in the hair follicle bulge contribute to wound repair but not to homeostasis of the epidermis. *Nat Med*. 11:1351-1354.

Itoh, S., F. Itoh, M.J. Goumans, and P. Ten Dijke. 2000. Signaling of transforming growth factor-beta family members through Smad proteins. *Eur J Biochem*. 267:6954-6967.

Jackson, S.M., M.L. Williams, K.R. Feingold, and P.M. Elias. 1993. Pathobiology of the stratum corneum. *West J Med*. 158:279-285.

Jaks, V., N. Barker, M. Kasper, J.H. van Es, H.J. Snippert, H. Clevers, and R. Toftgard. 2008. Lgr5 marks cycling, yet long-lived, hair follicle stem cells. *Nat Genet*. 40:1291-1299.

Jensen, K.B., and F.M. Watt. 2006. Single-cell expression profiling of human epidermal stem and transit-amplifying cells: Lrig1 is a regulator of stem cell quiescence. *Proc Natl Acad Sci U S A*. 103:11958-11963.

Jensen, U.B., S. Lowell, and F.M. Watt. 1999. The spatial relationship between stem cells and their progeny in the basal layer of human epidermis: a new view based on whole-mount labelling and lineage analysis. *Development*. 126:2409-2418.

Jones, D.L., and A.J. Wagers. 2008. No place like home: anatomy and function of the stem cell niche. *Nat Rev Mol Cell Biol*. 9:11-21.

Jones, P.H., S. Harper, and F.M. Watt. 1995. Stem cell patterning and fate in human epidermis. *Cell*. 80:83-93.

Jones, P.H., B.D. Simons, and F.M. Watt. 2007. Sic transit gloria: farewell to the epidermal transit amplifying cell? *Cell Stem Cell*. 1:371-381.

Jones, P.H., and F.M. Watt. 1993. Separation of human epidermal stem cells from transit amplifying cells on the basis of differences in integrin function and expression. *Cell*. 73:713-724.

Jung, E.G. 1995. Dermatologie. Hippokrates Verlag, Stuttgart.

Kaname, S., and E. Ruoslahti. 1996. Betaglycan has multiple binding sites for transforming growth factor-beta 1. *Biochem J*. 315 (Pt 3):815-820.

Kanda, T., K.F. Sullivan, and G.M. Wahl. 1998. Histone-GFP fusion protein enables sensitive analysis of chromosome dynamics in living mammalian cells. *Curr Biol*. 8:377-385.

Kanitakis, J. 2002. Anatomy, histology and immunohistochemistry of normal human skin. *Eur J Dermatol*. 12:390-399; quiz 400-391.

Kasper, M., U. Karsten, P. Stosiek, and R. Moll. 1989. Distribution of intermediate-filament proteins in the human enamel organ: unusually complex pattern of coexpression of cytokeratin polypeptides and vimentin. *Differentiation*. 40:207-214.

Kato, M., A. Ishizaki, U. Hellman, C. Wernstedt, M. Kyogoku, K. Miyazono, C.H. Heldin, and K. Funa. 1995. A human keratinocyte cell line produces two autocrine growth inhibitors, transforming growth factor-beta and insulin-like growth factor binding protein-6, in a calcium- and cell density-dependent manner. *J Biol Chem*. 270:12373-12379.

Kaur, P. 2006. Interfollicular epidermal stem cells: identification, challenges, potential. *J Invest Dermatol*. 126:1450-1458.

Kirkbride, K.C., T.A. Townsend, M.W. Bruinsma, J.V. Barnett, and G.C. Blobe. 2008. Bone morphogenetic proteins signal through the transforming growth factor-beta type III receptor. *J Biol Chem*. 283:7628-7637.

Kishimoto, T. 1989. The biology of interleukin-6. *Blood*. 74:1-10.

Kitano, Y., and N. Okada. 1983. Separation of the epidermal sheet by dispase. *Br J Dermatol*. 108:555-560.

Kottke, M.D., E. Delva, and A.P. Kowalczyk. 2006. The desmosome: cell science lessons from human diseases. *J Cell Sci*. 119:797-806.

Kuhn, U., A. Terunuma, W. Pfutzner, R.A. Foster, and J.C. Vogel. 2002. In vivo assessment of gene delivery to keratinocytes by lentiviral vectors. *J Virol*. 76:1496-1504.

Lahav, J., M.A. Schwartz, and R.O. Hynes. 1982. Analysis of platelet adhesion with a radioactive chemical crosslinking reagent: interaction of thrombospondin with fibronectin and collagen. *Cell*. 31:253-262.

Lane, E.B., B.L. Hogan, M. Kurkinen, and J.I. Garrels. 1983. Co-expression of vimentin and cytokeratins in parietal endoderm cells of early mouse embryo. *Nature*. 303:701-704.

Lau, J.Y., B.G. Oliver, M. Baraket, E.L. Beckett, N.G. Hansbro, L.M. Moir, S.D. Wilton, C. Williams, P.S. Foster, P.M. Hansbro, J.L. Black, and J.K. Burgess. 2010. Fibulin-1 is increased in asthma--a novel mediator of airway remodeling? *PLoS One*. 5:e13360.

Lawler, J. 2000. The functions of thrombospondin-1 and-2. *Curr Opin Cell Biol*. 12:634-640.

Lechler, T., and E. Fuchs. 2005. Asymmetric cell divisions promote stratification and differentiation of mammalian skin. *Nature*. 437:275-280.

Legg, J., U.B. Jensen, S. Broad, I. Leigh, and F.M. Watt. 2003. Role of melanoma chondroitin sulphate proteoglycan in patterning stem cells in human interfollicular epidermis. *Development*. 130:6049-6063.

Levy, V., C. Lindon, B.D. Harfe, and B.A. Morgan. 2005. Distinct stem cell populations regenerate the follicle and interfollicular epidermis. *Dev Cell*. 9:855-861.

Levy, V., C. Lindon, Y. Zheng, B.D. Harfe, and B.A. Morgan. 2007. Epidermal stem cells arise from the hair follicle after wounding. *FASEB J*. 21:1358-1366.

Li, A., N. Pouliot, R. Redvers, and P. Kaur. 2004. Extensive tissue-regenerative capacity of neonatal human keratinocyte stem cells and their progeny. *J Clin Invest*. 113:390-400.

Li, A., P.J. Simmons, and P. Kaur. 1998. Identification and isolation of candidate human keratinocyte stem cells based on cell surface phenotype. *Proc Natl Acad Sci U S A*. 95:3902-3907.

Li, C., D.A. Scott, E. Hatch, X. Tian, and S.L. Mansour. 2007. Dusp6 (Mkp3) is a negative feedback regulator of FGF-stimulated ERK signaling during mouse development. *Development*. 134:167-176.

Lim, X., S.H. Tan, W.L. Koh, R.M. Chau, K.S. Yan, C.J. Kuo, R. van Amerongen, A.M. Klein, and R. Nusse. 2013. Interfollicular epidermal stem cells self-renew via autocrine Wnt signaling. *Science*. 342:1226-1230.

Longley, J., T.G. Ding, C. Cuono, F. Durden, C. Crooks, S. Hufeisen, R. Eckert, and G.S. Wood. 1991. Isolation, detection, and amplification of intact mRNA from dermatome strips, epidermal sheets, and sorted epidermal cells. *J Invest Dermatol*. 97:974-979.

Longmate, W.M., R. Monichan, M.L. Chu, T. Tsuda, M.G. Mahoney, and C.M. DiPersio. 2014. Reduced fibulin-2 contributes to loss of basement membrane integrity and skin blistering in mice lacking integrin alpha3beta1 in the epidermis. *J Invest Dermatol*. 134:1609-1617.

Lopez-Casillas, F., S. Cheifetz, J. Doody, J.L. Andres, W.S. Lane, and J. Massague. 1991. Structure and expression of the membrane proteoglycan betaglycan, a component of the TGF-beta receptor system. *Cell*. 67:785-795.

Lopez-Casillas, F., J.L. Wrana, and J. Massague. 1993. Betaglycan presents ligand to the TGF beta signaling receptor. *Cell*. 73:1435-1444.

Lowell, C.A., and T.N. Mayadas. 2012. Overview: studying integrins in vivo. *Methods Mol Biol*. 757:369-397.

Lowell, S., P. Jones, I. Le Roux, J. Dunne, and F.M. Watt. 2000. Stimulation of human epidermal differentiation by delta-notch signalling at the boundaries of stem-cell clusters. *Curr Biol*. 10:491-500.

Lu, P., V.M. Weaver, and Z. Werb. 2012. The extracellular matrix: a dynamic niche in cancer progression. *J Cell Biol*. 196:395-406.

Lyle, S., M. Christofidou-Solomidou, Y. Liu, D.E. Elder, S. Albelda, and G. Cotsarelis. 1998. The C8/144B monoclonal antibody recognizes cytokeratin 15 and defines the location of human hair follicle stem cells. *J Cell Sci*. 111 (Pt 21):3179-3188.

Mackenzie, I.C. 1970. Relationship between mitosis and the ordered structure of the stratum corneum in mouse epidermis. *Nature*. 226:653-655.

Mackenzie, I.C., and J.R. Bickenbach. 1982. Patterns of epidermal cell proliferation. *Carcinog Compr Surv*. 7:311-317.

Mani, S.A., W. Guo, M.J. Liao, E.N. Eaton, A. Ayyanan, A.Y. Zhou, M. Brooks, F. Reinhard, C.C. Zhang, M. Shipitsin, L.L. Campbell, K. Polyak, C. Brisken, J. Yang, and R.A. Weinberg. 2008. The epithelial-mesenchymal transition generates cells with properties of stem cells. *Cell*. 133:704-715.

Marzluff, W.F., and R.J. Duronio. 2002. Histone mRNA expression: multiple levels of cell cycle regulation and important developmental consequences. *Curr Opin Cell Biol*. 14:692-699.

Mascre, G., S. Dekoninck, B. Drogat, K.K. Youssef, S. Brohee, P.A. Sotiropoulou, B.D. Simons, and C. Blanpain. 2012. Distinct contribution of stem and progenitor cells to epidermal maintenance. *Nature*. 489:257-262.

Massague, J. 2000. How cells read TGF-beta signals. *Nat Rev Mol Cell Biol*. 1:169-178.

Massague, J., and Y.G. Chen. 2000. Controlling TGF-beta signaling. *Genes Dev*. 14:627-644.

Massague, J., and R.A. Weinberg. 1992. Negative regulators of growth. *Curr Opin Genet Dev*. 2:28-32.

McMullan, R., S. Lax, V.H. Robertson, D.J. Radford, S. Broad, F.M. Watt, A. Rowles, D.R. Croft, M.F. Olson, and N.A. Hotchin. 2003. Keratinocyte differentiation is regulated by the Rho and ROCK signaling pathway. *Curr Biol*. 13:2185-2189.

Mese, G., G. Richard, and T.W. White. 2007. Gap junctions: basic structure and function. *J Invest Dermatol*. 127:2516-2524.

Miettinen, P.J., R. Ebner, A.R. Lopez, and R. Derynck. 1994. TGF-beta induced transdifferentiation of mammary epithelial cells to mesenchymal cells: involvement of type I receptors. *J Cell Biol*. 127:2021-2036.

Mishina, Y., M.C. Hanks, S. Miura, M.D. Tallquist, and R.R. Behringer. 2002. Generation of Bmpr/Alk3 conditional knockout mice. *Genesis*. 32:69-72.

Mistry, D.S., Y. Chen, Y. Wang, K. Zhang, and G.L. Sen. 2014. SNAI2 controls the undifferentiated state of human epidermal progenitor cells. *Stem Cells*. 32:3209-3218.

Moll, I. 2010. Dermatologie. Georg Thieme Verlag, Stuttgart

Mooradian, D.L., R.C. Lucas, J.A. Weatherbee, and L.T. Furcht. 1989. Transforming growth factor-beta 1 binds to immobilized fibronectin. *J Cell Biochem*. 41:189-200.

Moore, K.A., and I.R. Lemischka. 2006. Stem cells and their niches. *Science*. 311:1880-1885.

Morris, R.J., S.M. Fischer, and T.J. Slaga. 1985. Evidence that the centrally and peripherally located cells in the murine epidermal proliferative unit are two distinct cell populations. *J Invest Dermatol*. 84:277-281.

Morris, R.J., Y. Liu, L. Marles, Z. Yang, C. Trempus, S. Li, J.S. Lin, J.A. Sawicki, and G. Cotsarelis. 2004. Capturing and profiling adult hair follicle stem cells. *Nat Biotechnol*. 22:411-417.

Morris, R.J., and C.S. Potten. 1994. Slowly cycling (label-retaining) epidermal cells behave like clonogenic stem cells in vitro. *Cell Prolif*. 27:279-289.

Morris, R.J., and C.S. Potten. 1999. Highly persistent label-retaining cells in the hair follicles of mice and their fate following induction of anagen. *J Invest Dermatol*. 112:470-475.

Moustakas, A., S. Souchelnytskyi, and C.H. Heldin. 2001. Smad regulation in TGF-beta signal transduction. *J Cell Sci*. 114:4359-4369.

Muffler, S., H.J. Stark, M. Amoros, B. Falkowska-Hansen, K. Boehnke, H.J. Buhring, A. Marme, J.R. Bickenbach, and P. Boukamp. 2008. A stable niche supports long-term maintenance of human epidermal stem cells in organotypic cultures. *Stem Cells*. 26:2506-2515.

Nanba, D., N. Matsushita, F. Toki, and S. Higashiyama. 2013. Efficient expansion of human keratinocyte stem/progenitor cells carrying a transgene with lentiviral vector. *Stem Cell Res Ther*. 4:127.

Nead, M.A., and D.J. McCance. 1995. Poly-L-ornithine-mediated transfection of human keratinocytes. *J Invest Dermatol*. 105:668-671.

Nijhof, J.G., K.M. Braun, A. Giangreco, C. van Pelt, H. Kawamoto, R.L. Boyd, R. Willemze, L.H. Mullenders, F.M. Watt, F.R. de Gruijl, and W. van Ewijk. 2006. The cell-surface marker MTS24 identifies a novel population of follicular keratinocytes with characteristics of progenitor cells. *Development*. 133:3027-3037.

Ohyama, M., A. Terunuma, C.L. Tock, M.F. Radonovich, C.A. Pise-Masison, S.B. Hopping, J.N. Brady, M.C. Udey, and J.C. Vogel. 2006. Characterization and isolation of stem cell-enriched human hair follicle bulge cells. *J Clin Invest*. 116:249-260.

Orford, K.W., and D.T. Scadden. 2008. Deconstructing stem cell self-renewal: genetic insights into cell-cycle regulation. *Nat Rev Genet*. 9:115-128.

Pearson, C.A., D. Pearson, S. Shibahara, J. Hofsteenge, and R. Chiquet-Ehrismann. 1988. Tenascin: cDNA cloning and induction by TGF-beta. *EMBO J*. 7:2977-2982.

Perez-Moreno, M., C. Jamora, and E. Fuchs. 2003. Sticky business: orchestrating cellular signals at adherens junctions. *Cell*. 112:535-548.

Pfaffl, M.W. 2001. A new mathematical model for relative quantification in real-time RT-PCR. *Nucleic Acids Res*. 29:e45.

Ponec, M., A. Weerheim, J. Kempenaar, A.M. Mommaas, and D.H. Nugteren. 1988. Lipid composition of cultured human keratinocytes in relation to their differentiation. *J Lipid Res*. 29:949-961.

Porter, R.M. 2003. Mouse models for human hair loss disorders. *J Anat*. 202:125-131.

Potten, C.S. 1974. The epidermal proliferative unit: the possible role of the central basal cell. *Cell Tissue Kinet*. 7:77-88.

Potten, C.S. 1981. Cell replacement in epidermis (keratopoiesis) via discrete units of proliferation. *Int Rev Cytol*. 69:271-318.

Potten, C.S., and R.J. Morris. 1988. Epithelial stem cells in vivo. *J Cell Sci Suppl*. 10:45-62.

Prunieras, M., M. Regnier, and D. Woodley. 1983. Methods for cultivation of keratinocytes with an air-liquid interface. *J Invest Dermatol*. 81:28s-33s.

Ramos, J.W. 2008. The regulation of extracellular signal-regulated kinase (ERK) in mammalian cells. *Int J Biochem Cell Biol*. 40:2707-2719.

Reynisdottir, I., K. Polyak, A. Iavarone, and J. Massague. 1995. Kip/Cip and Ink4 Cdk inhibitors cooperate to induce cell cycle arrest in response to TGF-beta. *Genes Dev*. 9:1831-1845.

Rhee, H., L. Polak, and E. Fuchs. 2006. Lhx2 maintains stem cell character in hair follicles. *Science*. 312:1946-1949.

Rice, R.H., and H. Green. 1979. Presence in human epidermal cells of a soluble protein precursor of the cross-linked envelope: activation of the cross-linking by calcium ions. *Cell*. 18:681-694.

Roberts, A.B., F. Tian, S.D. Byfield, C. Stuelten, A. Ooshima, S. Saika, and K.C. Flanders. 2006. Smad3 is key to TGF-beta-mediated epithelial-to-mesenchymal transition, fibrosis, tumor suppression and metastasis. *Cytokine Growth Factor Rev*. 17:19-27.

Rowe, L., and W.J. Dixon. 1972. Clustering and control of mitotic activity in human epidermis. *J Invest Dermatol*. 58:16-23.

Ruhland, C., E. Schonherr, H. Robenek, U. Hansen, R.V. Iozzo, P. Bruckner, and D.G. Seidler. 2007. The glycosaminoglycan chain of decorin plays an important role in collagen fibril formation at the early stages of fibrillogenesis. *FEBS J*. 274:4246-4255.

Ruoslahti, E. 1989. Proteoglycans in cell regulation. *J Biol Chem*. 264:13369-13372.

Sadagurski, M., S. Yakar, G. Weingarten, M. Holzenberger, C.J. Rhodes, D. Breitkreutz, D. Leroith, and E. Wertheimer. 2006. Insulin-like growth factor 1 receptor signaling regulates skin development and inhibits skin keratinocyte differentiation. *Mol Cell Biol*. 26:2675-2687.

Sage, E.H., and P. Bornstein. 1991. Extracellular proteins that modulate cell-matrix interactions. SPARC, tenascin, and thrombospondin. *J Biol Chem*. 266:14831-14834.

Sakaguchi, M., M. Miyazaki, H. Sonegawa, M. Kashiwagi, M. Ohba, T. Kuroki, M. Namba, and N.H. Huh. 2004. PKCalpha mediates TGFbeta-induced growth inhibition of human keratinocytes via phosphorylation of S100C/A11. *J Cell Biol*. 164:979-984.

Sakaguchi, M., M. Miyazaki, M. Takaishi, Y. Sakaguchi, E. Makino, N. Kataoka, H. Yamada, M. Namba, and N.H. Huh. 2003. S100C/A11 is a key mediator of Ca(2+)-induced growth inhibition of human epidermal keratinocytes. *J Cell Biol*. 163:825-835.

Salic, A., and T.J. Mitchison. 2008. A chemical method for fast and sensitive detection of DNA synthesis in vivo. *Proc Natl Acad Sci U S A*. 105:2415-2420.

Sankar, S., N. Mahooti-Brooks, M. Centrella, T.L. McCarthy, and J.A. Madri. 1995. Expression of transforming growth factor type III receptor in vascular endothelial cells increases their responsiveness to transforming growth factor beta 2. *J Biol Chem*. 270:13567-13572.

Scadden, D.T. 2006. The stem-cell niche as an entity of action. *Nature*. 441:1075-1079.

Schaefer, L., and R.V. Iozzo. 2008. Biological functions of the small leucine-rich proteoglycans: from genetics to signal transduction. *J Biol Chem*. 283:21305-21309.

Schluter, H., S. Paquet-Fifield, P. Gangatirkar, J. Li, and P. Kaur. 2011. Functional characterization of quiescent keratinocyte stem cells and their progeny reveals a hierarchical organization in human skin epidermis. *Stem Cells*. 29:1256-1268.

Schluter, H., H.J. Stark, D. Sinha, P. Boukamp, and P. Kaur. 2013. WIF1 is expressed by stem cells of the human interfollicular epidermis and acts to suppress keratinocyte proliferation. *J Invest Dermatol*. 133:1669-1673.

Schmidt, M., G. Hoffmann, M. Wissler, N. Lemke, A. Mussig, H. Glimm, D.A. Williams, S. Ragg, C.U. Hesemann, and C. von Kalle. 2001. Detection and direct genomic sequencing of multiple rare unknown flanking DNA in highly complex samples. *Hum Gene Ther*. 12:743-749.

Schmidt, M., K. Schwarzwaelder, C. Bartholomae, K. Zaoui, C. Ball, I. Pilz, S. Braun, H. Glimm, and C. von Kalle. 2007. High-resolution insertion-site analysis by linear amplification-mediated PCR (LAM-PCR). *Nat Methods*. 4:1051-1057.

Schmidt, M., K. Schwarzwaelder, C.C. Bartholomae, H. Glimm, and C. von Kalle. 2009. Detection of retroviral integration sites by linear amplification-mediated PCR and tracking of individual integration clones in different samples. *Methods Mol Biol*. 506:363-372.

Schneider, T.E., C. Barland, A.M. Alex, M.L. Mancianti, Y. Lu, J.E. Cleaver, H.J. Lawrence, and R. Ghadially. 2003. Measuring stem cell frequency in epidermis: a quantitative in vivo functional assay for long-term repopulating cells. *Proc Natl Acad Sci U S A*. 100:11412-11417.

Seidler, D.G. 2012. The galactosaminoglycan-containing decorin and its impact on diseases. *Curr Opin Struct Biol*. 22:578-582.

Shin, K., V.C. Fogg, and B. Margolis. 2006. Tight junctions and cell polarity. *Annu Rev Cell Dev Biol*. 22:207-235.

Sirard, C., J.L. de la Pompa, A. Elia, A. Itie, C. Mirtsos, A. Cheung, S. Hahn, A. Wakeham, L. Schwartz, S.E. Kern, J. Rossant, and T.W. Mak. 1998. The tumor suppressor gene Smad4/Dpc4 is required for gastrulation and later for anterior development of the mouse embryo. *Genes Dev*. 12:107-119.

Snippert, H.J., A. Haegebarth, M. Kasper, V. Jaks, J.H. van Es, N. Barker, M. van de Wetering, M. van den Born, H. Begthel, R.G. Vries, D.E. Stange, R. Toftgard, and H. Clevers. 2010. Lgr6 marks stem cells in the hair follicle that generate all cell lineages of the skin. *Science*. 327:1385-1389.

Sotiropoulou, P.A., and C. Blanpain. 2012. Development and homeostasis of the skin epidermis. *Cold Spring Harb Perspect Biol*. 4:a008383.

Spradling, A., D. Drummond-Barbosa, and T. Kai. 2001. Stem cells find their niche. *Nature*. 414:98-104.

Staedel, C., J.S. Remy, Z. Hua, T.R. Broker, L.T. Chow, and J.P. Behr. 1994. High-efficiency transfection of primary human keratinocytes with positively charged lipopolyamine:DNA complexes. *J Invest Dermatol*. 102:768-772.

Stark, H.J., K. Boehnke, N. Mirancea, M.J. Willhauck, A. Pavesio, N.E. Fusenig, and P. Boukamp. 2006. Epidermal homeostasis in long-term scaffold-enforced skin equivalents. *J Investig Dermatol Symp Proc*. 11:93-105.

Stark, H.J., M.J. Willhauck, N. Mirancea, K. Boehnke, I. Nord, D. Breitkreutz, A. Pavesio, P. Boukamp, and N.E. Fusenig. 2004. Authentic fibroblast matrix in dermal equivalents normalises epidermal histogenesis and dermoepidermal junction in organotypic co-culture. *Eur J Cell Biol*. 83:631-645.

Steinert, P.M., and L.N. Marekov. 1995. The proteins elafin, filaggrin, keratin intermediate filaments, loricrin, and small proline-rich proteins 1 and 2 are isodipeptide cross-linked components of the human epidermal cornified cell envelope. *J Biol Chem*. 270:17702-17711.

Steinert, P.M., and L.N. Marekov. 1997. Direct evidence that involucrin is a major early isopeptide cross-linked component of the keratinocyte cornified cell envelope. *J Biol Chem*. 272:2021-2030.

Sterry, W., Burgdorf, W., and Paus, R. . 2005. Checkliste Dermatologie. Georg Thieme Verlag KG, Stuttgart.

Stingl, J., P. Eirew, I. Ricketson, M. Shackleton, F. Vaillant, D. Choi, H.I. Li, and C.J. Eaves. 2006. Purification and unique properties of mammary epithelial stem cells. *Nature*. 439:993-997.

Strachan, L.R., and R. Ghadially. 2008. Tiers of clonal organization in the epidermis: the epidermal proliferation unit revisited. *Stem Cell Rev*. 4:149-157.

Streuli, C.H., C. Schmidhauser, M. Kobrin, M.J. Bissell, and R. Derynck. 1993. Extracellular matrix regulates expression of the TGF-beta 1 gene. *J Cell Biol*. 120:253-260.

Stuart, K., J. Paderi, P.W. Snyder, L. Freeman, and A. Panitch. 2011. Collagen-binding peptidoglycans inhibit MMP mediated collagen degradation and reduce dermal scarring. *PLoS One*. 6:e22139.

Tan, D.W., K.B. Jensen, M.W. Trotter, J.T. Connelly, S. Broad, and F.M. Watt. 2013. Single-cell gene expression profiling reveals functional heterogeneity of undifferentiated human epidermal cells. *Development*. 140:1433-1444.

Taraboletti, G., D. Roberts, L.A. Liotta, and R. Giavazzi. 1990. Platelet thrombospondin modulates endothelial cell adhesion, motility, and growth: a potential angiogenesis regulatory factor. *J Cell Biol*. 111:765-772.

Taraboletti, G., D.D. Roberts, and L.A. Liotta. 1987. Thrombospondin-induced tumor cell migration: haptotaxis and chemotaxis are mediated by different molecular domains. *J Cell Biol*. 105:2409-2415.

Terunuma, A., R.P. Limgala, C.J. Park, I. Choudhary, and J.C. Vogel. 2010. Efficient procurement of epithelial stem cells from human tissue specimens using a Rho-associated protein kinase inhibitor Y-27632. *Tissue Eng Part A*. 16:1363-1368.

Toyoshima, K., and P.K. Vogt. 1969. Enhancement and inhibition of avian sarcoma viruses by polycations and polyanions. *Virology*. 38:414-426.

Tran, H., W.J. VanDusen, and W.S. Argraves. 1997. The self-association and fibronectin-binding sites of fibulin-1 map to calcium-binding epidermal growth factor-like domains. *J Biol Chem*. 272:22600-22606.

Trempus, C.S., R.J. Morris, C.D. Bortner, G. Cotsarelis, R.S. Faircloth, J.M. Reece, and R.W. Tennant. 2003. Enrichment for living murine keratinocytes from the hair follicle bulge with the cell surface marker CD34. *J Invest Dermatol*. 120:501-511.

Tumbar, T., G. Guasch, V. Greco, C. Blanpain, W.E. Lowry, M. Rendl, and E. Fuchs. 2004. Defining the epithelial stem cell niche in skin. *Science*. 303:359-363.

Turksen, K., T. Kupper, L. Degenstein, I. Williams, and E. Fuchs. 1992. Interleukin 6: insights to its function in skin by overexpression in transgenic mice. *Proc Natl Acad Sci U S A*. 89:5068-5072.

Unsold, C., M. Hyytiainen, L. Bruckner-Tuderman, and J. Keski-Oja. 2001. Latent TGF-beta binding protein LTBP-1 contains three potential extracellular matrix interacting domains. *J Cell Sci*. 114:187-197.

van den Bogaard, E.H., D. Rodijk-Olthuis, P.A. Jansen, I.M. van Vlijmen-Willems, P.E. van Erp, I. Joosten, P.L. Zeeuwen, and J. Schalkwijk. 2012. Rho kinase inhibitor Y-27632 prolongs the life span of adult human keratinocytes, enhances skin equivalent development, and facilitates lentiviral transduction. *Tissue Eng Part A*. 18:1827-1836.

Vasioukhin, V., C. Bauer, L. Degenstein, B. Wise, and E. Fuchs. 2001. Hyperproliferation and defects in epithelial polarity upon conditional ablation of alpha-catenin in skin. *Cell*. 104:605-617.

Vidal, V.P., M.C. Chaboissier, S. Lutzkendorf, G. Cotsarelis, P. Mill, C.C. Hui, N. Ortonne, J.P. Ortonne, and A. Schedl. 2005. Sox9 is essential for outer root sheath differentiation and the formation of the hair stem cell compartment. *Curr Biol*. 15:1340-1351.

Vlodavsky, I., J. Folkman, R. Sullivan, R. Fridman, R. Ishai-Michaeli, J. Sasse, and M. Klagsbrun. 1987. Endothelial cell-derived basic fibroblast growth factor: synthesis and deposition into subendothelial extracellular matrix. *Proc Natl Acad Sci U S A*. 84:2292-2296.

Votteler, M., P.J. Kluger, H. Walles, and K. Schenke-Layland. 2010. Stem cell microenvironments--unveiling the secret of how stem cell fate is defined. *Macromol Biosci*. 10:1302-1315.

Wagers, A.J., and I.L. Weissman. 2006. Differential expression of alpha2 integrin separates long-term and short-term reconstituting Lin-/loThy1.1(lo)c-kit+ Sca-1+ hematopoietic stem cells. *Stem Cells*. 24:1087-1094.

Wang, X.P., M. Schunck, K.J. Kallen, C. Neumann, C. Trautwein, S. Rose-John, and E. Proksch. 2004. The interleukin-6 cytokine system regulates epidermal permeability barrier homeostasis. *J Invest Dermatol*. 123:124-131.

Watabe, T., and K. Miyazono. 2009. Roles of TGF-beta family signaling in stem cell renewal and differentiation. *Cell Res*. 19:103-115.

Watanabe, K., M. Ueno, D. Kamiya, A. Nishiyama, M. Matsumura, T. Wataya, J.B. Takahashi, S. Nishikawa, S. Nishikawa, K. Muguruma, and Y. Sasai. 2007. A ROCK inhibitor permits survival of dissociated human embryonic stem cells. *Nat Biotechnol*. 25:681-686.

Watt, F.M. 2002. Role of integrins in regulating epidermal adhesion, growth and differentiation. *EMBO J*. 21:3919-3926.

Watt, F.M., and R.R. Driskell. 2010. The therapeutic potential of stem cells. *Philos Trans R Soc Lond B Biol Sci*. 365:155-163.

Watt, F.M., S. Estrach, and C.A. Ambler. 2008. Epidermal Notch signalling: differentiation, cancer and adhesion. *Curr Opin Cell Biol*. 20:171-179.

Watt, F.M., and H. Fujiwara. 2011. Cell-extracellular matrix interactions in normal and diseased skin. *Cold Spring Harb Perspect Biol*. 3.

Watt, F.M., and B.L. Hogan. 2000. Out of Eden: stem cells and their niches. *Science*. 287:1427-1430.

Watt, F.M., and P.H. Jones. 1993. Expression and function of the keratinocyte integrins. *Dev Suppl*:185-192.

Webb, A., A. Li, and P. Kaur. 2004. Location and phenotype of human adult keratinocyte stem cells of the skin. *Differentiation*. 72:387-395.

Weissman, I.L., and D. Baltimore. 2001. Disappearing stem cells, disappearing science. *Science*. 292:601.

Wilkes, G.L., I.A. Brown, and R.H. Wildnauer. 1973. The biomechanical properties of skin. *CRC Crit Rev Bioeng*. 1:453-495.

Williams, A. 2003. Transdermal and topical drug delivery, London, UK.

Wilson, A., E. Laurenti, G. Oser, R.C. van der Wath, W. Blanco-Bose, M. Jaworski, S. Offner, C.F. Dunant, L. Eshkind, E. Bockamp, P. Lio, H.R. Macdonald, and A. Trumpp. 2008. Hematopoietic stem cells reversibly switch from dormancy to self-renewal during homeostasis and repair. *Cell*. 135:1118-1129.

Yamaguchi, Y., D.M. Mann, and E. Ruoslahti. 1990. Negative regulation of transforming growth factor-beta by the proteoglycan decorin. *Nature*. 346:281-284.

Yan, C., W.A. Grimm, W.L. Garner, L. Qin, T. Travis, N. Tan, and Y.P. Han. 2010. Epithelial to mesenchymal transition in human skin wound healing is induced by tumor necrosis factor-alpha through bone morphogenic protein-2. *Am J Pathol*. 176:2247-2258.

Yang, Y., M. Gil, S.M. Byun, I. Choi, K.H. Pyun, and H. Ha. 1996. Transforming growth factor-beta1 inhibits human keratinocyte proliferation by upregulation of a receptor-

type tyrosine phosphatase R-PTP-kappa gene expression. *Biochem Biophys Res Commun*. 228:807-812.

Young, P., O. Boussadia, H. Halfter, R. Grose, P. Berger, D.P. Leone, H. Robenek, P. Charnay, R. Kemler, and U. Suter. 2003. E-cadherin controls adherens junctions in the epidermis and the renewal of hair follicles. *EMBO J*. 22:5723-5733.

Yugawa, T., K. Nishino, S. Ohno, T. Nakahara, M. Fujita, N. Goshima, A. Umezawa, and T. Kiyono. 2013. Noncanonical NOTCH signaling limits self-renewal of human epithelial and induced pluripotent stem cells through ROCK activation. *Mol Cell Biol*. 33:4434-4447.

Zhu, A.J., I. Haase, and F.M. Watt. 1999. Signaling via beta1 integrins and mitogen-activated protein kinase determines human epidermal stem cell fate in vitro. *Proc Natl Acad Sci U S A*. 96:6728-6733.

Zhu, J., and R.A. Clark. 2014. Fibronectin at select sites binds multiple growth factors and enhances their activity: expansion of the collaborative ECM-GF paradigm. *J Invest Dermatol*. 134:895-901.

6 Appendix

Table 6: Complete list of differentially expressed genes revealed by the microarray analysis analyzed with chipster.

	gene symbol	gene	Fold change
1	DCN	decorin	22,40631251
2	IL6	interleukin 6 (interferon, beta 2)	19,27065005
3	FBLN2	fibulin 2	16,42134054
4	FN1	fibronectin 1	9,741653484
5	IGFBP4	insulin-like growth factor binding protein 4	9,285631315
6	TIMP2	TIMP metallopeptidase inhibitor 2	8,534657944
7	COL6A1	collagen, type VI, alpha 1	8,0556444
8	COL1A1	collagen, type I, alpha 1	7,981537412
9	C1S	complement component 1, s subcomponent	7,754318535
10	RASD1	RAS, dexamethasone-induced 1	7,498835972
11	AEBP1	AE binding protein 1	7,34451216
12	FBLN1	fibulin 1	7,279749911
13	PTGS2	prostaglandin-endoperoxide synthase 2	6,700025873
14	CTSK	cathepsin K	6,415966756
15	LUM	lumican	6,190259974
16	THBS1	thrombospondin 1	5,958709852
17	VASN	vasorin	5,769048265
18	NPTX2	neuronal pentraxin II	5,540437872
19	DPYSL3	dihydropyrimidinase-like 3	5,502167273
20	VIM	vimentin	5,256733755
21	SERPINE2	serpin peptidase inhibitor, clade E (nexin, plasminogen activator inhibitor type 1), member 2	5,58
22	LEP	leptin	5,55
23	C11orf96	chromosome 11 open reading frame 96	5,43
24	IL1RL1	interleukin 1 receptor-like 1	5,41
25	CDR1	cerebellar degeneration-related protein 1, 34kDa	5,14
26	MMP1	matrix metallopeptidase 1 (interstitial collagenase)	5,05
27	COL6A3	collagen, type VI, alpha 3	4,91
28	APOD	apolipoprotein D	4,88
29	HMOX1	heme oxygenase (decycling) 1	4,67
30	SFRP2	secreted frizzled-related protein 2	4,67
31	COL1A2	collagen, type I, alpha 2	4,13
32	MFAP4	microfibrillar-associated protein 4	4,12
33	NDN	necdin, melanoma antigen (MAGE) family member	4,07
34	DPT	dermatopontin	3,93
35	STC1	stanniocalcin 1	3,92
36	RGS2	regulator of G-protein signaling 2, 24kDa	3,87
37	TNFAIP6	tumor necrosis factor, alpha-induced protein 6	3,65

38	KIAA1199	KIAA1199	3,62
39	CNFN	cornifelin	3,57
40	RARRES2	retinoic acid receptor responder (tazarotene induced) 2	3,53
41	COL3A1	collagen, type III, alpha 1	3,32
42	MEDAG	mesenteric estrogen-dependent adipogenesis	3,24
43	PDGFRA	platelet-derived growth factor receptor, alpha polypeptide	3,20
44	ATP8B2	ATPase, aminophospholipid transporter, class I, type 8B, member 2	3,15
45	PTX3	pentraxin 3, long	3,11
46	METTL7A	methyltransferase like 7A	2,97
47	OLFML3	olfactomedin-like 3	2,96
48	S100P	S100 calcium binding protein P	2,95
49	CRISPLD2	cysteine-rich secretory protein LCCL domain containing 2	2,90
50	LGALS1	lectin, galactoside-binding, soluble, 1	2,86
51	NID1	nidogen 1	2,85
52	CXCL12	chemokine (C-X-C motif) ligand 12	2,84
53	CRCT1	cysteine-rich C-terminal 1	2,79
54	CXCL5	chemokine (C-X-C motif) ligand 5	2,77
55	TNC	tenascin C	2,77
56	KLK7	kallikrein-related peptidase 7	2,74
57	HSPB8	heat shock 22kDa protein 8	2,73
58	APCDD1	adenomatosis polyposis coli down-regulated 1	2,64
59	S100A4	S100 calcium binding protein A4	2,64
60	FLNC	filamin C, gamma	2,53
61	GEM	GTP binding protein overexpressed in skeletal muscle	2,50
62	SAA1	serum amyloid A1	2,49
63	THY1	Thy-1 cell surface antigen	2,35
64	FST	follistatin	2,33
65	CFD	complement factor D (adipsin)	2,32
66	TMEM119	transmembrane protein 119	2,32
67	COL4A1	collagen, type IV, alpha 1	2,31
68	CIDEA	cell death-inducing DFFA-like effector a	2,26
69	STMN2	stathmin-like 2	2,25
70	PPARGC1A	peroxisome proliferator-activated receptor gamma, coactivator 1 alpha	2,25
71	SVEP1	sushi, von Willebrand factor type A, EGF and pentraxin domain containing 1	2,21
72	CLDN11	claudin 11	2,18
73	LCN2	lipocalin 2	2,16
74	NNMT	nicotinamide N-methyltransferase	2,15
75	CTHRC1	collagen triple helix repeat containing 1	2,14
76	PRRX1	paired related homeobox 1	2,13
77	LOXL4	lysyl oxidase-like 4	2,04

78	CRYAB	crystallin, alpha B	2,04
79	GREM1	gremlin 1, DAN family BMP antagonist	2,00
80	EDNRB	endothelin receptor type B	1,98
81	COL5A1	collagen, type V, alpha 1	1,96
82	TNFRSF11B	tumor necrosis factor receptor superfamily, member 11b	1,96
83	SLC39A14	solute carrier family 39 (zinc transporter), member 14	1,91
84	CXCL6	chemokine (C-X-C motif) ligand 6	1,90
85	PODN	podocan	1,86
86	AP1S2	adaptor-related protein complex 1, sigma 2 subunit	1,83
87	NCCRP1	non-specific cytotoxic cell receptor protein 1 homolog (zebrafish)	1,81
88	ISLR	immunoglobulin superfamily containing leucine-rich repeat	1,80
89	RCAN2	regulator of calcineurin 2	1,80
90	LOR	loricrin	1,79
91	CPE	carboxypeptidase E	1,77
92	SCNN1D	sodium channel, non-voltage-gated 1, delta subunit	1,77
93	DIO2	deiodinase, iodothyronine, type II	1,76
94	DUSP6	dual specificity phosphatase 6	0,40
95	HIST1H2BG	histone cluster 1, H2bg	0,39
96	HIST1H4H	histone cluster 1, H4h	0,39
97	GOLGA7B	golgin A7 family, member B	0,38
98	CXCL14	chemokine (C-X-C motif) ligand 14	0,38
99	KRT14	keratin 14	0,37
100	MCM3	minichromosome maintenance complex component 3	0,36
101	HIST1H2BK	histone cluster 1, H2bk	0,36
102	ITGB4	integrin, beta 4	0,33